NASA CR 71207

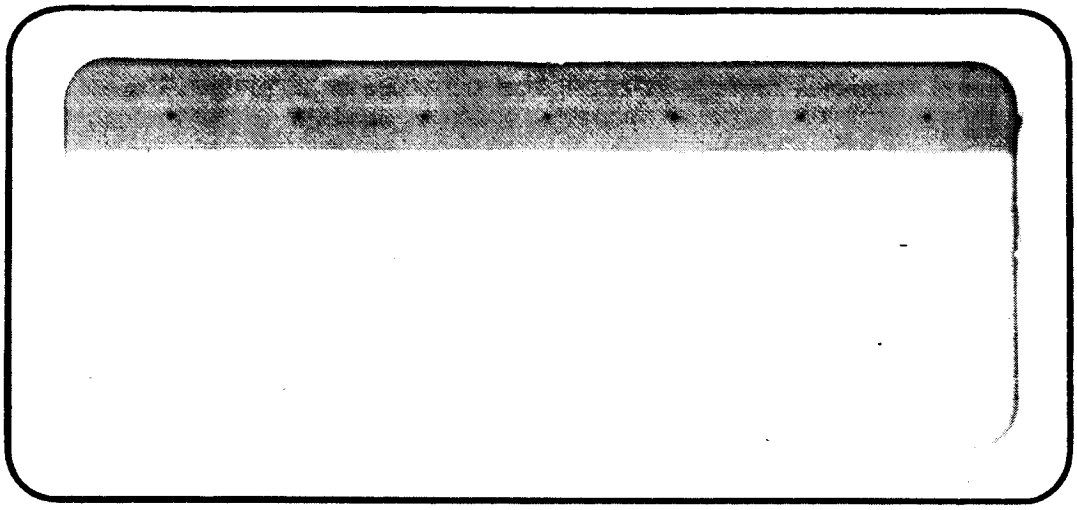

TRW SYSTEMS

ONE SPACE PARK • REDONDO BEACH, CALIFORNIA

MID-TERM TECHNICAL PROGRESS REPORT

ADVANCED PLANETARY PROBE STUDY

15 March 1966

Prepared for Jet Propulsion Laboratory
under Contract 951311

This work was performed for the Jet Propulsion Laboratory, California Institute of Technology, sponsored by the National Aeronautics and Space Administration under Contract NAS7-100.

TRW Systems
1 Space Park
Redondo Beach, California

CONTENTS

CONTENTS (Continued)

ILLUSTRATIONS

ILLUSTRATIONS (Continued)

TABLES

1. INTRODUCTION

This volume and a classified appendix constitute the Mid-Term Technical Progress Report of the Advanced Planetary Probe Study. This study is being conducted by TRW Systems under Contract No. 951311 of the Jet Propulsion Laboratory, California Institute of Technology. As this report is being submitted on March 15, 1966, and as it incorporates the subject matter normally embodied in the Monthly Technical Progress Letter Report, due the same date, this monthly letter report will not be submitted separately.

The mid-term report covers the progress resulting from approximately one-third of the programmed effort of the study. This effort has been directed towards establishing the conceptual design of classes of spacecraft which conform to the study constraints discussed below, with emphasis on the requirements resulting from the mission analysis, and a first look, or parametric study, of subsystem characteristics.

The more detailed aspects of subsystem quantitative requirements and implementation, reliability analyses, cost effectiveness analyses, and preliminary estimates of schedule and cost are not included in this report, but will be addressed in the remainder of the study.

Although the classes of spacecraft design concepts which have been considered are illustrated by specific samples, it is intended that this report be applicable to a broad spectrum of spacecraft capabilities. It is recognized that the remaining work of the study, more detailed in nature, will be best accomplished if the number of specific spacecraft configurations is reduced. Therefore, it is anticipated that as a result of this report and the subsequent briefing, agreement will be reached with the effect of reducing the number of specific configurations carried forward.

2. SCOPE OF STUDY

2.1 TIME PERIOD

The Advanced Planetary Probe Study applies to missions to be conducted during the period 1970-1980. This is interpreted to mean that the launches of the spacecraft destined to the various target planets will take place during this period. Because of substantial transit times for missions to the more distant planets, the end of the mission, as determined by the arrival time, could be as much as eight years later.

On the other hand, for purposes of subsystem design, a reasonable lead time is necessary so that the design is established sufficiently in advance of the launch date. For this purpose, it is felt that the earliest launches in the 1970-1980 time period must be accomplished with hardware which essentially reflects the 1966 state of the art. The later launches may reasonably be based on developments in technology expected to occur at appropriately later times.

2.2 MISSIONS CONSIDERED

The Advanced Planetary Probe, according to the Work Statement, is directed towards: "(1)basic flyby missions of the planets Jupiter, Saturn, and Neptune, and (2) examination of the growth potential of the basic concepts through the use of a modular design concept to perform orbiter and planetary capsule entry missions." The planet Uranus has been included in certain aspects of the study, because it is a planet of the same class as those specified, and because its orbital characteristics make it intermediate to the extremes specified.

The major emphasis is on the flyby missions of the planets. The growth to an orbiter mission is relatively straightforward, in terms of the implications on the experiment complement and the subsystem implementation of the spacecraft. On the other hand, the incorporation of capsule missions, particularly for the major planets—Jupiter and Saturn, carries feasibility implications, the complete resolution of which is beyond the scope of this study. Such implications have to do with the extreme guidance accuracy which may be required for such a capsule to make meaningful atmospheric measurements.

2.3 EXPERIMENTAL OBJECTIVES

The experimental objectives of the Advanced Planetary Probe missions are identified in the Work Statement as follows:

1) Measurement of the spatial distribution of interplanetary and planetary particles and fields

2) Measurement of the salient features of planetary atmospheres, with particular emphasis upon remote measurements from a flyby spacecraft

3) Observations of the planets, i.e., visual, infrared, etc.

2.4 SPACECRAFT CONFIGURATION CONSTRAINTS

The conceptual design of spacecraft configurations suitable for the Advanced Planetary Probe have been generated observing the following constraints:

1) Spacecraft power is to be supplied by radioisotope thermoelectric generators (RTG's)

2) A large body-fixed antenna is employed for the primary communication between the probe and the earth

3) The cruise attitude stabilization directs the axis of this antenna toward the earth.

A further constraint is the specification of launch vehicles (see next Section) which are to be employed in injecting the spacecraft onto the interplanetary trajectory. It has been assumed that all primary propulsion to direct the spacecraft to the target planet is produced by the launch vehicle, and the use of onboard propulsion is limited to midcourse trajectory correction maneuvers and, in the case of an orbiter mission, the propulsion for orbit insertion.

2.5 LAUNCH VEHICLES

The launch vehicles considered for the Advanced Planetary Probe are the following six vehicle combinations specified by JPL:*

Saturn V/Centaur

*W. A. Ogram, "Launch Vehicle Future Missions Study Guideline."

Saturn V

Saturn IB/Centaur

Titan IIICx/Centaur

Atlas SLV3x/Centaur/HEKS

Atlas SLV3x/Centaur

The reference gives performance data for the Launch Vehicles, and prescribes mounting provisions and envelope limits for the spacecraft.

For certain missions it is desirable to incorporate into the spacecraft design a solid propulsion motor, for the purpose of enhancing the capability of the launch vehicle. Although this solid motor is physically a part of the spacecraft design, it is functionally a part of the launch vehicle system.

2.6 DOMINATING CHARACTERISTICS

The extension of interplanetary and planetary missions from the region of those planets near the earth (Venus and Mars) to the outer planets of the solar system introduces the following characteristics which dominate:

1) The extreme reduction in the amount of solar energy which might be available for spacecraft power

2) The extreme increase in the communication distances between the spacecraft and the earth

3) Substantial increases in the mission lifetime requirement, due to the large interplanetary transit times.

The first two characteristics are coped with by the defining characteristics of spacecraft configurations studied, and discussed in 2.4. These are the use of radioisotope power aboard the spacecraft, and the emphasis on communication ability inherent in the large antenna design.

The long lifetime characteristics of the missions makes system reliability an important criterion in the maintenance of adequate probabilities of success. For a first generation spacecraft, this reliability is to be achieved to a large extent by design simplicity. One of the classes of spacecraft presented in this report—the spin-stabilized spacecraft—

represents an approach to inherent reliability through operational simplicity. As a consequence of the basic mission characteristics, and the experimental objectives of the mission, the attitude control and data handling subsystems are also subject to unique requirements. The attitude control requirements, whether for a spin-stabilized spacecraft or a fully attitude-controlled spacecraft, arise not only from the experimental objectives, but also from the requirement of directing a narrow antenna beam at the earth. The data handling requirements stem from a desire to utilize to the largest extent the data rate capability of the communication link, recognizing that, at least for a flyby mission, the scientific data of greatest interest are generated during the comparatively brief period of planetary encounter.

3. MISSION ANALYSIS

3.1 LAUNCH ENERGY REQUIREMENTS

The injection energy requirements of the launch vehicle for ballistic interplanetary trajectories from the earth to Jupiter, Saturn, Uranus, and Neptune are shown in Figure 3.1-1. Both direct trajectories (earth-target planet) and swingby trajectories (earth-Jupiter-target planet) are included. The trajectories represented are the following, with the sources of data from which the curves were generated indicated by the references:

- Earth-Jupiter. Type I and Type II Trajectories. Launch opportunities: 1969-70, 71, 72, 73, 74. Reference 3.1.1.
- Earth-Saturn (direct trajectories). Type I. Launch opportunities: 1970, 71, 72, 73, 74, 75. Reference 3.1.2
- Earth-Uranus (direct trajectories).
- Earth-Neptune (direct trajectories).
- Earth-Saturn (Jupiter swingby trajectories). Launch opportunity: 1979. Reference 3.1.3.
- Earth-Uranus (Jupiter swingby trajectories). Launch opportunity: 1979. Reference 3.1.3.
- Earth-Neptune (Jupiter swingby trajectories). Launch opportunity: 1979. Reference 3.1.3.

For all the trajectories except direct trajectories from the earth to Uranus and Neptune, the curves give minimum injection energy requirements over a 20-day launch opportunity.

For the direct earth-Uranus and earth-Neptune trajectories, in the absence of more precise data, the curves were based on these assumptions:

- The earth's orbit is circular, with a radius of 1 AU.
- The target planet is at a constant distance from the sun. This distance, 18.2 AU for Uranus and 30.3 AU for Neptune, approximates the actual distance from the sun to these planets during the 1980's.

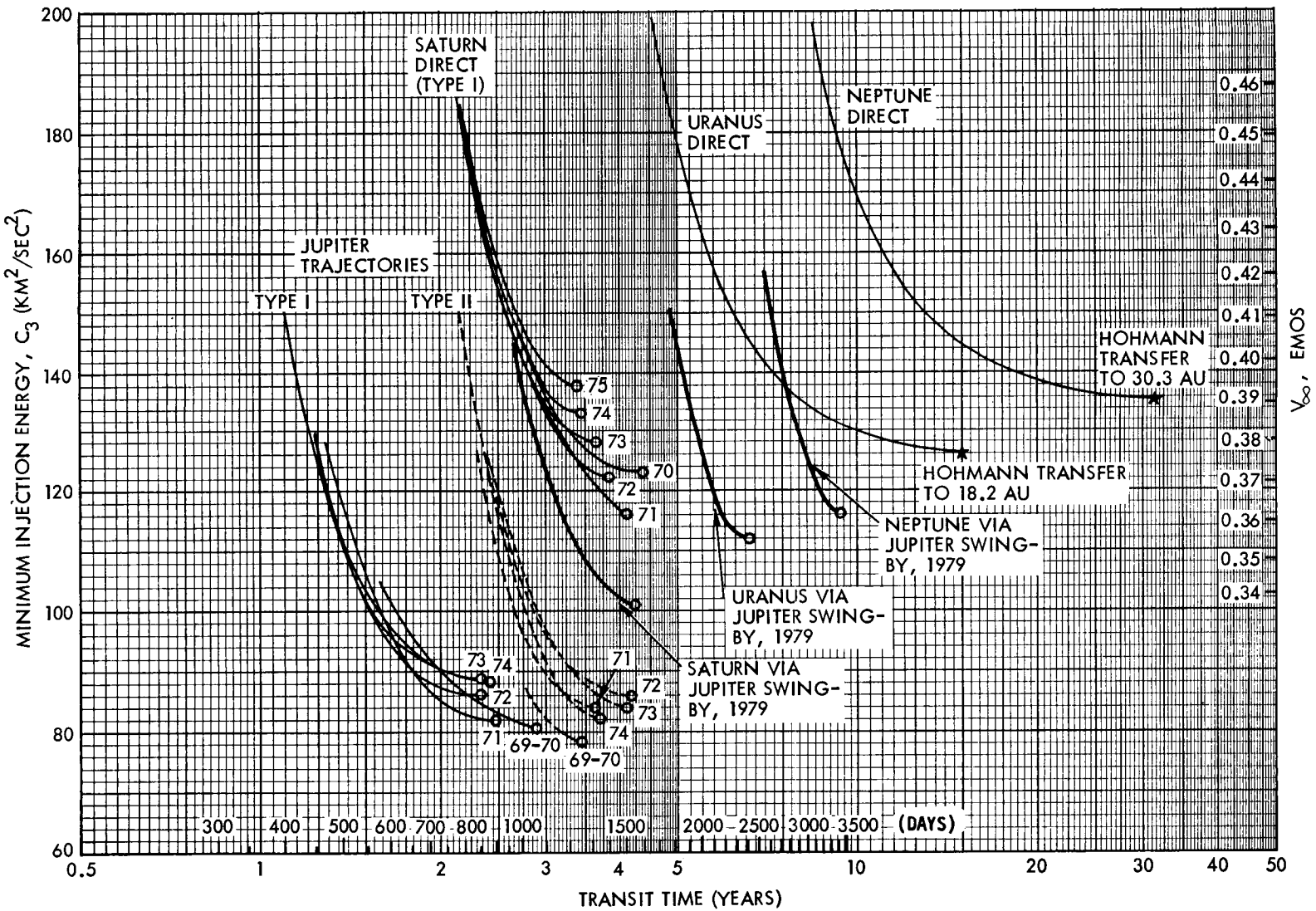

Figure 3.1-1. Injection Energy Versus Transit Time

- The orbits of the earth and the target planets are co-planar.

As a result of these assumptions, the curves show no distinction between the different (annual) launch opportunities and show no division into Type I and Type II categories. Also, no provision for a finite launch-opportunity duration was made. (Redrawing the curves to accommodate the penalty imposed by the requirement of a 20-day launch opportunity would increase C_3 by 3.5 km^2/sec^2.) The limiting case of these curves, reflecting the minimum-energy trajectories, corresponds to the Hohmann transfers.

The interpretation of the minimum energy requirement over a 20-day launch opportunity is illustrated by a point on one of the curves. For example, the 1975 curve for direct trajectories to Saturn passes through the point 3.1 years, 140 km^2/sec^2. We may state that for the 1975 opportunity, the minimum injection energy which need not be exceeded to produce trajectories to Saturn with transit times no greater than 3.1 years or 20 consecutive launch days is 140 km^2/sec^2. Or, conversely, given an injection energy of 140 km^2/sec^2, the smallest transit time which need not be exceeded for 20 consecutive launch days is 3.1 years.

Figure 3.1-1 indicates the expected progressive increases in transit time and required injection energy for target planets more distant from the sun. In addition, the family of curves for any one target planet shows the tradeoff between C_3 and transit time. Thus increasing C_3 (for a Jupiter mission) from 90 to 130 km^2/sec^2 reduces transit time from 2 years to about 1.25 years. Since C_3 is related to the spacecraft weight which may be injected by a given launch vehicle (discussed in Section 3.2), comparison of curves of Figures 3.1-1 and 3.2-1 will show (for a given launch vehicle and a given target planet) the cost (in transit time) of additional spacecraft weight. This comparison is illustrated in Figure 3.1-2. As an example, the launch vehicle Atlas SLV3x/Centaur/HEKS can send a 400-lb spacecraft to Jupiter in 1.25 years, or a 950-lb spacecraft in 2 years.

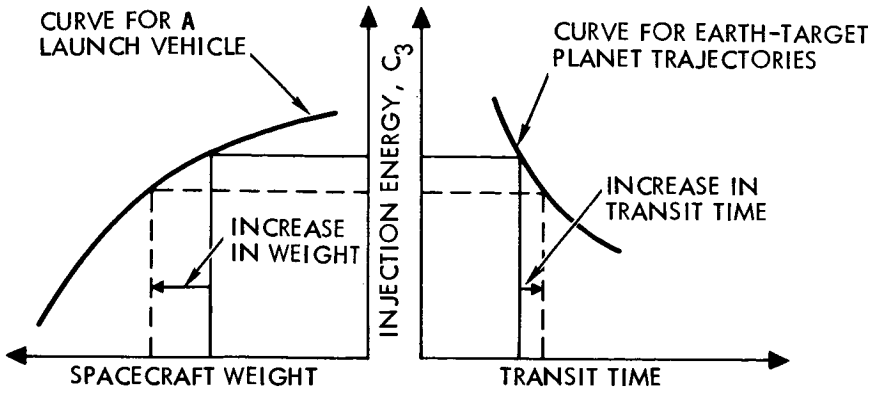

Figure 3.1-2. Influence of Spacecraft Weight on Transit Time

For missions to the outer planets, the advantages of swingby trajectories, which use the gravitational attraction of Jupiter to boost the heliocentric velocities, over direct trajectories are seen in Figure 3.1-1. For Saturn missions, the reduction in transit time for a given launch energy is not extreme. At best, the swingby trajectories reduce transit time from 4 to 3 years. However, the swingby technique reduces the minimum energy requirement to about 100 km^2/sec^2. For direct trajectories the corresponding minima are 116 to 138 km^2/sec^2, depending on the launch year. Thus, the swingby technique probably has more value in reducing C_3 requirements than in reducing transit time for Saturn missions.

For missions to Uranus and Neptune, however, although launch energy requirements are reduced appreciably by the swingby technique, the striking advantage appears to lie in the substantial reduction in transit times for values of C_3 in the range 130 to 150 km^2/sec^2.

Of course, it is recognized that the swingby trajectories are related to the long (12 to 20 years) synodic periods between Jupiter and the outer planets, and are not available annually, as the direct trajectories are. Reference 3.1.3 points out that 1979 and adjacent years appear to provide the best opportunities for the swingby missions considered here. Other characteristics of the swingby missions are reviewed in Section 3.7.

REFERENCES

3.1.1 TR 32-77, "Design Parameters for Ballistic Interplanetary Trajectories, Part II. One-Way Transfers to Mercury and Jupiter," V. C. Clarke, W. E. Bollman, P. H. Fetis, and R. Y. Roth.

3.1.2 NASA TMX 53046, "Interplanetary Trajectory Analysis for Missions from Earth to Mercury, Jupiter, and Saturn."

3.1.3 JPL Space Programs Summary No. 37-35, Vol. IV, p. 12. "Utilization of Energy Derived from the Gravitational Field of Jupiter for Reducing Flight Time to the Outer Solar System," G. A. Flandro.

3.2 LAUNCH VEHICLE CAPABILITIES

3.2.1 Weight Vs. Injection Energy

Performance data for eight launch vehicle combinations have been generated on a common basis. These combinations include the six configurations identified by JPL for use in the study (Reference 3.2.1).

A. Saturn V/Centaur

B. Saturn V

C. Saturn IB/Centaur/HEKS

D. Titan IIICx/Centaur

E. Atlas SLV3x/Centaur/HEKS

F. Atlas SLV3x/Centaur

In addition, two combinations have been created by the incorporation of a solid motor, based on the TE-364, into the injection sequence as a final stage:

D1. Titan IIICx/Centaur/TE-364

F1. Atlas SLV3x/Centaur/TE-364

The common basis for performance data corresponds to that employed in the reference, except that the spacecraft-to-vehicle adapter weight and nose fairing weight, estimated as suggested in the reference, are not included in the payload weight.

The performance data of these launch vehicle combinations are shown in Figure 3.2-1. (Vehicle F cannot achieve C_3 of 60 km^2/sec^2, and does not appear in the figure.)

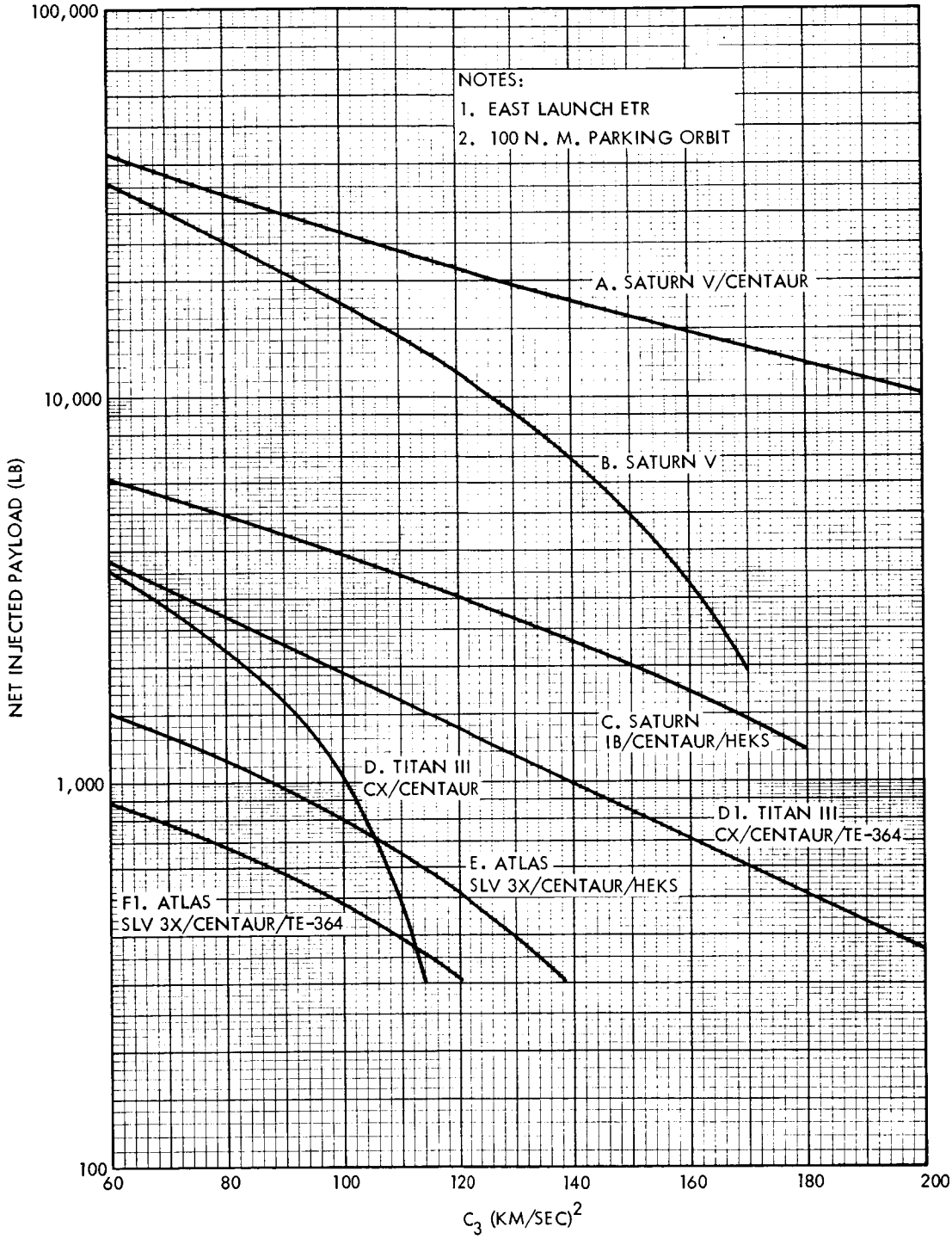

Figure 3.2-1. Launch Vehicle Performance Capability

In considering the payload capability of the Atlas SLV3x/Centaur and the Titan IIICx/Centaur, it becomes apparent that the equivalent of an additional injection stage is required. The Atlas/Centaur is just not capable of providing the required injection energy for even the minimum spacecraft and the Titan/Centaur suffers a high degree of efficiency degradation when C_3 exceeds 100 km^2/sec^2 without such an injection stage. To remedy this situation, a Surveyor TE-364 solid rocket motor is assumed for this function. In the case of the minimum module flyby mission, this rocket motor would be integrated into the spacecraft and the spent motor would be carried along the flyby mission to achieve a compact vehicle layout and simplify the design. In keeping with a modular concept, the same motor would be used for deboost propulsion when compatible with the related propulsive requirement. Performance data for the TE-364 are given below:

Propellant weight	=	1197 lb
Burnout weight	=	137 lb
Total weight	=	1334 lb
Specific Impulse	=	290 sec.

These correspond to a version of the TE-364 which is consistent with the current motor casing design size.

3.2.2 Limitations on Launch Capability

For the configurations being considered, a restart of either the Centaur stage or the S-IVB stage will be required to establish the transfer orbit. Both of these stages have restart capability; however, the use of LOX/Hydrogen in these stages will require that the coast time be kept to a minimum in order to reduce boil off. The coast time for the Centaur stage is currently limited to 25 minutes for the Surveyor mission. Either an increase in this allowable coast time or a limitation on the spectrum of acceptable transfer orbits would be required by the Advanced Planetary Probe missions. The S-IVB stage has the capability of restarting after coasting for a full revolution and therefore should present no problem in this regard. For the high energy missions being considered, restart of the HEKS and TE-364 motor would not be required for injection into the transfer orbit since these stages would be utilized only in this phase.

The launch azimuth from ETR is currently limited to between 72 and 108 degrees. This limitation will restrict the selection of the transfer orbit in conjunction with the coast time limitations previously discussed. Detailed analyses of these limitations would have to be conducted separately for each mission and each launch opportunity. If it is required to increase the range of allowable launch azimuths, detailed range safety analysis would be required.

3.2.3 Injection Accuracy

The injection error is also influenced by the 3σ variation in the total impulse of the solid motor (± 1 percent) from Reference 3.2.2 and by the 3σ tip off error (assumed to be 1 degree in this case). For the Atlas SLV3x/Centaur/TE-364 configuration, the ΔV imparted by the TE-364 solid motor is approximately 3.0 km/sec (for $C_3 = 97$, $W_{pl} = 500$ lb). A 3σ error in burnout velocity of approximately 30 m/sec would then be expected due to the total impulse variation alone. In addition, if a tip off error of 1 degree is assumed, this would yield an error of approximately 0.06 degree in burnout flight path angle.

By taking the root-sum-square of the errors at Centaur burnout (from the Surveyor data) and the solid motor contributions, an estimate of the injection accuracy for the Atlas SLV3x/Centaur/TE-364 configuration is determined. This yields a 3σ burnout velocity error of 30.5 m/sec and a 3σ burnout flight path angle error of 0.118 degree.

The error contributed by the TE-364 solid motor will be significantly less for the Titan IIICx/Centaur/TE-364 configuration since a smaller ΔV is imparted by the solid stage. This is due to the increased payload provided by this vehicle. In this case, a 3σ burnout velocity error of 12 m/sec and a 3σ burnout a flight path angle error of 0.02 degree would be attributed to the solid motor.

The transformation from injection accuracy to figure of merit, in which the effect of the earth's gravitation is removed, should be performed in order to provide the most useful guidance information; however, this transformation is a function of the C_3 of the launch. It should be pointed out that the accuracy data quoted above are of a preliminary nature. A

more detailed analysis is required to determine the injection accuracies and figures of merit of the various configurations being considered.

3.2.4 Longitudinal Accelerations

The maximum longitudinal accelerations imposed on the payload by the various launch vehicle configurations are listed in Table 3.2-1.

Table 3.2-1. Maximum Longitudinal Acceleration

	Launch Vehicle	~ g's
A	Saturn V/Centaur	4.35
B	Saturn V	4.35
C	Saturn IB/Centaur/HEKS	4.0
D1	Titan III Cx/Centaur/TE-364	4.07
E	Atlas SLV3x/Centaur/HEKS	6.0
F1	Atlas SLV3x/Centaur/TE-364	13.45

For configurations A, B, C, and E the maximum acceleration is obtained during the operation of the first stage. On the other hand, configurations D1 and F1 will encounter maximum acceleration at the termination of the TE-364 solid motor burning phase. The acceleration in the latter case is highly dependent on payload weight. The payload at $C_3 = 100$ $(km/sec)^2$ was used in determining the peak acceleration for these two configurations. For reduced payloads corresponding to higher values of C_3, the peak acceleration will be higher than the above values. This increase is most pronounced for D1 and F1.

An estimate of the injection accuracy which is achieved with the Atlas SLV3x/Centaur/TE-364 configuration has been determined based on similar error data for the Surveyor mission and on the errors contributed by the solid motor burning phase. The 3σ injection accuracy, quoted in Reference 3.2.3 for the Surveyor mission is approximately 5 m/sec in velocity and 0.09 degree in flight path angle for an Atlas/

Centaur configuration utilizing two burns of the Centaur stage and a coast time of 1500 seconds.

3.2.5 Launch Vehicle Dynamic Environments

The dynamic environments for the launch vehicles presently considered are given below. These vehicles are Atlas SLV3x/Centaur/ with or without upper stage or solid, Titan IIICx/Centaur/with or without upper stage, Saturn IB/Centaur/HEKS.

3.2.5.1 Atlas/Centaur

The data (Reference 3.2.4) are preliminary and are intended for use for feasibility and/or preliminary calculations.

A requirement to design a rigid payload structure is given. A recommended lowest cantilever frequency is 20 cps or higher.

a. Vibration

The payload's structure and small components (up to approximately 50 pounds) should be designed to withstand the following sinusoidal and random vibrations without adverse effects.

i) Sinusoidal

0.25 inch single amp. (O-P) 5 to 13 cps
3.15 g (rms) 13 to 500 cps
4.5 g (rms) 500 to 2000 cps

ii) Random Vibration (see Note 1)

0.0013 g^2/cps at 50 cps increasing 6 db per octave to 0.225 g^2/cps at 600 cps. Constant at 0.225 g^2/cps from 600 to 1100 cps. Decreasing at 12 db/octave to 0.0205 g^2/cps at 2000 cps.

Sweep rate 2 minutes per octave, duration 17.3 minutes in each of three mutually perpendicular axes.

Note 1. Payload composite vibration tests may be conducted with these input levels subject to the condition that the maximum permissible load factor not exceed the following values (taken from plot).

Payload Weight, lb.	100	200	400	1000	2000	5000
Permissible load factor, g's	10	7.5	5.4	3.2	2.5	1.8

b. Shock

The only significant shock in the Centaur environment is due to the separation of insulation panels on Centaur and the nose fairing jettison or spacecraft separation. This may be represented by a sinusoidal shock for one-half wavelength in which maximum shock amplitude shall be 1000 g's and the duration 0.0004 seconds. The shock shall be applied along any axis.

c. Acoustical Noise

Equipment, while operating, shall undergo a maximum, broadband, random incidence, sound pressure field with an overall sound pressure level of 141 decibels. (The detailed levels are given in Reference 3.2.6.)

3.2.5.2 Titan IIICx/Centaur/Upper Stage

Data are from Reference 3.2.5. This document applies to Titan IIIC with Transtage. However, test levels are not expected to deviate with use of Centaur as opposed to the Transtage.

a. Random Vibration

The vibration environment described is applicable for periods of approximately 10 seconds during launch and 40 seconds during the transonic and maximum dynamic pressure regions of flight. During the remaining portions of powered flight, the overall rms vibration levels will be less than half the values described.

For payload weights less than 2000 lbs:

Flat 22 to 180 cps at 0.065 g^2/cps

Roll-off at 3 db/oct below 22 cps

Flat 550 to 1000 cps at 0.2 g^2/cps

Roll-off at 3 db/oct below 550 cps

Roll-off at 6 db/oct above 1000 cps

Overall 15.8 g rms

Notes: (1) Reduce spectra by 3 db for total weights of 2,000 to 10,000 lbs., overall 11.3 g rms.
(2) Reduce spectra by 6 db for total weight of 10,000 to 20,000 lbs., overall 7.9 g rms.

b. Shock

Transient accelerations at shroud and spacecraft separation are to be considered. Shock input can be represented by a sinusoidal shock for one-half wavelength which maximum shock amplitude shall be 850 g's and the duration 0.00035 seconds.

c. Acoustic Sound Field

The maximum noise levels for test is 150 db-qualification level (includes 5 db margin for test), 1 minute for test. This covers both the launch and the transonic and maximum dynamic pressure flight conditions.

3.2.5.3 Saturn IB/Centaur

Data from Reference 3.2.4.

a. Vibration

i) Low Frequency Vibration

The low frequency flight vibration, covering all events from liftoff to spacecraft injection, is estimated to be a sinusoidal input as follows:

Lateral	0.6 g rms	5 to 200 cps
Axial	1.2 g rms	5 to 200 cps

ii) Random Vibration

The liftoff and transonic vibration environment, with the exception of low frequency, is assumed to be the following omnidirectional input to the spacecraft separation plane: power spectral density peaks of 0.07 g^2 cps ranging from 100 to 1500 cps with a 6 db/octave rolloff in the envelope defining peaks below and above these frequencies. Maximum total time is 60 seconds. Random vibration at other mission times is predicted to be insignificant by comparison.

b. Shock

Transient accelerations at shroud and spacecraft separation will be investigated. Depending on the launch vehicle characteristics, shock response during other mission events is predicted to be insignificant by comparison. The shock response to these environments may be

approximated by an input consisting of a 200 g terminal peak sawtooth of 0.7 to 1.0 millisecond rise time.

c. Acoustic Sound Field

The maximum acoustic field, for either liftoff or transonic, is assumed to be a reverberant field as follows: Overall sound pressure level (SPL) is approximately 142 db. Total duration about 2 minutes.

REFERENCES

3.2.1 W. A. Ogram, "Launch Vehicle Future Missions Study Guideline"

3.2.2 Spherical Rocket Motors (U), EB7-64, Thiokol Chemical Corporation, Elkton Division, dtd: January 1965

3.2.3 Centaur Guidance System Accuracy Bimonthly Report, AC-8 Accuracy Analysis (U), GD/C-BTD 64-013-10, General Dynamics, dtd: 01 January 1966

3.2.4 Centaur Capability Handbook, GD/A Project Centaur, Report No. GD/A-BTD 64-119-1

3.2.5 Interface Specification, Standard Space Launching System to Spacecraft Environmental, Standard Interface Capabilities and Requirements, Specification No. IFS-T111-20004

3.2.6 TRW/System, Phase IA Study Report, Voyager Spacecraft, Volume 2, Page 369

3.3 DISPLAY OF SAMPLE TRAJECTORIES

This section of the mid-term report contains an analysis of several representative direct and planetary swingby missions to the outer planets for selected earth launch dates in the 1970-1980 decade. These sample trajectories have been graphically displayed on a map of the solar system. The salient heliocentric communications parameters and orientation angles have been plotted as a function of time from earth launch date.

3.3.1 Solar System Maps, 1970-1980

Figure 3.3-1 depicts the variations of the positions of the planets specified, assuming mean circular orbits, during the 1970-1980 period. The mean longitudes of the ascending node and of perihelion are noted. For purposes of clarity, earth's orbit size has been doubled; its orbital positions during the year 1970 are indicated.

Figure 3.3-2 illustrates the orbital arcs traversed by the specified planets in the 1970-1980 period. This figure has been constructed from planetary ephemeris data and thus is an accurate representation of the relative planetary positions during the time period of interest.

3.3.2 Definition and Display of Sample Trajectories

Five sample trajectories have been chosen for analysis and graphical representation. Two direct transfers to Jupiter and one to Saturn have been selected. They are:

Mission Designation	From	To	Launch Date	Transfer Time	Launch Energy (C_3)
A.	Earth	Jupiter	2-11-71	650 days	95.9 km^2/sec^2
B.	Earth	Jupiter	3-24-72	450 days	142.4 km^2/sec^2
C.	Earth	Saturn	10-4-75	1,600 days	131.8 km^2/sec^2

In addition, two Jupiter swingbys have been analyzed. They are:

Mission Designation	Earth Depart Date	Jupiter Encounter Date	Target Planet Arrive Date	C_3 at Launch (km^2/sec^2)
D. Earth-Jupiter-Saturn	11-10-79	5-5-81	6-24-83	111.5
E. Earth-Jupiter-Neptune	11-8-79	5-5-81	8-29-88	110.6

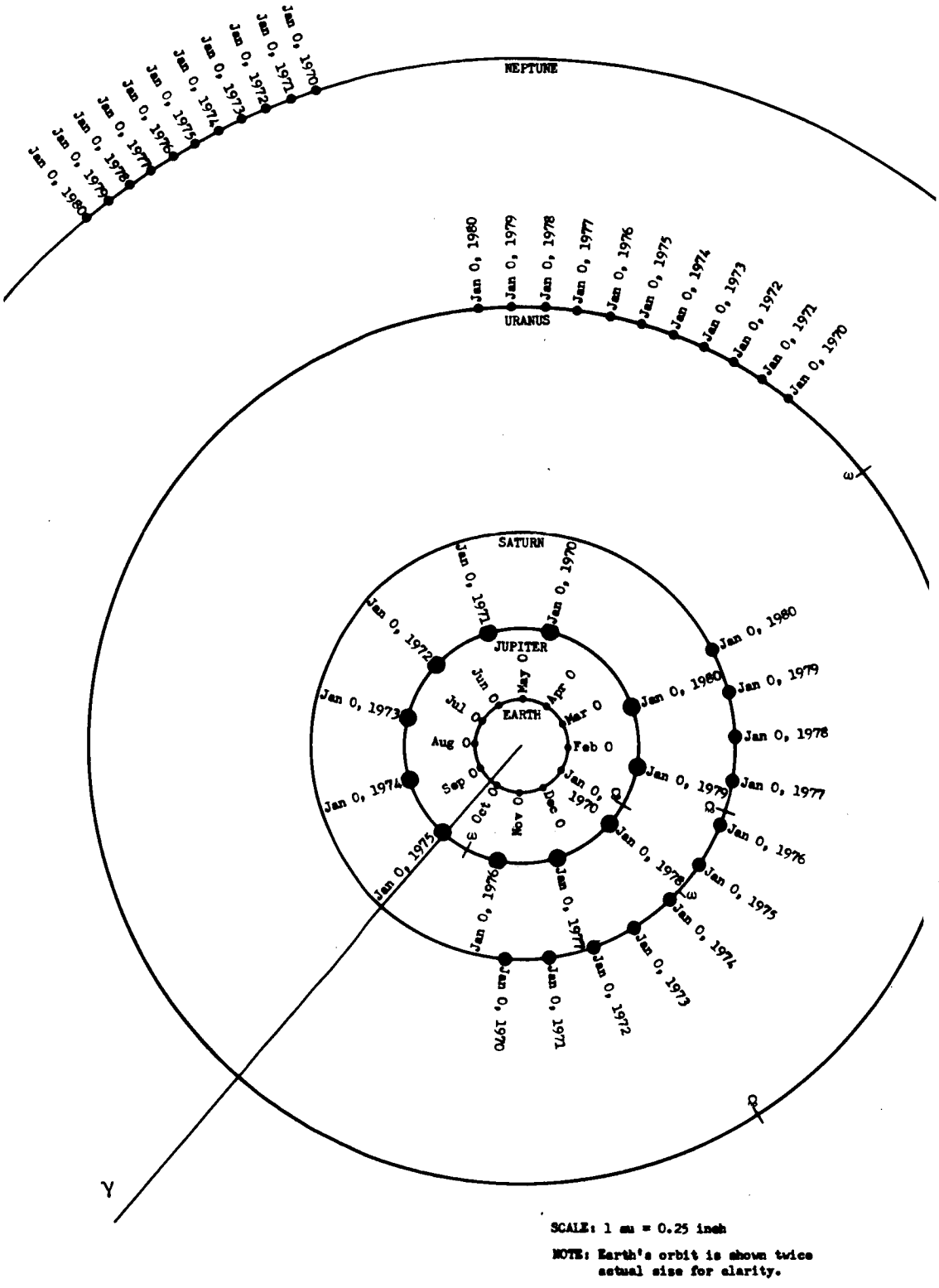

Figure 3.3-1. Partial Map of Solar System

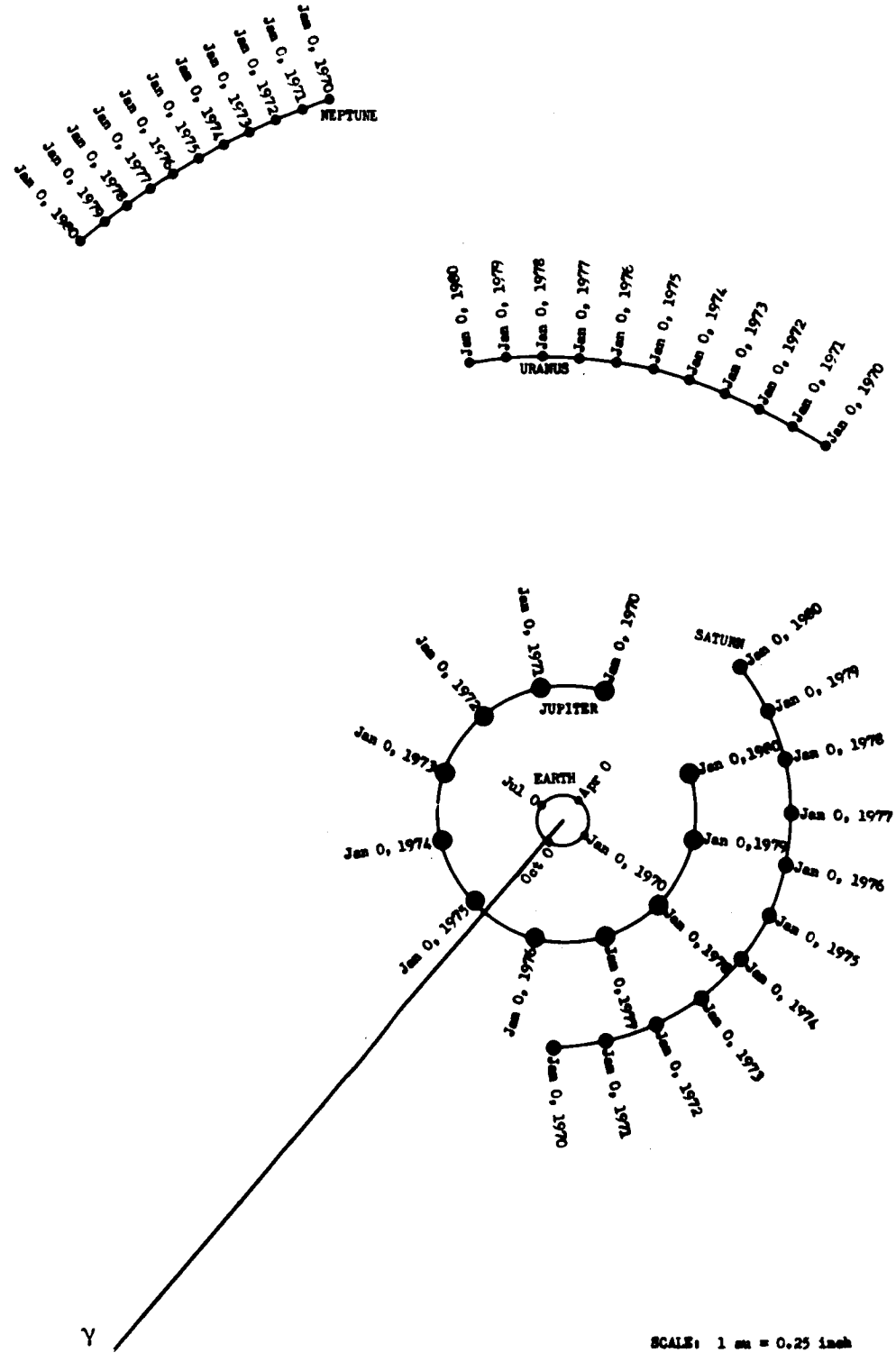

Figure 3.3-2. Partial Map of Solar System—1970 to 1980

Figures 3.3-3 and 3.3-4 graphically display sample trajectories A and B. Several elapsed times from earth launch are noted with tick marks for each trajectory. Sample trajectories C, D and E are now being plotted. Completed graphs will be transmitted as soon as possible.

3.3.3 Orientation Angles and Communication Distances versus Elapsed Time from Launch

Figures 3.3-5 through 3.3-10 compare the following heliocentric orientation angles and communications distances for several of the sample trajectories:

i) Sun-spacecraft-earth angle

ii) Earth-spacecraft-target planet angle

iii) Spacecraft-earth-sun angle

iv) Heliocentric longitude of projection of earth-spacecraft line on plane of ecliptic

v) Spacecraft-earth distance

vi) Spacecraft-target planet distance.

3.3.4 Spacecraft Attitude after Injection

The geometry of the injection process and particularly the orientation of the spacecraft are examined to evaluate these points:

- If the spin (antenna) axis is directed more than 90 degrees away from the sun, the spacecraft's passive thermal control system may be unable to maintain suitable temperatures. If this situation exists after injection and separation from the launch vehicle, it may be necessary to initiate an orientation maneuver promptly to relieve it. However, passage through the earth's shadow may delay the necessity for the maneuver.

- Because the high-gain antenna has a very narrow beam, and because the rotation of the spacecraft-earth line is initially very rapid, it is fruitless (for communications purposes) to adhere to the earth-pointing cruise attitude, until some time has elapsed. To delay the start of earth-pointing cruise attitude, however, does not prejudice the communication links, because low-gain antennas are adequate for these initially short communication distances.

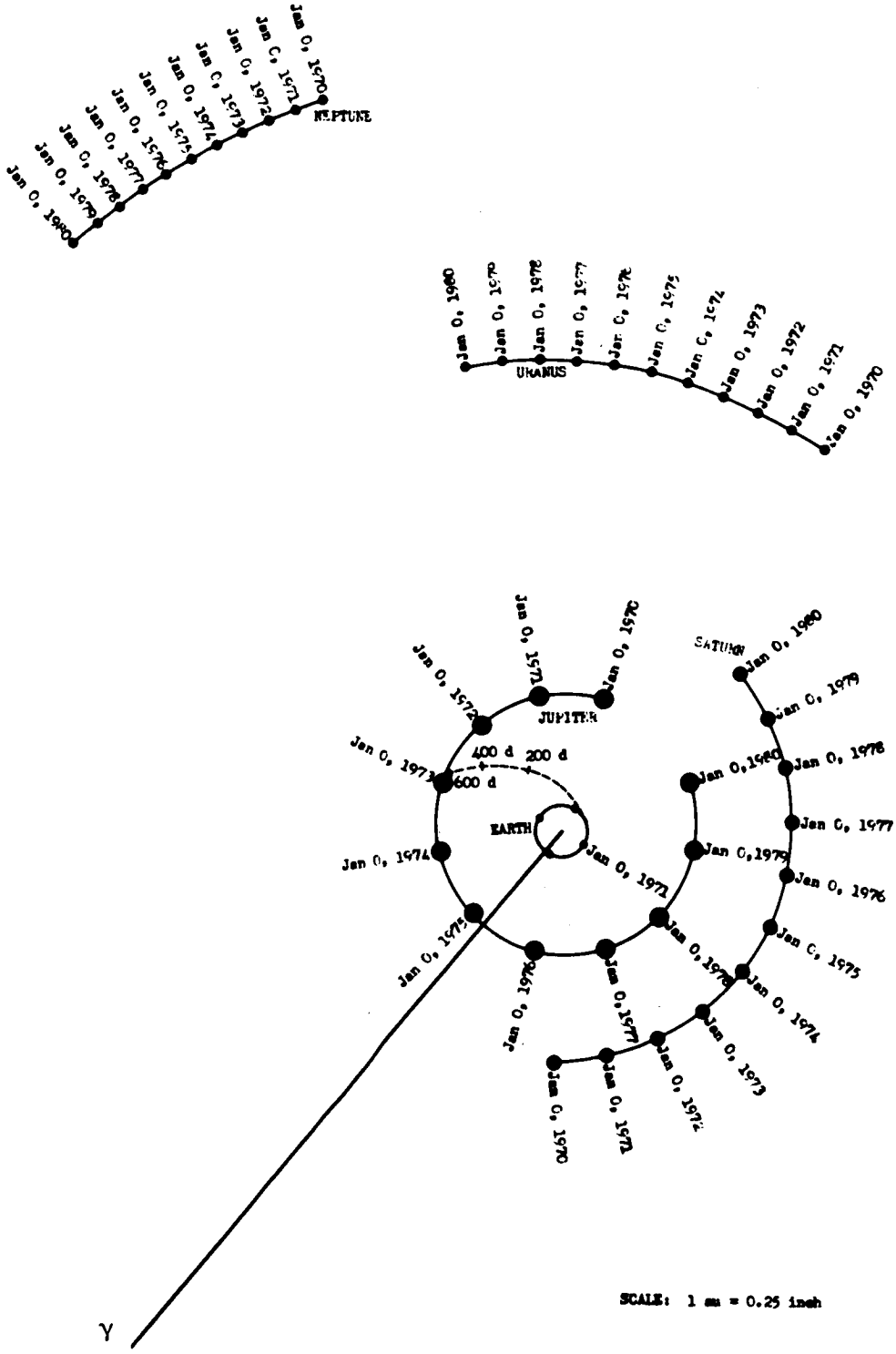

Figure 3.3-3. Display of Sample Trajectory A

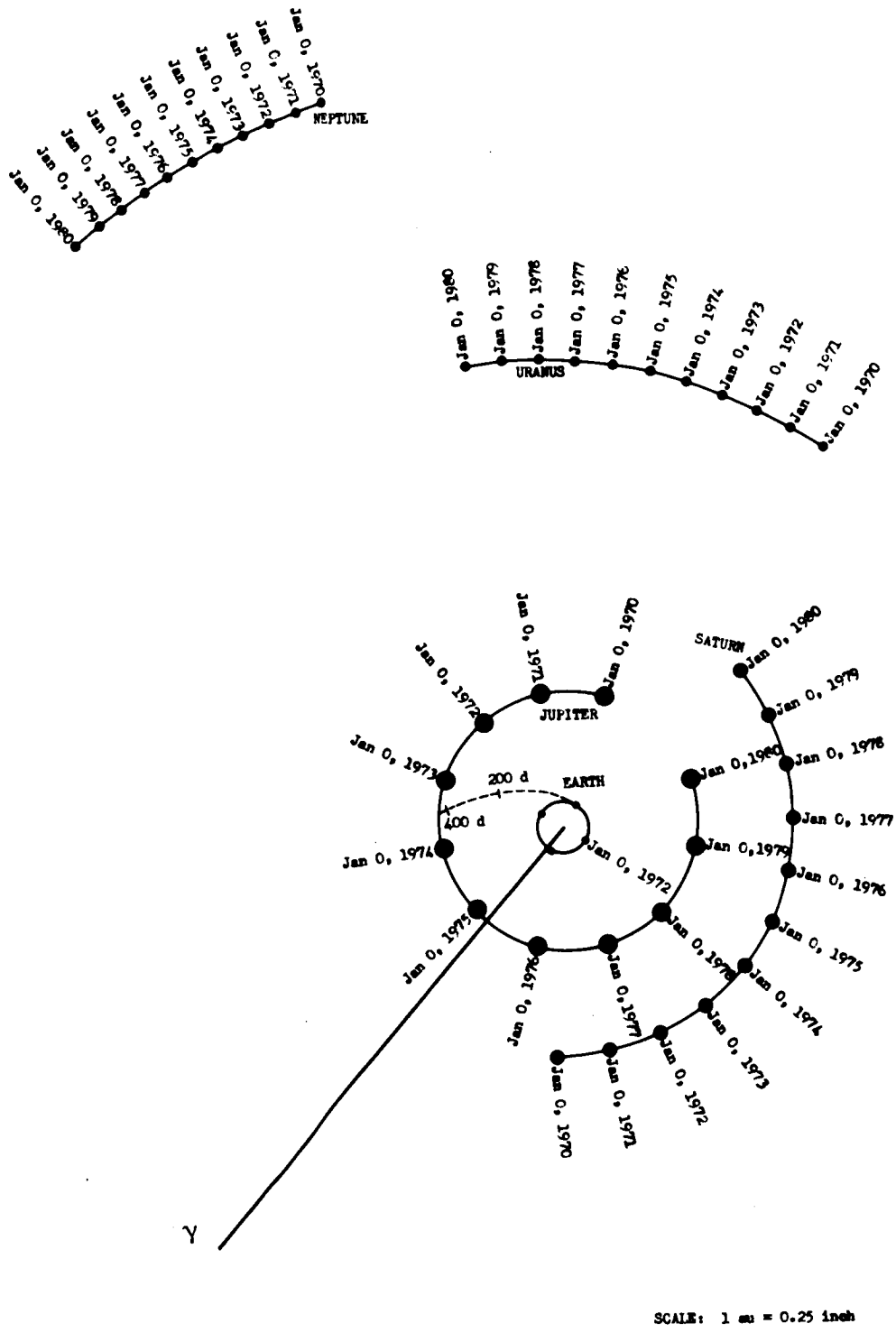

Figure 3.3-4. Display of Sample Trajectory B

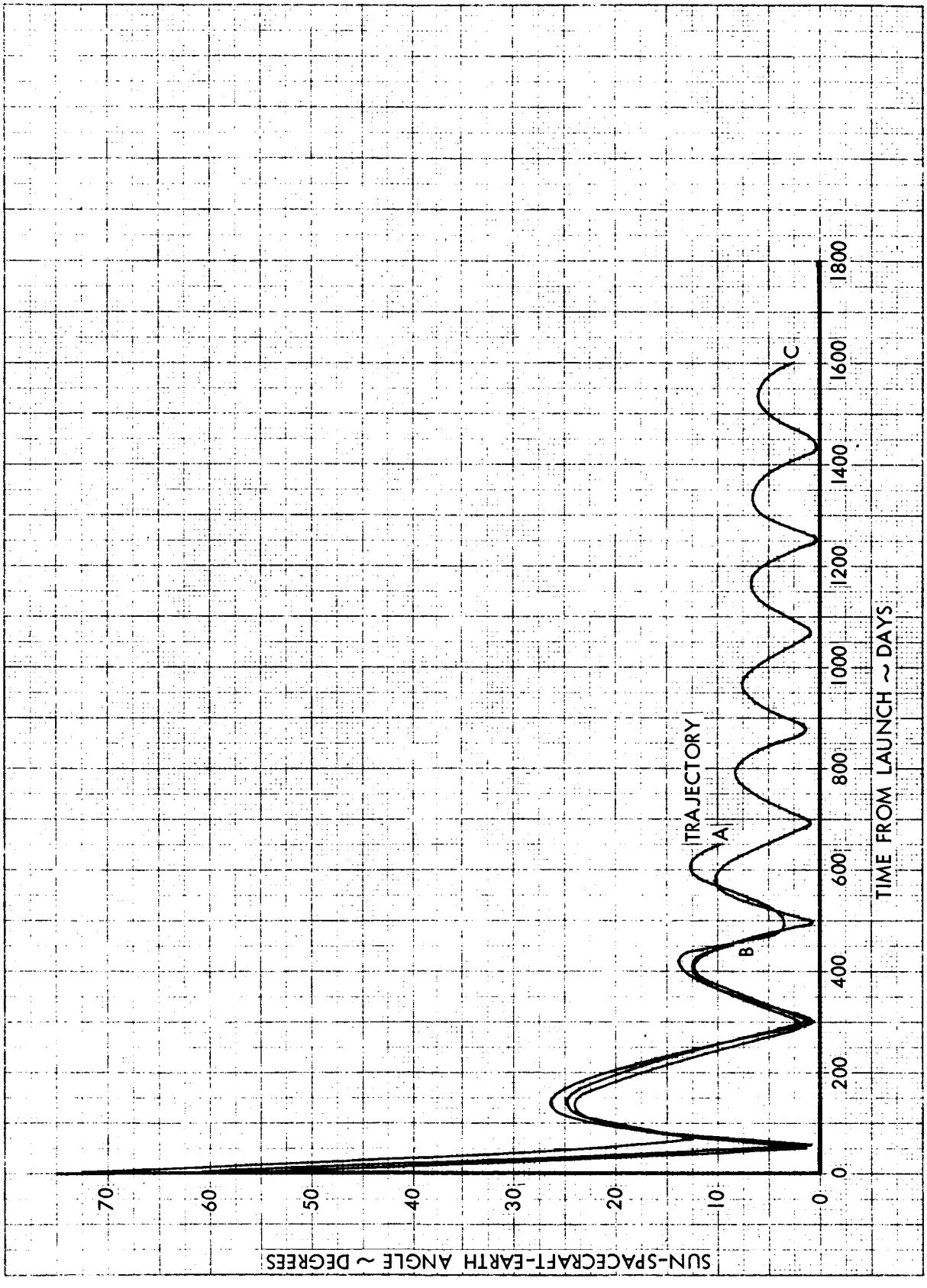

Figure 3.3-5. Sun-Spacecraft-Earth Angle Versus Time from Launch

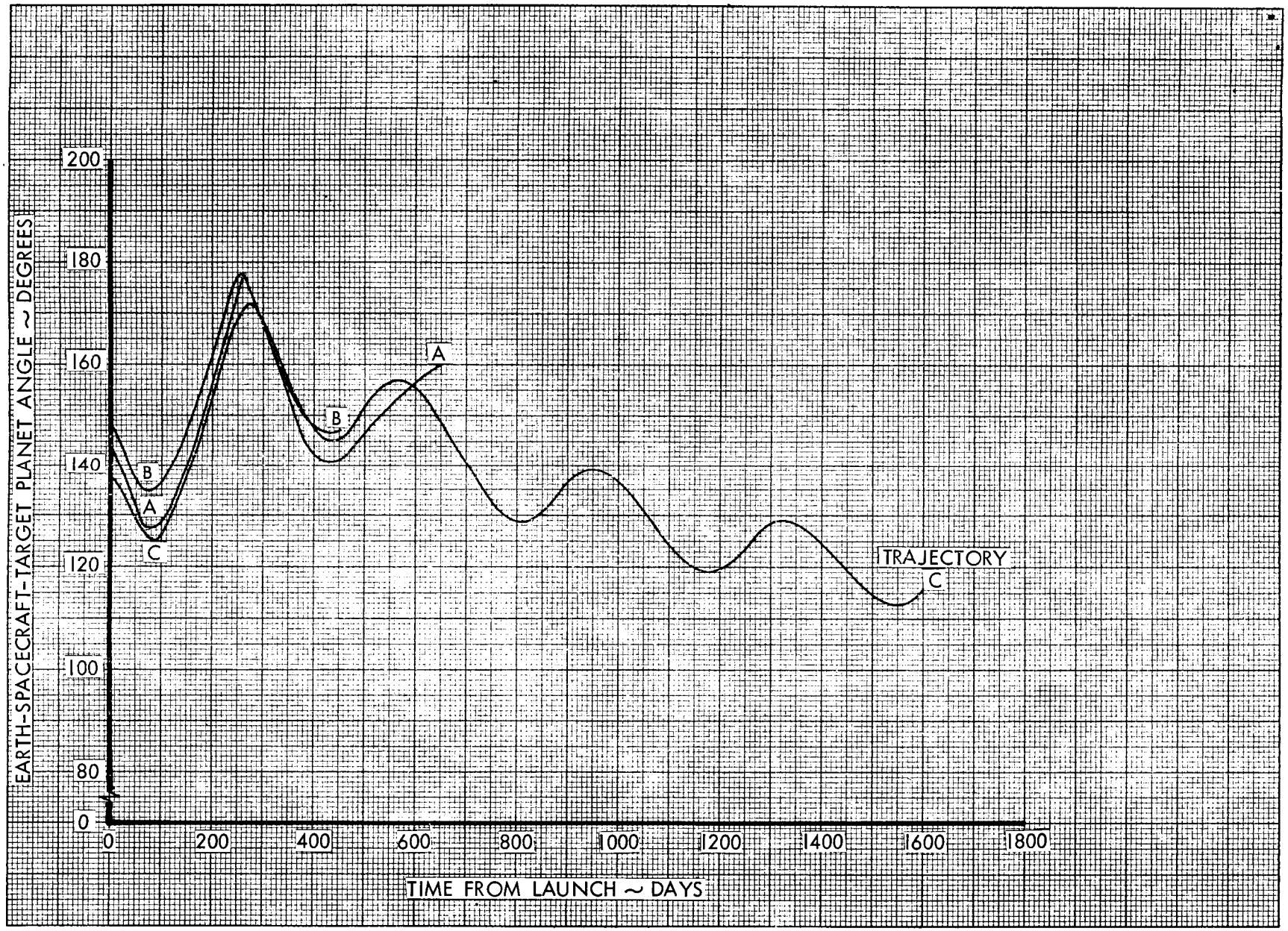

Figure 3.3-6. Earth-Spacecraft-Target Plane Angle Versus Time from Launch

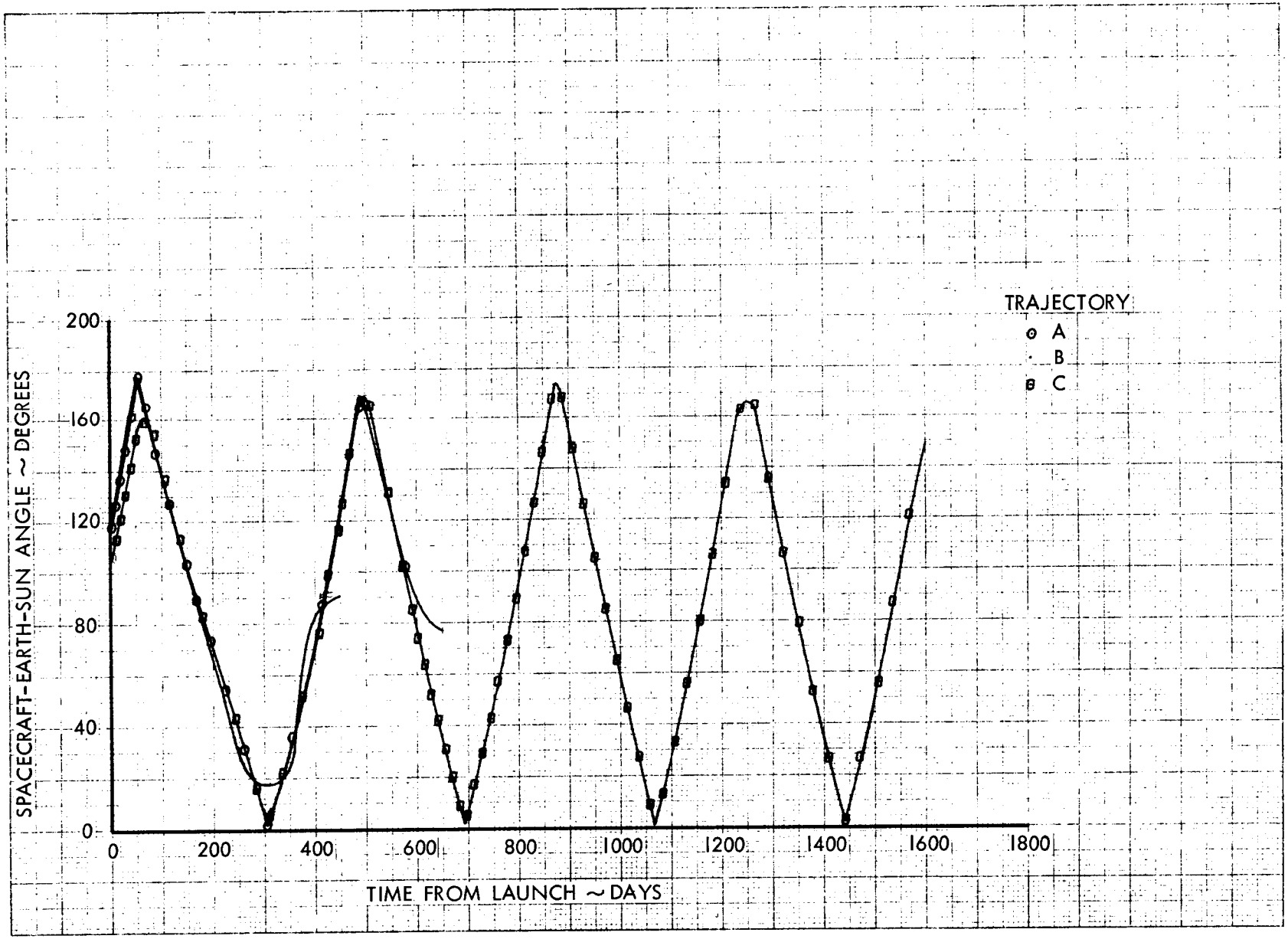

Figure 3.3-7. Spacecraft-Earth-Sun Angle Versus Time from Launch

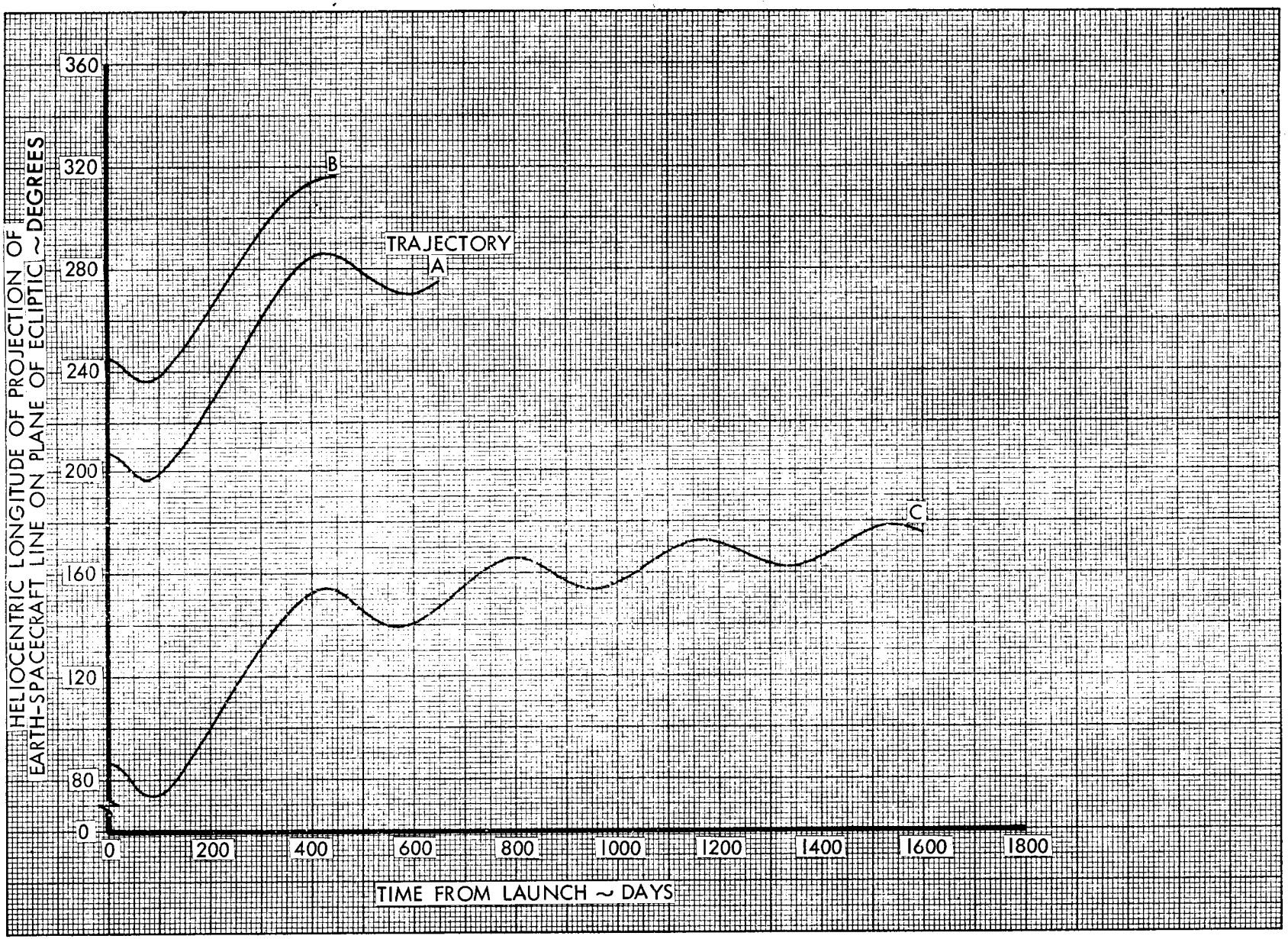

Figure 3.3-8. Heliocentric Longitude of Projection of Earth-Spacecraft Line on Plane of Ecliptic Versus Time from Launch

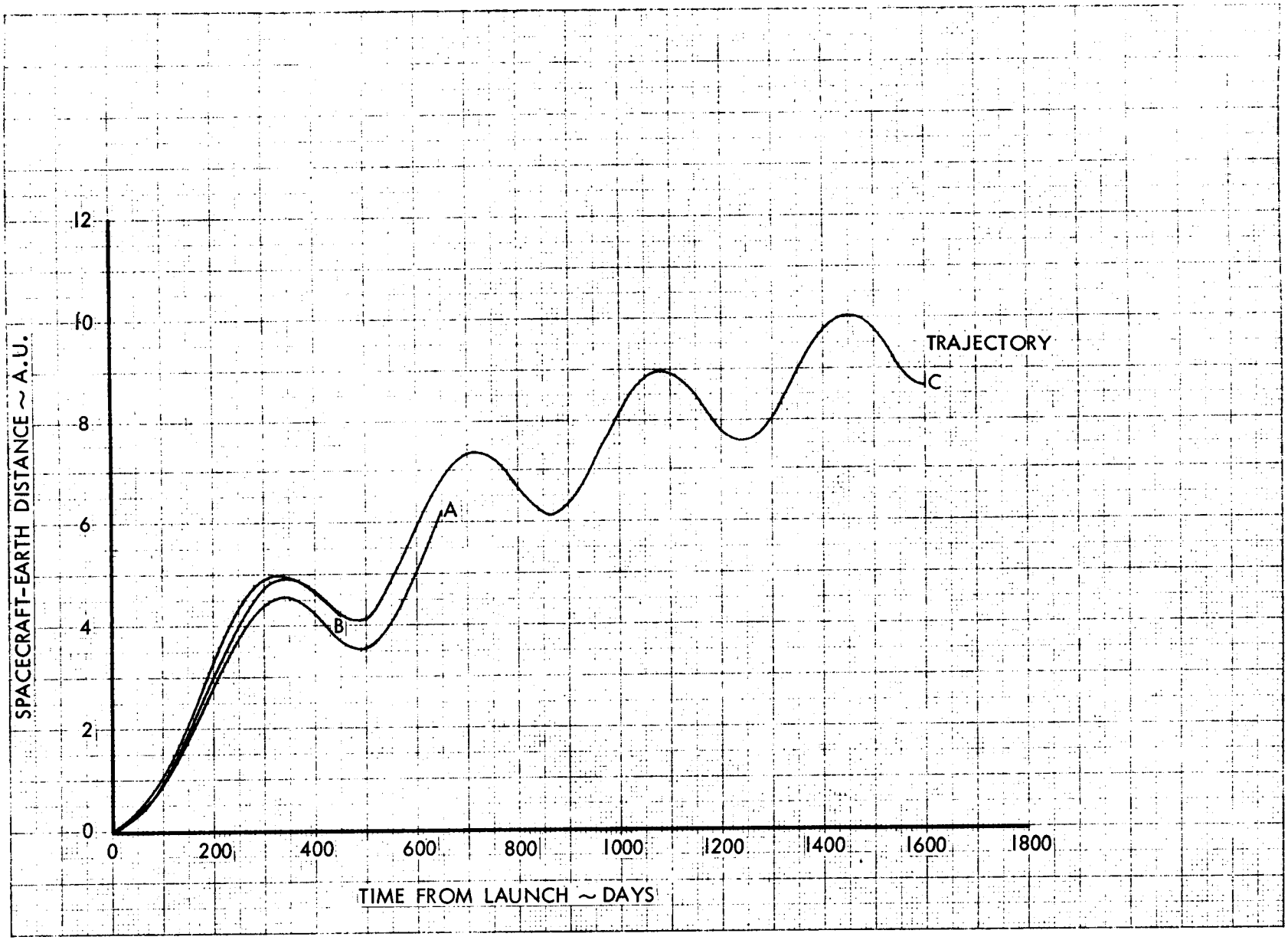

Figure 3.3-9. Spacecraft-Earth Distance Versus Time from Launch

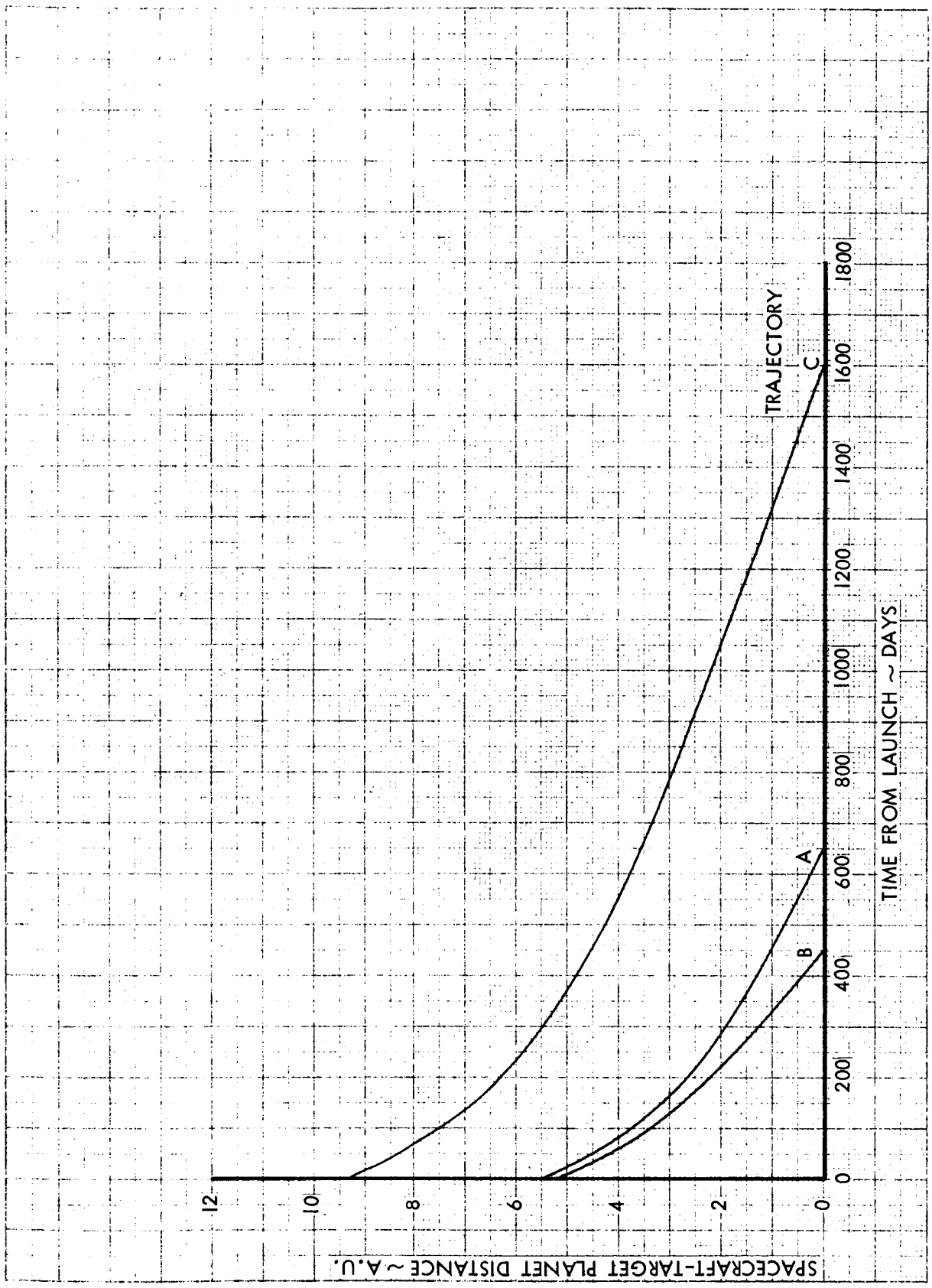

Figure 3.3-10. Spacecraft-Target Planet Distance Versus Time from Launch

Figure 3.3-11 illustrates the injection and near-earth geometry for typical trajectories to Jupiter or other outer planets. Two paths are shown—one corresponding to a minimum energy transfer, and one corresponding to a transfer which uses higher injection energy to reduce transit time. For simplicity the paths are shown in the plane of the ecliptic.

It is seen that the eastward launch carries the spacecraft ~~through~~ INTO the earth's shadow soon after or slightly before injection. The time spent in the shadow will be of the order of 30 to 50 minutes. It is also seen that in the injection attitude, the antenna axis is pointed more than 90 degrees from the sun. This angle is always less than 90 degrees after the earth-pointing cruise attitude is attained. (See also Figure 3.3-5.)

The following conclusions may be drawn:

- The injection attitude, with the antenna axis more than 90 degrees away from the sun, may jeopardize spacecraft thermal control
- Because the spacecraft enters the earth's shadow within minutes of injection, initiation of an orientation away from the injection attitude may be delayed 30 to 50 minutes
- The earth-pointing cruise attitude for any point in the trajectory is satisfactory for thermal control. It is not necessary (for communication purposes) to adopt this attitude early.

It might, therefore, be reasonable to make the initial orientation from the injection attitude, not to the current earth-pointing attitude, but to the attitude which will be earth-pointing after several days. By then, the rotation rate of the spacecraft-earth line will have slowed down so that holding this attitude does not require such frequent adjustments, and the range will be great enough that the antenna beam will illuminate the entire earth.

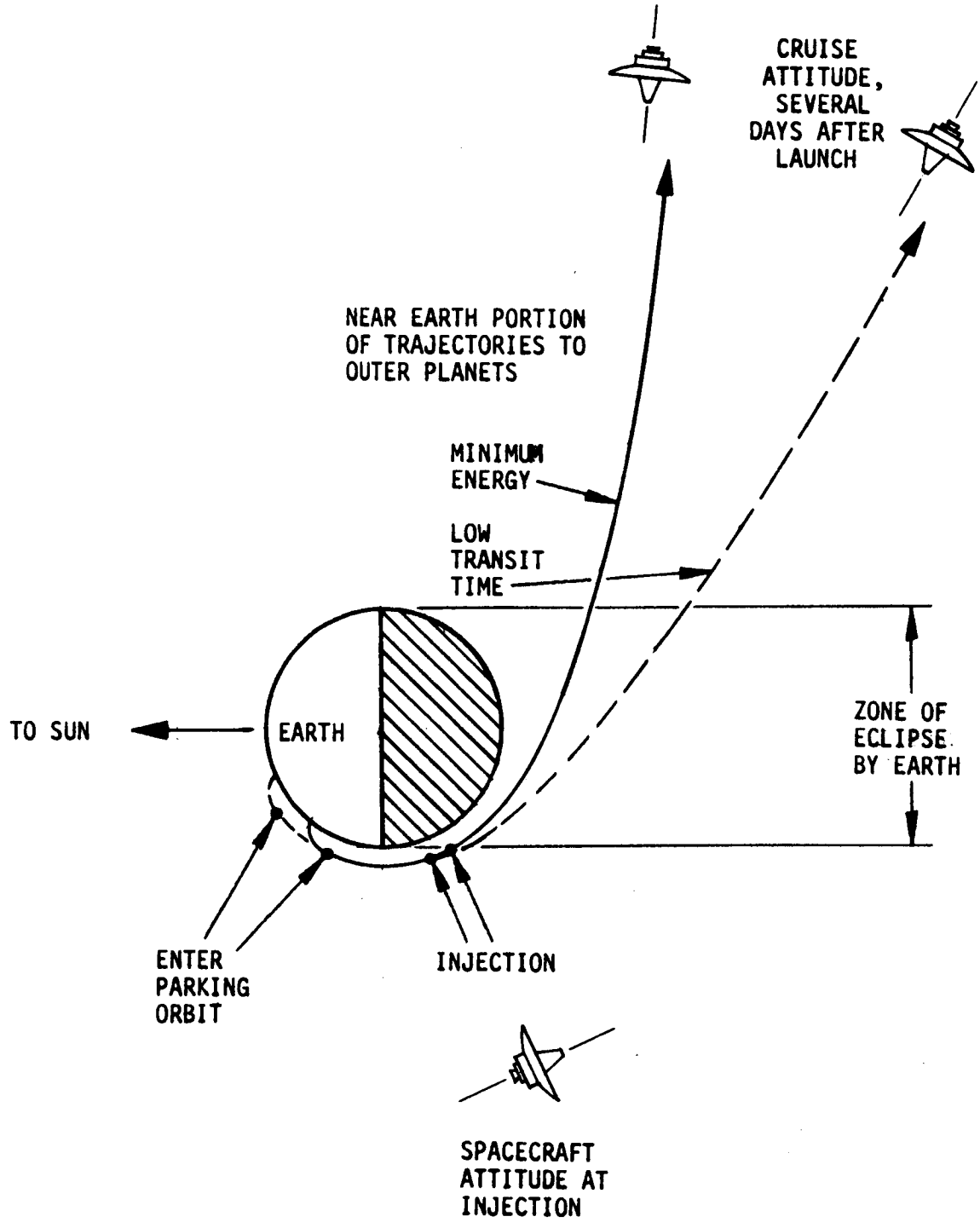

Figure 3.3-11. Injection Geometry

3.4 RADIO TRACKING

After injection, the spacecraft will be tracked by the tracking stations in the NASA/JPL Deep Space Network (DSN), with stations at Goldstone, California, Johannesburg, South Africa, and Woomera, Australia. The DSN stations transmit a highly stable signal to the spacecraft which multiplies the frequency of the signal by a constant and retransmits to earth. The doppler shift is then counted over evenly spaced intervals and divided by the interval to give an average doppler-frequency shift. All DSN stations have rubidium frequency standards that are stable to a few parts in 10^{12} over periods of one hour or more. Mariner 4 data have shown that the observed noise was 0.01 cps which is approximately equivalent to 0.6 mm/sec of error in range rate.

The sources of orbit prediction uncertainties will be tracking measurement errors and systematic errors such as uncertainty in station location and physical constants. The objective of the data reduction is to produce the best estimate of the orbit (in a least squares sense) from a set of imperfect observations. The observation errors are assumed to be gaussian with known variances. If the biases, the means of these gaussian distributions, are not known they may be estimated along with the orbit parameters. In effect, the estimate of the orbit must minimize a weighted sum of the squares of the residuals, the first differences between the measured observations and the observations computed from the estimated orbit. The differential correction to the original orbit is computed from first order partial derivatives about the reference trajectory. If the original estimate is poor, the partial derivatives employed by the linear model will not be accurate, and a new correction must be computed. The regression may be repeated for several iterations until the sum of squares converges to a stable value.

The results of an interplanetary orbit determination study are most easily viewed in the B · T, B · R coordinate system. The impact parameter, B, is defined as a vector originating at the center of the target and perpendicular to the incoming asymptote of the target

centered approach hyperbola. The impact parameter is resolved into two components which lie in a plane normal to the incoming asymptote. The unit vector T is parallel to the ecliptic plane and R = S x T where S is a unit vector in the direction of the approach asymptote. Thus, the impact parameter, B, lies in the R - T plane and has components B · T and B · R.

The estimated state vector at the tracking epoch will be transformed into a point in the impact parameter plane while the uncertainties in the estimated state vector will be transformed into an ellipse in the impact parameter plane. The expected value of the semi-major axis of the 1σ miss ellipse resulting from doppler tracking by the DSN net is shown below for various trajectories. These numbers have been scaled from Mariner 4 results. It was assumed that a midcourse maneuver was made 10 days after injection.

Target	Tracking Interval	1 Semi-Major Axis km
Jupiter	0^D - 10^D	3,000
Jupiter	10^D - 20^D	4,000
Jupiter	10^D - 100^D	900
Jupiter	10^D - 580^D	300
Saturn	0^D - 10^D	7,000
Saturn	10^D - 20^D	10,000
Saturn	10^D - 100^D	2,300
Saturn	10^D - 1530^D	300

3.5 MIDCOURSE CORRECTIONS - NORMAL PROGRAM

The usual procedure is to make the first midcourse trajectory correction from 5 to 20 days after launch. In the normal sequence the thrust may be applied in any fixed direction by properly orienting the spacecraft. For the actual trajectory onto which the spacecraft is injected, there is a unique direction and velocity magnitude which will null out errors in time of flight and in the impact parameter, i.e., B · T and B · R. If time of flight corrections are not of interest, impulsive fuel may be saved by making the firings in a fixed plane. This is called the critical plane.

The 5 to 20 day sensitivities are roughly independent of trajectory and of the destination planet. The JPL Mariner and Mars trajectories indicate sensitivities of 10,000 km/m/s at the first midcourse correction. This is more or less independent of time if it is made between 5 and 20 days. For example, an impact plane analysis for a Jupiter 760 day trajectory indicates a B · R sensitivity of 10,000 km/m/sec and a B · T of 2,000 km/m/sec. If in addition the flight time is to be corrected at the first midcourse, approximately 25% additional ΔV must be carried. However, it is probably unnecessary to correct the time of arrival to a specific or nominal day. It may be desired (for ground station visibility at encounter) to fix the time of day of arrival, but this will incur only a negligible increase in propellant required over that needed for critical-plane corrections.

The amount of fuel required depends on the magnitude of the velocity correction which must be made, and for early corrections, this is essentially equal to the injection error of the launch vehicle. Typical launch vehicle figures of merit are 10 to 15 meters per second (1σ), and 3σ to 5σ capability represents the typical propellant sizing.

Section 3.4 considers the uncertainty in knowledge of the spacecraft's position and velocity, projected to the target planet. In evaluating a program of midcourse trajectory corrections we are concerned with the uncertainty of control of the spacecraft's trajectory, projected to the target planet. For a single midcourse correction, the uncertainty in control of the trajectory has these contributing components:

- The execution error of the midcourse maneuver
- The uncertainty of orbit determination at the time of the maneuver
- The uncertainty in the knowledge of Jupiter's ephemeris

The first contribution depends on the mode of attaining attitude control. For a 3-axis stabilized spacecraft the 1σ execution errors are typically 0.1% of the magnitude of the velocity increment and 0.5 degrees in direction (about 2 axes). This assumes an accelerometer output is integrated to control the magnitude, and orientation is gyroscopically controlled from a cruise attitude established by optical celestial

sensors. The 1σ error is predominantly that due to the direction of ΔV, and is about 1%. If the 1σ injection error is 15 meters/sec, the error after midcourse execution is about 0.15 meters/sec, leading to 1,500 km, 1σ error in B, for a Jupiter flyby mission. For a spin-stabilized spacecraft, the orientation error for the maneuver could run to 1.5 degrees, 1σ if the orientation is open loop, or 0.5 degrees if it is closed loop (for example, if scanning star sensors are used to accurately ascertain the spin axis orientation before firing the engine). Because engine firing duration must be controlled by a timer rather than an accelerometer in a spinning spacecraft, the magnitude accuracy is no better than 1%. Thus the total error may be 1.5 to 3%, 1σ, leading to a velocity error of 0.2 to 0.4 meters/sec, and 2,000 to 4,000 km error in B. To account for the nongaussian distribution introduced by the fact that the execution errors are proportional to injection errors, we will raise these numbers to 2,000 km and 5,000 km, 1σ error in B, for fully-attitude stabilized and spin-stabilized spacecraft, respectively.

The second source of error, the uncertainty of orbit determination, is indicated in Section 3.4 to be about 3,000 km, 1σ. The third source, Jupiter position error, is probably less than either of the first two sources.

Thus we conclude that a normal program of a single midcourse trajectory correction can control the approach asymptote of a Jupiter flyby mission to about 4,000 km or 6,000 km, 1σ, for spacecraft with 3-axis- or spin-stabilization, respectively.

3.6 MIDCOURSE CORRECTIONS - SPECIAL PROGRAM

A special program of midcourse trajectory corrections which is primarily applicable to a spin-stabilized spacecraft employs thrusters oriented parallel to the spin axis. All midcourse maneuvers are performed without having the spacecraft directed from its normal cruise spinning attitude. For the Advanced Planetary Probe, this attitude is such that the positive spin axis (that is, the direction of the large antenna beam center line) is aimed at the earth. To accomplish trajectory correction roughly equivalent to that achieved by the normal

program of 3.5, the special program consists of midcourse engine operation at two separate times in the transit phase. Velocity increment along the earth-spacecraft line produces differing relative changes in $\overline{B} \cdot \overline{R}$ and $\overline{B} \cdot \overline{T}$ at the target approach according to the date it is performed, and this may be illustrated by a sensitivity "trace" drawn on the R-T plane. Thus a known trajectory error can be corrected by resolving the $\Delta\overline{B}$ vector into two components, one parallel to the R-T trace due to an earth-directed ΔV on one date, and the second parallel to that of the second date.

A choice may be made between having one midcourse engine only, directed along the (say) positive spin axis, or having two engines, one pointed in either direction. If the single engine is employed, a trajectory bias must be employed in the injection to insure that the velocity increments of the two propulsion maneuvers have the appropriate polarity.

The advantages of the special program over the normal program, for a spin stabilized spacecraft, are (1) the increase in reliability if no orientation maneuver is required, (2) the continuously maintained communications via the high-gain antenna (an advantage particularly if the earth-spacecraft range at midcourse is too great for low-gain antenna usage), and (3) the saving in attitude control gas expenditure.

The disadvantages are (1) the increase in total propellant required, (2) the duplicate engines required if no trajectory bias is used to insure firing in only the (say) positive direction, (3) the decrease in reliability with two firings rather than one, and (4) the constraint imposed on trajectory choices in order to insure adequate rotation of R-T traces as the transit phase proceeds.

These advantages and disadvantages should be evaluated, and the accuracy expected of the special program should be compared with that of the normal program.

3.7 PLANETARY SWINGBY TRAJECTORIES VIA JUPITER AND SATURN

The planetary swingby mode is receiving considerable attention as a technique for reducing launch energies and trip times for missions

to the outer planets. Flandro (Reference 3.7.1) has investigated the launch energies and trip times for missions to Saturn, Neptune, Uranus, and Pluto utilizing a Jupiter swingby mode. This section of the mid-term report compares these swingby missions with direct flights from earth to the outer planets.

3.7.1 Earth-Jupiter-Saturn Swingbys

In addition to direct, free-fall transfers, it is sometimes feasible to utilize an unpowered or powered swingby of an intermediate planet such as Jupiter in order to reduce launch energies and flight times to the outer planets. Figure 3.7-1 shows the vis viva launch energies (C_3) and transfer times required for direct earth-Saturn missions in late 1979. Type I transfers (heliocentric transfer angles less than 180 degrees) are not displayed because the associated values of C_3 are all greater than 180 km^2/sec^2. Figure 3.7-2 illustrates the launch energies and transfer times required for earth-Jupiter-Saturn swingby missions during the same launch period. A comparison of these two figures shows that for a given C_3 of 140 km^2/sec^2, for example, the swingby missions offer considerable savings in transit time. Niehoff (Reference 3.7.2) has found that favorable launch opportunities for these unpowered swingby missions occur in the period 1977-1981; they do not recur until 1997.

As may be seen from Figure 3.7-2, the unpowered earth-Jupiter-Saturn swingbys require transfer times on the order of 3 years for values of $C_3 < 140$ km^2/sec^2. These transfer times may be further reduced by utilizing a propulsive maneuver in the vicinity of Jupiter in order to reach Saturn in advance of the date predicated by the mechanics of an unpowered swingby.

3.7.2 Planetary Swingbys to Uranus and Neptune

Either a Saturn or Jupiter swingby mode may be utilized for missions to Uranus and Neptune. The next favorable launch periods for these swingbys have been tabulated by Niehoff as:

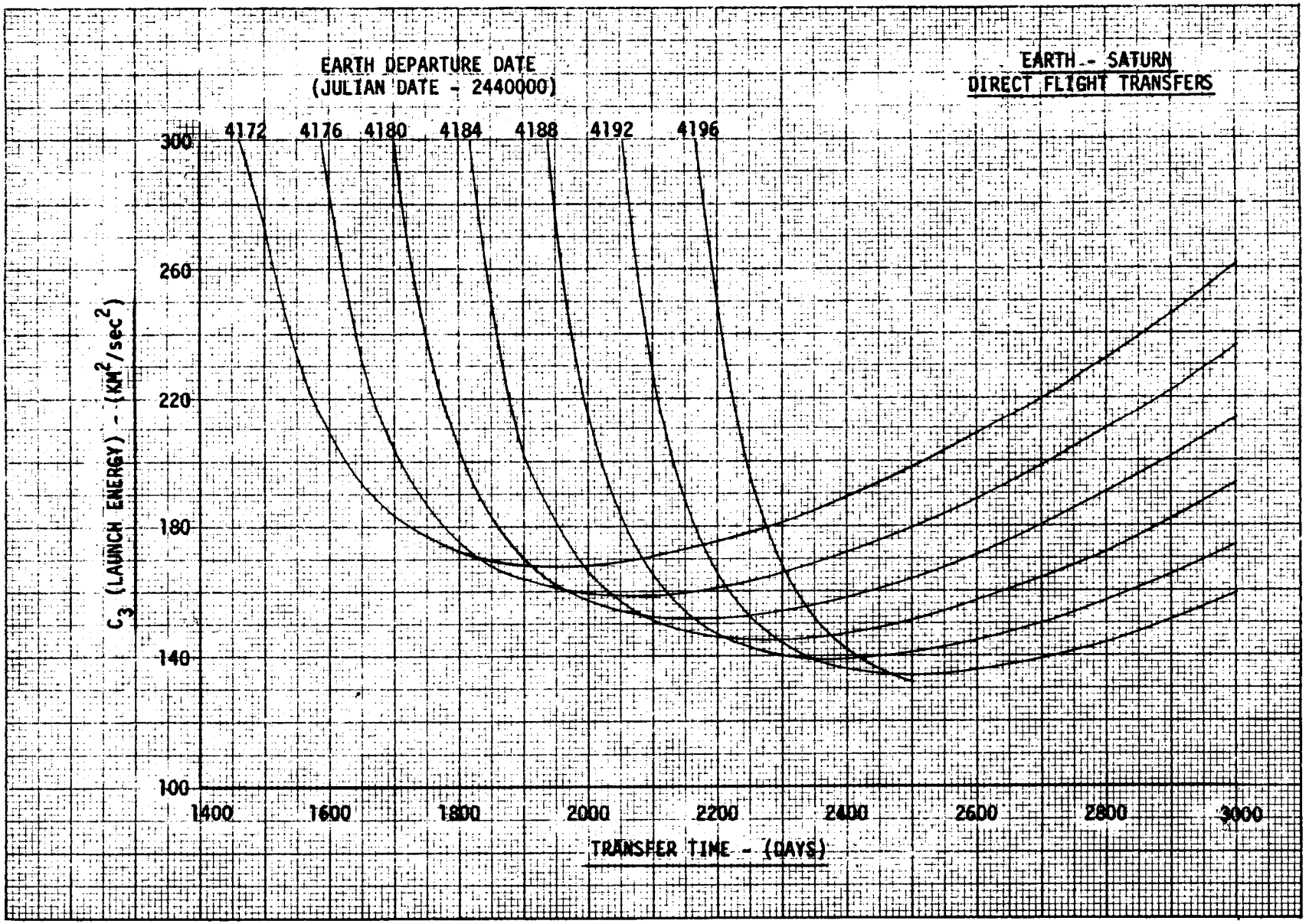

Figure 3.7-1. Earth-Saturn Direct Flight Transfers

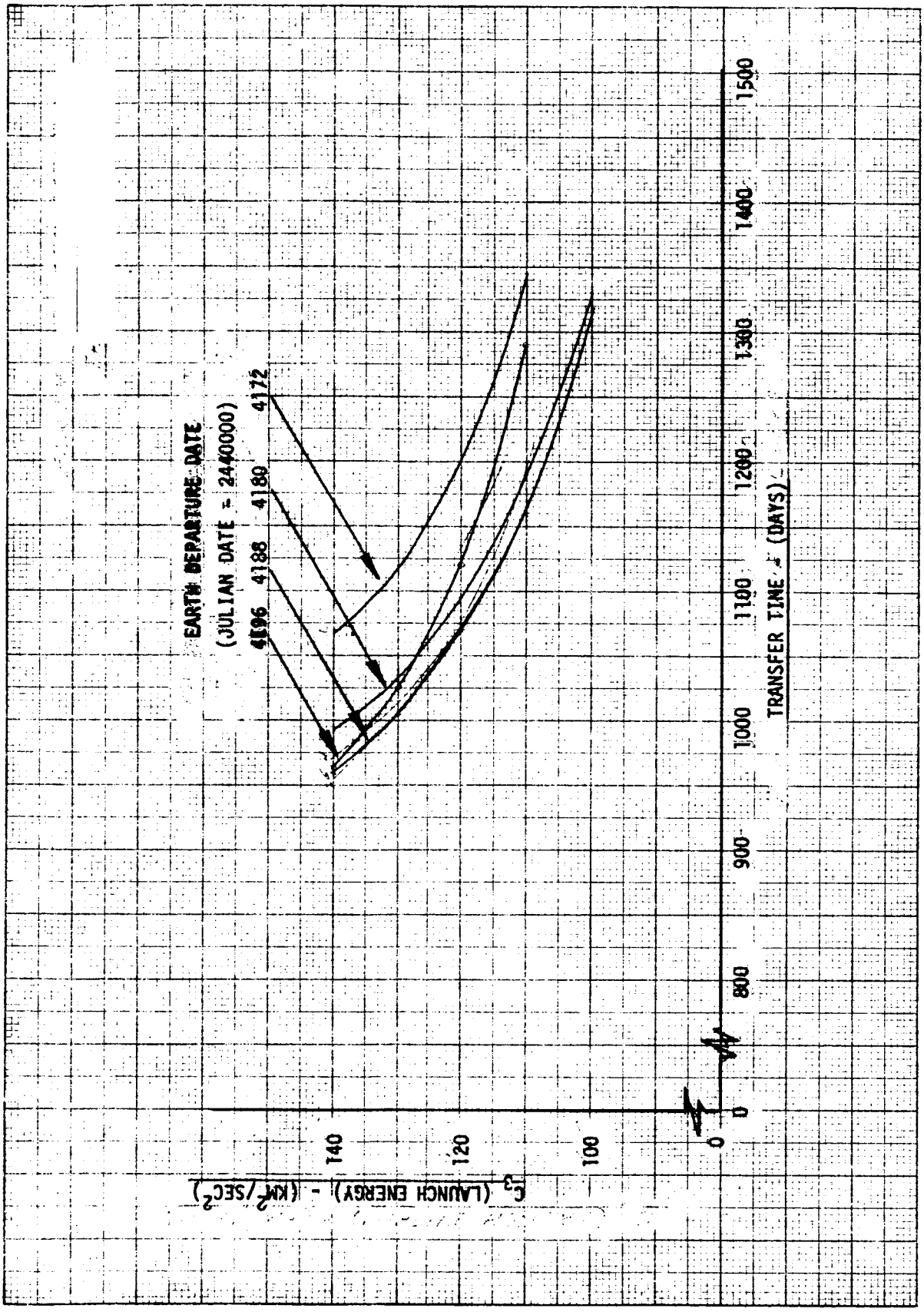

Figure 3.7-2. Earth-Jupiter-Saturn Transfers

Mission	Next Launch Period	Start of Following Period
Earth-Jupiter-Uranus	1978-1981	1992
Earth-Saturn-Uranus	1977-1985	2023
Earth-Jupiter-Neptune	1978-1980	1991
Earth-Saturn-Neptune	1979-1984	2015

As may be seen from this table, the utiliazation of Saturn as the intermediate planet considerably widens the next launch period of feasible transfers to Uranus and Neptune.

3.7.3 Additional Guidance and Propulsion Requirements Associated with Planetary Swingby Missions

The utilization of a planetary swingby mode requires the application of a third midcourse maneuver in addition to (a) the injection error correction maneuver and (b) the swingby planet approach maneuver. This third maneuver is initiated subsequent to planetary swingby encounter. This maneuver must correct the errors remaining from the second midcourse maneuver; errors which are magnified by the planetary swingby. The initiation time of the third maneuver is determined by a tradeoff between requirements for (1) the acquisition of sufficient orbit determination data and (2) propulsion requirements which, in general, increase as the maneuver time is delayed.

REFERENCES

3.7.1 G. A. Flandro, "Utilization of Energy Derived from the Gravitational Field of Jupiter for Reducing Flight Time to the Outer Solar System," JPL Space Programs Summary No. 37-35 Volume 4, Pages 12 through 23, dated 31 August 1965.

3.7.2 J. C. Niehoff, "An Analysis of Gravity Assisted Trajectories to Solar System Targets," AIAA Pre-print 66-10 dated 24-26 January 1966.

3.8 INTERPLANETARY METEOROID ENVIRONMENT

The most significant environmental hazard to the spacecraft in the interplanetary region is due to the presence of micrometeoroid particles. The extent of this hazard is uncertain, because the spatial distribution of meteoroids beyond Mars, both in and out of the plane of the ecliptic, are not well known. This section accumulates and summarizes the data and assumptions pertinent to this environment.

3.8.1 Near-Earth Flux

For the near-earth region (geocentric radius 6,500 - 260,000 km) and for $M > 10^{-5}$ gm, the meteoroid flux, in impacts/meter^{2}sec, due to particles of M grams or more, is N, where:

$$\log N = -1.34 \log M + 2.68 \log\left(\frac{0.44}{\rho}\right) - 14.18 \qquad (A)$$

This is from Reference 3.8.1, modified to remove effect of earth shielding. A meteoroid density of 0.44 gm/cm^3 will be used as a base. The mean velocity used is 22 km/sec. For 10^{-10} gm $< M < 10^{-6}$ gm:

$$\log N = -16.87 - 1.7 \log M \qquad (B)$$

This equation is from Reference 3.8.2, and represents the earth satellite results. The equation was modified to the form above to remove the earth shielding effects based on a shielding factor of 0.74. This is the factor for an average orbit altitude of 2500 miles, the average for the satellites involved.

3.8.2 At 1 AU (away from earth)

The flux at 1 AU is reduced from the near-earth levels because of the dust belt around the earth. Beard, Reference 3.8.3, gives a reduction of 10^4 in dust particles. Mariner 4 data, Reference 3.8.4, gives a reduction by 10^4 to 10^5 in the mass range 4×10^{-11} to 6×10^{-10} grams from the levels measured by earth satellites, equation B, above. Both the Mariner data and Beard's conclusion fall below the flux proposed by van de Hulst, recommended in Reference 3.8.1 as applicable to "deep space" (5×10^4 to 2×10^5 km) for the small particles.

Whipple, Reference 3.8.1, sees no basis for there being a great terrestrial concentration of the larger particles ($M > 10^{-5}$ gms).

Consequently, the interplanetary flux at 1 AU will be assumed given by using equation A for the larger particles, and van de Hulst's equation, below, for the smaller particles.

$$\log N = -0.65 \log M - 10.44 \qquad (C)$$

Fluxes representing equations A, B, and C and the Mariner data are shown in Figure 3.8-1.

3.8.3 From 1 AU to 2 AU

Whipple, Reference 3.8.1 believes the variation in the meteoroid flux will be at least an inverse law of the solar distance.

Beard, Reference 3.8.3, based on scattered light observations, concludes that for small dust particles the distribution varies inversely with the solar distance to the ν power, where ν is possibly less than but probably equal to 1.5 for small elongations. For large elongations, the observations of zodiacal light favor $\nu = 1.5$.

The Mariner 4 data, for mass range from 4×10^{-11} to 5×10^{-10} gm, is in disagreement with both the above conclusions. The preliminary data from Mariner, Reference 3.8.4, shows an increase in flux by 4 to 6 times going from 1.0 - 1.2 AU to 1.4 to 1.47 AU, Figure 3.8-1. In Reference 3.8.5, the meteoroid flux model used for the Voyager studies given by JPL, the factor covering the increase in flux extended to solar distances to 1.56 AU. At this distance, the flux is 2.5 that at 1 AU. The flux used in the study will comply with the Mariner data. JPL will be contacted for extensions, if any, on the Mariner data.

Reference 3.8.6, page 283, credits Whipple with the estimate that the incidence of larger particles (>0.1 gm) will remain equal to that observed at earth for decreasing solar distance at least to the orbit of Venus, and should increase as the asteroid belt is approached to a value perhaps 10 times greater at the orbit of Mars (1.53 $\pm$0.12 AU).

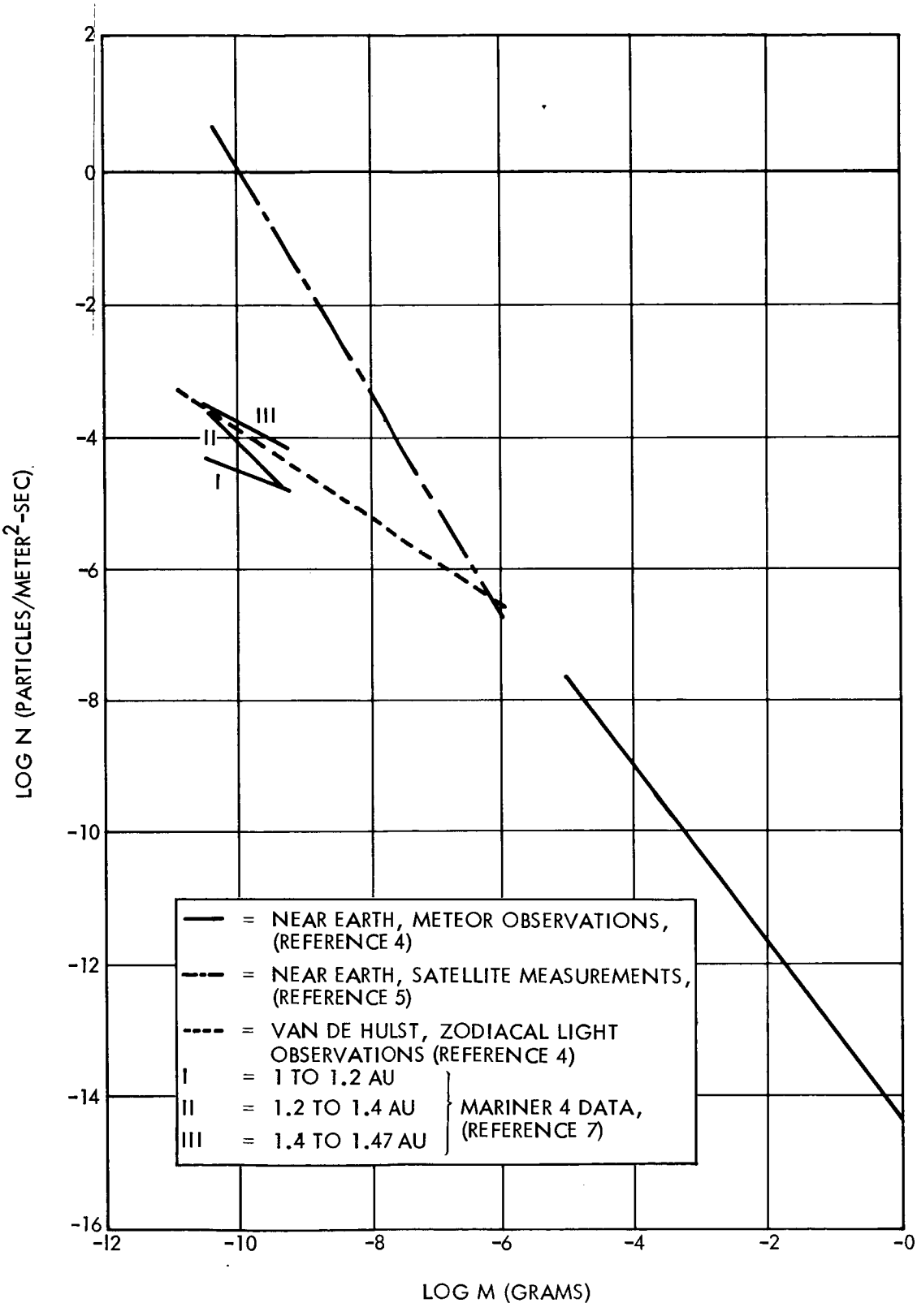

Figure 3.8-1. Micrometeoroid Fluxes

3.8.4 Asteroid Region (Approximately 2 - 4 AU)

It is expected, by interaction only, that the meteoroid hazard will be increased in this region.

Notes on the Asteroid Region (References 3.8.7 and 3.8.8.). The asteroid region covers solar distances from 2 to 4 AU with a mean at 2.8 AU. Approximately 40 percent of the asteroids have orbits within 15 degrees inclination to the ecliptic with a mean inclination of 10 degrees. The orbit eccentricities vary from 0 to 0.25 with an average of 0.15. There is a definite tendency for small asteroids to occur farther from the sun. There are conspicuous gaps in the asteroid distribution. Of the 1500 major asteroid bodies found, none move around the sun in retrograde motion.

It is of interest to note there is a concentration of meteors with aphelion distances in the 3 to 5 AU range and with inclinations mainly below 20 degrees but with many inclinations between 20 and 40 degrees.

Of space debris (dust and meteoroids), 90 percent is credited to cometary ejection and disintegration while grinding and fragmentation of asteroids accounts for between 2 to 10 percent of the total. Reference 3.8.7 increases the density of meteoroids in the region to a value of 0.75 gm/cm^3 from the normal mean density of 0.443 gm/cm^3.

The only estimate found for the flux in the asteroid region is in Reference 3.8.7, which assumes the particle concentration is 20 or 30 times that of interplanetary space but for the model of that reference a conservatively assumed 100 times is used. It is probable that the out-of-ecliptic distribution of dust and micrometeoroids is much less dispersed than the corresponding distribution of meteors and minor planets. Observations have placed the thickness of this belt of small particles at about $\pm$0.1 AU from the ecliptic.

In order that the spacecraft withstand the micrometeoroid environment it is pertinent to consider not only the use of structural protection against impact and penetration, but also the adoption of trajectory constraints to insure that the spacecraft avoids passage through the denser regions of the asteroid belt. An out-of-ecliptic displacement of 0.1 to 0.2 AU while 2 to 4 AU from the sun would not represent a severe trajectory constraint.

REFERENCES

3.8.1 F. L. Whipple, "On Meteoroids and Penetration," Journal of Geophysical Research, Vol. 68, No. 17, 1 September 1963.

3.8.2 M. Dubin, and C. W. McCracken, NASA RP-103, "Measurements of Distributions of Interplanetary Dust," (Reprint of Astronautical Journal, Vol. 67, No. 5, pgs. 248-256, June 1962).

3.8.3 D. R. Beard, "Interplanetary Dust Distribution," Astrophysical Journal, Vol. 129, No. 2, pgs. 496-505, March 1959.

3.8.4 W. G. Fawcett, et al, "Scientific Exploration with Mariner 4," Astronautics and Aeronautics, pgs. 23 and 28, October 1965.

3.8.5 TRW Systems Memo VV-331, "Interpretation of Meteoroid Data for Voyager," by W. J. Dixon, dated 30 November 1965.

3.8.6 E. Manring, "Interplanetary Matter," in Advances in Space Science and Technology," edited by F. I. Ordway, Vol. 3, pg. 276.

3.8.7 J. J. Volkoff, "JPL - TR - 32 - 410."

3.8.8 R. L. Newburn, "The Exploration of Mercury, the Asteroids--," in Advances in Space Science and Technology, edited by F. I. Ordway, Vol. 3, pg. 216.

3.8.9 J. J. Volkoff, "System Protection Requirements for the Resistance of Meteoroid Penetration Damage," Journal of Spacecraft, Vol. 3, No. 1, January 1966.

3.9 ENVIRONMENT OF JUPITER

For the spacecraft to operate in the near-Jupiter region, we must be concerned with the nature of this environment. Of course, the purpose of the probe is to measure this environment; the present knowledge of it has uncertainties of several orders of magnitude.

3.9.1 Micrometeoroids

Whether Jupiter has a cloud of dust particles which increases the near-Jupiter micrometeoroid flux several decades above the interplanetary flux, as in the case of the earth, is not known. If we accept the premise that the intensification of the interplanetary micrometeoroid flux near the earth is primarily due to secondary particles ejected from the moon, it might be reasonable to assume that a similar phenomenon exists at Jupiter. However, the degree of intensification would be less than that at earth, because the ratio of satellite cross section area to the volume of the affected space is much less. Since the interplanetary micrometeoroid flux at Jupiter's distance from the sun is less than that at 1 AU, the net flux in the near-Jupiter environment should be substantially less than that near the earth.

3.9.2 Radiation Belts

It would appear from the decimeter radio noise that the Jovian radiation belt may contain as much as 10^3 times as many high energy electrons (10 Mev) as the terrestrial radiation belts; the flux of lower energy electrons is uncertain. If we take a flux of 10^6 electrons/cm^2 sec and assume no bremsstrahlung loss or shielding, the radiation intensity delivered/cm^2 would be about 3×10^{-5} roentgens/sec. It would not appear that this dose represents a serious radiation damage problem to a vehicle in transit through the belt, unless either the flux at lower energies is very intense or a significant high energy proton flux is present. The latter, of course, is quite easily shielded out. Damage to solid state circuitry would be expected at integrated exposures of $\sim 10^5$ R.

4. SCIENTIFIC OBJECTIVES AND INSTRUMENTS

4.1 CLASSES OF OBSERVATIONS

In accordance with the Statement of Work, the scientific experiments to be performed are divided into the three categories:

1) Measurement of interplanetary particles and fields
   Measurement of planetary particles and fields

2) Measurement of the salient features of planetary atmospheres

3) Observations of the planets.

In the present discussion, the desired planetary observations will be limited primarily to Jupiter and will be expanded to the outer planets later.

4.2 PARTICLES AND FIELDS

4.2.1 Interplanetary Particles and Fields

The measurements are intended to give information about the plasma-magnetic field configuration in the interplanetary medium, the temporal variations in this configuration and their correlation with solar phenomena. An additional objective is the determination of the spatial distribution of dust throughout the interplanetary medium with, for the specific missions under consideration, particular emphasis on the asteroid belt and planetary vicinity.

Local measurements of the plasma-magnetic field configuration can be obtained directly with plasma probes and magnetometers. The present knowledge of the interplanetary configuration beyond the orbit of Mars has been derived from a study of Comet Humason;[1] here the tail deflection indicates that at anti solar distances as large as 5 AU the flow properties of the solar wind are not significantly modified from those determined in

[1] W. Bernstein, "The Solar Plasma - Its Detection, Measurement and Significance," Space Physics, editors D. P. LeGalley and A. Rosen, John Wiley and Sons, Inc., New York, 1964.

the near earth environment. Extrapolation of near earth data would indicate a flux of ~2 x 10^6 particles/cm^2 sec and a magnetic field of ~1 gamma at Jupiter distances from the sun (flux α d^{-2} and B α d^{-1}) provided significant changes, many of which have been theoretically predicted,[2,3] do not occur.

Significant information about the non-local plasma-magnetic field configuration can be derived from measurements of solar cosmic rays, emitted in association with solar flares, and of galactic cosmic rays, since the trajectories of these particles are determined primarily by the magnetic field configuration. Lastly, radio propagation measurements provide an estimate of the integrated electron density between the spacecraft and earth. Although these last measurements have, in the past, yielded high values for the average electron density in the interplanetary medium, this is a particularly valuable technique for the study of temporal variations in the electron density.

It is therefore suggested, that desirable interplanetary measurements include (1) solar plasma directed velocity distribution, estimates of the thermal velocity distribution, and flux; (2) continuous vector measurements of the interplanetary magnetic field; (3) intensity and energy of the solar cosmic ray flux; (4) intensity of the galactic cosmic ray flux; and (5) flux, momentum and possibly energy of dust particles.

4.2.2 Planetary Particle and Field Measurements

The intensity of radio noise[4,5] received from Jupiter in the 10 cm and 10-meter wavelength regions is far greater than that associated with temperatures of 130°K derived from infrared and microwave measurements. The 10 cm radiation, the intensity of which has a fair correlation with solar activity, has been attributed to synchrotron radiation of energetic electrons in the Jovian magnetic field. The 10-meter radiation

---

[2] J. C. Brandt, Icarus, 1, 1 (1962).

[3] K. McCracken, Journal of Geophysical Research, 67, 423 (1962).

[4] M. S. Roberts and G. R. Huguenin, "Physics of Planets," Proceedings of the Eleventh International Astrophysical Symposium, Liege, Belgium, July 9-12, 1962.

[5] J. W. Warwick, "Radio Emission from Jupiter," Annual Review of Astronomy and Astrophysics, editors L. Goldberg, A. J. Deutch and D. Layzer, Annual Reviews, Inc., Palo Alto, California, 1964.

has been attributed to cyclotron radiation produced by energetic electrons penetrating to regions of relatively strong magnetic field. These measurements suggest the presence of a large Jovian magnetic field, the existence of trapped particle radiation belts and perhaps even of auroral phenomena. Measurements of the magnetic field configuration of Jupiter, the characteristics of the Jovian radiation belts, and the possible presence of auroral activity can contribute greatly to our, as yet, relatively poor knowledge of radiation belt physics by providing an opportunity to study these phenomena under a set of conditions significantly different from that of the earth. It may be noted that attempts to observe Jovian auroral phenomena terrestrially are under study.[6]

Some estimates of the Jovian magnetic field and particle densities in the radiation belts are:[4]

1) A surface magnetic field of ~50 gauss; the magnetic axis is probably tilted about 10 degrees from the rotation axis

2) Electron energies of ~10 Mev and fluxes of 10^5 - $10^6/cm^2$ sec

3) Dimensions roughly a torus with the major radius $3R_J$ and a minor radius of 0.1 - 0.5 R_J.

With a surface magnetic field of ~50 gauss, assumed to be dipolar, the solar wind-magnetosphere interaction could be expected to occur at ~100 R_J. Interplanetary plasma probe and magnetometer instrumentation should be adequate for the investigation of this region.

It is therefore suggested that instrumentation suitable for the vector determination of the planetary magnetic field and for the determination of the flux and qualitative energy distribution of both protons and electrons be available. Lastly, the identification of auroral activity would be of great interest.

---

[6] J. V. Jelley and A. D. Petford, "Physics of Planets," Proceedings of the Eleventh International Astrophysical Symposium, Liege, Belgium, July 9-12, 1962.

4.3 ATMOSPHERIC MEASUREMENTS

Consistent with Öpik,[7] this discussion of the Jovian atmosphere is restricted to the region above the cloud layer since the existence of a Jovian "surface" has not been established. The primary areas of interest in this region include the atmospheric scale height and the atomic and molecular abundances. Current estimates of the scale height have been derived from a single observation of the fading of the light from σ Arietis during an occultation by Jupiter. This observation indicated an approximate scale height of 8 km; with an assumed atmospheric temperature of ~130°K, this yields a mean molecular weight of ~4 for the Jovian atmosphere. Based on this result and spectroscopic observations of NH_3, CH_4, and H_2 in the Jovian atmosphere, Öpik[7] suggests the following composition of the Jovian atmosphere:

Molecule	He	H_2	Ne	CH_4	A	NH_3
%	97.2	2.3	0.39	0.063	0.042	0.0029

Such a model atmosphere requires that hydrogen has escaped from the planet despite the fact that the large gravitational field inhibits escape since the "cosmic abundance" of hydrogen is significantly greater than helium. Theoretical arguments which permit the escape of hydrogen have been advanced by both Urey[8] and Öpik.

The isotopic abundances of the noble gases and the deuterium/hydrogen ratio are of great interest at Jupiter,[9] since our current knowledge of these abundances are at present limited to terrestrial observations. The latter appears to be characteristic of only earth because of the almost complete escape of primitive material and the influence of nuclear transmutation during the formative period of the solar system. Jupiter is expected to be far more representative of the primitive material because of the inhibition of escape by the large gravitational field and its

---

[7] E. J. Öpik, Icarus 1, 200 (1962).

[8] H. C. Urey, "Some Cosmochemical Problems," Thirty-Seventh Annual Priestly Lectures, Pennsylvania State University, View Park, Pennsylvania, 1963.

[9] W. A. Fowler, J. L. Greenstein, and F. Hoyle, Geophysical Journal of the Royal Astronomical Society, 6, 2, 148 (1962).

remoteness from the sun which reduced the flux of bombarding particles. The determination of these isotopic ratios requires a mass analysis of the atmosphere with instrumentation of very high mass resolution.

It is believed that a simple determination of the H/He ratio would represent an important contribution to the knowledge of the structure and evolution of Jupiter. It does not appear feasible to attempt such a measurement employing either resonant scattering of solar radiation or direct particle analysis. However, if auroras do occur on Jupiter, and the current interpretation of the 10-meter radio noise is assigned to auroral activity, then emission spectrography in the visible region may yield estimates of the H/He ratio. In the case of terrestrial auroras, the bulk of the light intensity is produced by excitation of O_2 and N_2 by precipitating particles; the H_α and H_β light arise from charge exchange reactions of precipitating protons with the ambient atmosphere and He_I light is not observed.[10] In the Jovian case where H_2 and He are the abundant atmospheric gases, excitation of the H_α, H_β and He_I by precipitating particles should be the dominant source of light.

Estimates of the atmospheric and ionospheric scale heights above the clouds can be derived from radio occultation measurements similar to those employed in the Mariner-Mars experiment.[11] In addition, observation of the attenuation of the sun at the limb during solar occultation can yield scale height information similar to that obtained from the stellar occultation observation.

4.4 PLANETARY OBSERVATIONS

Terrestrial infrared and microwave temperature measurements indicate a temperature of $\sim 130^{\circ}K$. However, terrestrial infrared measurements are limited to the region 8-14 μ and are probably characteristic of the cloud layer rather than the surface because of the strong absorption

---

[10] J. W. Chamberlain, "Physics of the Aurora and Airglow," Academic Press, New York, 1961.

[11] Kliore and Fjeldko, California Institute of Technology Lunar and Planetary Conference, September 13-18, 1965.

of NH_3 in this wavelength region; the same is probably true for the microwave measurements. Therefore it would be desirable to determine the infrared temperature at other wavelengths where absorption is not an important factor.

Spectroscopic measurements also indicate that specific molecular components have velocities significantly different from each other and that the atmosphere is probably quite turbulent. Also certain marked planetary features, such as the Red Spot, appear to move in longitude. These temporal variations in the Jovian surface configurations may best be observed by photographic (television) techniques perhaps in different wavelength (particularly infrared) regions.

4.5 EXTENSION TO OTHER PLANETS

It should be briefly mentioned that many of the statements about the Jovian atmosphere are applicable to the outer planets.[12] Since the temperature falls with anti-solar distance, the abundance of NH_3 is reduced and Uranus is primarily CH_4, H_2, and He. Therefore similar measurements would be planned for these planets.

4.6 REPRESENTATIVE SCIENCE COMPLEMENTS

Representative experiment payloads are shown on Tables 4.6.1 and 4.6-2 for a small and medium spacecraft, respectively. A large payload would be in the 250-lb class and would correspond to the listing in Technical Direction Memorandum No. 1, dated March 7, 1966. Whether the spacecraft is spin or attitude-stabilized will not affect the selection of any particular experiment so much as the method of orienting and positioning the experiment in relation to the direction of flight, the sun or the angle and direction of the phenomena that the experiment is expected to measure.

During the early part of the trajectory, the earth-sun angle seen by the spacecraft is constantly changing over large angles and imposes some constraints on the look angles of the solar plasma and solar cosmic ray instruments when on a spinning vehicle.

---

[12] J. C. Brandt, and P. W. Hodge, "Solar System Astrophysics, McGraw Hill Book Co., Inc., New York, 1964.

Table 4.6-1. Representative 50-Pound Class Jupiter Flyby Payload

Experiment	(1)	SENSOR						
		No. Req.	Weight (lb)	Size (in.)	Aperture Size (in.)	View Angle	Pointing Direction	
							Spin	Stable
TV experiment	B	1	8	12 x 7 x 5	4D	1.05^{o} x 1.05^{o}	Fixed angle to spin axis	Scan platform
Magnetometer	A-B	1	1.5	2D x 3	-	-	One axis parallel to spin	Any
Trapped radiation	B	1	Sensor and electronics combined		3D	2π	Any	Any
Solar plasma	A	1	Sensor and electronics combined		.8 x .4	160^{o} x 20^{o}	Towards sun	
Micrometeoroid	A-B	1	Sensor and electronics combined		5D	2π	---	
Solar cosmic ray	A	2	2 x 1.5	2 (3 x 3 x 6)	3D	60^{o}	Towards sun Away from sun	
Radio occultation	A-B	2*	1.5	36 and 6	-	-	---	
Infrared radiometer	B	1	Sensor and electronics combined		2D	2^{o}	Perpendicular to spin	Scan platform
Galactic cosmic ray	A	1	Sensor and electronics combined		4.5D	60^{o}	Away from sun	

(1) A - Interplanetary
B - Planetary Flyby

*Antenna Whip

Table 4.6-1. Representative 50-Pound Class Jupiter Flyby Payload (Continued)

Experiment	(1)	REMOTE ELECTRONICS						
		Weight (lb)	Size (in.)	Power (watts)	Data Rate Bits/Sample	Commands (including on/off)	Diagnostic Telemetry	
TV experiment	B	6	8 x 6 x 6	10	A B	4	2T	2V
Magnetometer	A-B	4	6 x 6 x 6	4	A-24 B-24	4	2T	2V
Trapped radiation	B	5	5 x 5 x 4	2	A-0 B-24	2	1T	2V
Solar plasma	A	5.5	7 x 6 x 6.5	1.5	A-24 B-0	3	1T	1V
Micrometeoroid	A-B	4	6 x 6 x 6	1	A-14 B-14	2	1T	2V
Solar cosmic ray	A	3	5 x 5 x 6	2	A-32 B-32	3	3T	1V
Radio occultation	A-B	5	6 x 7 x 7	1.5	A-6 B-72	2	1T	1V
Infrared radiometer	B	3	4 x 5 x 7	3	A-0 B-28	4	2T	2V
Galactic cosmic ray	A	6	6 x 6 x 6	2	A-5 B-5	3	2T	1V

(1) A - Interplanetary
B - Planetary Flyby

Table 4.6-2. Representative 100-Pound Class Jupiter Flyby Payload

Experiment	(1)	SENSOR						
		No. Req.	Weight (lb)	Size (in.)	Aperture Size (in.)	View Angle	Pointing Direction	
							Spin	Stable
TV experiment	B	1	8	12 x 7 x 5	4D	2°	Fixed angle to spin axis	Scan platform
Microwave radiometer	B	*	8	20D	20D	2.5° cone	Fixed angle to spin axis	Scan platform
Solar cosmic ray	A	2	2 x 1.5	2 (3 x 3 x 6)	3D	60°	Towards sun Away from sun	
Magnetometer tri-axial fluxgate	B	1	1	2D x 3	-	-	One axis parallel to spin	Any
Magnetometer helium	A	1	2	6 x 3 x 3	-	-	One axis parallel to spin	Any
Trapped radiation analyzer	B	Sensor and electronics combined			3D	2π	Any	
Solar plasma	A	Sensor and electronics combined			.8 x .4	160° x 20°	Towards sun	
Micrometeoroid	A-B	Sensor and electronics combined			5D	2π	---	
Galactic cosmic ray	A	Sensor and electronics combined			4.5 D	60°	Away from sun	
Radio occultation	A-B	2**	1.5	36 and 6	-	-	---	
Low energy proton monitor	B	2	2 x 1	2 (3 x 3 x 6)	1D	2π	Perpendicular to flight	
Auroral	B	2	2 x 1	2 (3 x 3 x 6)	2D	5°	135° from spin	Scan platform
Solar visual occultation	B	1	1.5	2D x 6	1D	5°	Towards sun	Scan platform

(1) A - Interplanetary
B - Planetary Flyby

*Dish Antenna
**Antenna Whip

Table 4.6-2. Representative 100-Pound Class Jupiter Flyby Payload (Continued)

Experiment	(1)	REMOTE ELECTRONICS						
		Weight (lb)	Size (in.)	Power (watts)	Data Rate Bits/Sample	Commands	Diagnostic Telemetry	
TV experiment	B	6	8 x 6 x 6	10	B-250,000 A-0	4	2T	2V
Microwave radiometer	B	24	8 x 8 x 14	4	B-70 A-0	4	2T	2V
Solar cosmic ray	A	3	5 x 5 x 6	2	A-32 B-32	3	3T	2V
Magnetometer triaxial fluxgate	B	4	6 x 6 x 6	2	B-24 A-0	4	2T	2V
Magnetometer helium	A	5	6 x 6 x 6	5	A-30 B-0	4	2T	2V
Trapped radiation analyzer	B	5	4 x 5 x 5	2	B-24 A-0	2	1T	2V
Solar plasma	A	5.5	7 x 6 x 6.5	1.5	A-24 B-0	3	1T	1V
Micrometeoroid	A-B	4	6 x 6 x 6	1	A-14 B-14	2	1T	2V
Galactic cosmic ray	A	6	6 x 6 x 6	2	A-5 B-5	3	2T	1V
Radio occultation	A-B	6.5	6 x 7 x 7	1.5	A-6 B-72	2	1T	1V
Low energy proton monitor	B	4	5 x 4 x 4	2	B-20 A-0	2	3T	3V
Auroral	B	3	4 x 4 x 5	2	B-30 A-0	2	3T	3V
Solar visual occultation	B	3	4 x 4 x 4	2	B-30 A-0	2	1T	2V

(1) A - Interplanetary
B - Planetary Flyby

At the other end of the trajectory, that is, when the spacecraft is in the planetary flyby stage, pointing directions and look angles of many experiments are also constrained by a spinning vehicle, unless of course, some mechanism is used to change the look angle of the experiment in relation to the planet, as it passes by.

If an attitude-stabilized spacecraft is contemplated along with a scanning or movable platform on which the experiments which require a pointing direction can be placed, most, if not all the conditions placed by the experiments on the spacecraft attitude are met; however, movable platforms impose large penalties on the spacecraft regarding the additional weight, power, magnetics, and ground commands or other means of pointing the platform and varying the rate of scan. With regard to the ability to compensate for unplanned deviations from the nominal trajectory, the rotation of the spin-stabilized spacecraft is equivalent to one gimbal axis for the fully attitude-stabilized spacecraft. For an instrument on a spinning spacecraft scanning a relatively broad conical field, substantial trajectory errors might cause it to view the target planet at a time which differs from the nominal time, and from a direction which differs (in one coordinate) from the nominal direction; however, the planet certainly will cross the field of view of the instrument. The same accommodation can be provided by a single-gimballed platform on an attitude-stabilized spacecraft. However, unless the platform were programmed to scan automatically about this axis, the required displacement to accommodate a substantial trajectory error would have to be commanded.

The attitude-controlled spacecraft has an advantage over the spinning spacecraft for instruments with marginal sensitivity. For example, an infrared mapping instrument might require a longer exposure time while pointed at a given region of the disc of the planet than is possible from the spin-generated scan.

The most significant factor in the choice between spinning or stabilized spacecraft appears to be the television camera and infrared imaging devices. Section 4.8 is devoted to a discussion of the television experiment.

4.7 EXPERIMENT REQUIREMENTS ON THE SPACECRAFT

4.7.1 Power Requirements

The representative 50 and 100-lb class of scientific payloads are not over-demanding in their power requirements, the largest single consumer being the television camera, requiring 10 watts of power during the planet flyby phase. One must, however, add to these 10 watts, most of the power required by the onboard data storage unit, which is there mainly to fulfill the television experiment requirements.

As the mission is both interplanetary and planetary, many of the planetary experiments are not turned on during the interplanetary flight, the total power required by the experiments is not additive. For example, on the 100-lb class payload, two magnetometers are shown, one covering the low magnetic field of interplanetary space and the other covering the extremely high field expected in the vicinity of the planet. To ease the power load it is expected that the interplanetary magnetometer will be switched off as the spacecraft approaches the planet, for, with its upper dynamic range fixed at 200 gamma, it should be completely saturated and therefore serve no useful purpose in being on.

The maximum power required at any one time for the 50-lb payload is 17.5 watts and for the 100-lb payload 26.5 watts.

4.7.2 Volume Requirements

Our experience has shown that the volume of individual experiments and therefore the total volume of the experiment payload, is seldom one of the limiting factors on the spacecraft.

With the advent of microminiaturization, experiments are kept within the limits of a given size. Very little can be done in reducing the sensor portion of the experiment which is fixed regarding the aperture size and the look angles required. Several of the proposed experiments, however, have more than one sensor, thus increasing the experiment volume. This approach has been taken so that each sensor of any one experiment covers a narrow band, rather than selecting a more complex instrument which uses only one sensor, but involves switched filters or other moving parts within the instrument.

With those experiments that utilize photomultiplier tubes for their operation, the sensor volumes have been increased to allow for magnetic shielding necessary to prevent defocussing of the tubes during the planet flyby period. It is also expected that the volumes of some other experiments will increase to a small extent to combat radiation and micrometeoroid damage. This is especially so for the more exposed experiments like the boom-mounted magnetometer sensor.

4.7.3 Command Requirements

To turn the experiment on, place it in the calibrate mode or change its dynamic range, requires either an earth-spacecraft rf link, spacecraft onboard automatic sequencer or both.

Flights to unknown areas of the universe where the expected range of phenomena to be measured might be very different from that calculated, necessitates large dynamic ranges from the experiment, or several smaller switched ranges. Commands are required in quantities over and above the normal.

The vast distances involved from the earth to the spacecraft places great limitations time-wise on an earth command. If we were reading on the ground some measurement from a spacecraft at 5 AU, the information is already 40 minutes late. By the time a command has reached the spacecraft to change the experiment to a higher or lower range, 80 minutes flight time has elapsed. The experiment could well be in and out of the phenomena of interest during this time.

Automatic commands from an onboard sequencer would seem the likely solution. By sensing the data output, and if saturated, e.g., reading all "ones" or above a certain analog level, the sequencer would command the experiment to the next higher range.

Great flexibility exists in limiting the number of commands required by the payload and hence, the size and complexity of the uplink decoder or automatic sequencer, for instance, one calibrate command might suffice for all experiments, or, on the heavier payload where both magnetometers are not required at the same time, the command that switches one on, would switch the other off.

Many other tradeoffs exist between the number of commands, the complexity of the experiment and even the number of experiments required.

4.7.4 Telemetry Requirements

The experiments requiring the largest telemetry rate are the visual experiments and in particular, a television camera, the output of which can range from something like 2×10^4 bits per frame to 1.5×10^6 bits per frame, depending on the requirements and spacecraft limitations.

This amount of information has an enormous impact on the spacecraft, affecting the weight, volume and power, to the extent that it completely governs.

The remainder of the experiments are low on their telemetry demands to the extent that during the interplanetary phase, not all the proposed spacecraft telemetry capacity is used, even taking into consideration the spacecraft engineering measurements.

Many tradeoffs exist to best fit any payload to the telemetry capacity of the downlink.

Experiments can be sampled at slower or faster rates, data compression can be used, or if during some phase of the mission, the telemetry information being gathered onboard the spacecraft is less than the downlink handling capacity, it can be stored and unloaded periodically at the higher downlink rate. This has the subsidiary advantage of releasing the DSN from continuous attention to one spacecraft, an important consideration in view of the extended flight times—two years and more—of Advanced Planetary Probes.

A data handling system is presently being studied by TRW, involving a central data processing unit. Rather than each and every experiment doing its own data processing, the signals would be taken from the sensors and processed and formatted in a system common to all. It is believed that this will save weight, power and volume. This could well be the most suitable approach for a mission of this nature.

4.7.5 Thermal Requirements

The thermal requirements of the experiments are no different from that required of the spacecraft electronic packages and should not pose a problem. An exception to this is the boom-mounted magnetometer sensor mounted remote to achieve magnetic isolation from the remainder of the spacecraft. As negligible power is generated within the sensor, passive thermal layers of insulation will be used, the thermal balance being made up with a small heater if necessary. Most other instruments will be within the confines of the temperature controlled compartment along with the spacecraft electronics. Experiments mounted in a gimballed external planet sensor package may require additional heater power.

4.7.6 Pointing Accuracy Requirements

Whether the spacecraft be spin or attitude-stabilized, the experiments in use during the interplanetary stage of the mission place no exacting requirements on the spacecraft. The cosmic and plasma probes have wide fields of view and are not confined to small angular limits. During the planetary flyby stage, the experiments seeking atmospheric or surface information impose more rigid constraints on the spacecraft and the trajectory due to their more narrow look angles, The infrared radiometer, microwave radiometer and the TV experiments fall into this category and are critical to a 1 degree pointing accuracy. Due to the long ground link transmission times and the limited flyby times, a planet seeking sensor seems desirable to trigger these instruments on at the correct time.

4.7.7 Magnetic Requirements

The inclusion of a magnetometer experiment to measure the low magnetic fields during the interplanetary phase of the mission imposes severe restraints on the materials used on the spacecraft, the positioning of the assemblies on the spacecraft and the manufacturing techniques involved with assemblies to reduce stray fields due to current loops. With interplanetary magnetic field levels of one gamma, the magnetometer should be sensitive to changes as low as 0.1 gamma. The spacecraft magnetic field contribution at the sensor must be kept below the resolution of the magnetometer.

On large spacecraft involving many large electronic assemblies, the positioning of the sensor on a 20-foot boom still makes this low level difficult to achieve. TWT's and RTG's are particularly troublesome in this respect. Some compromise must be made between the cost of exacting magnetic controls on the spacecraft and the contributing magnetic field at the magnetometer sensor.

When in the vicinity of Jupiter, the magnetic compatibility problems of the spacecraft are totally different in nature. The planet's expected magnetic field is very large, the calculated upper limit being 1000 gauss. Dependent on the flyby distance, the spacecraft might be subjected to 100-gauss fields. This can have the effect of defocussing the TWT's of the communication subsystem and the PM tubes used in several experiments, unless adequate shielding is used. It is also expected that any core storage units of the telemetry subsystem would require magnetic shielding.

4.8 TELEVISION CAMERA FOR JUPITER PROBE

Two types of television cameras are described here, one for use on a three axis stabilized probe, the other for a spin-stabilized version. The intention is to briefly describe the design approach and give approximate weight, power, data and performance parameters in each case. These figures are summarized in Table 4.8-1. Further definition of the TV experiment for various science payload classes will be performed in conjunction with JPL.

4.8.1 Three-Axis Stabilized Vehicle

A television camera of the Mariner-C type is appropriate for the three-axis stabilized probe. This camera system has one mechanical scan axis and consists of a narrow field optical system, slow scan vidicon with a shutter and digital processing electronics. Mounting the camera in a two-degree-of-freedom Planet Sensor Package (PSP) offers better coverage but increased complexity. Some differences exist in the design parameters of the Jupiter camera as opposed to the Mariner unit due to the desire for higher resolution for the former and the somewhat lower planetary brightness of Jupiter.

The Jupiter disc will fill the field of view of such a television camera at a range of approximately 100 planet radii. Prior to this time a PSP mounted camera would be actuated and, if desirable, operated at a repetition rate limited only by data storage and transmission constraints. Picture taking by a camera mounted as in Mariner-C would be delayed until Jupiter entered the scan field. With the parameters shown in Table 4.8.1 the resolution will be ~10 sec, corresponding to 300 km on the planetary surface at the 100-radius range. As the probe nears the planet the ground resolution is enhanced but the picture will encompass a smaller portion of the disc.

Since data handling is probably the most severe problem associated with the television it is appropriate to display briefly some tradeoff possibilities. Figure 4.8-1 shows the data readout, storage, and transmission requirements for possible picture formats.

4.8.2 Spin-Stabilized Vehicle

The second type of television described is to be used on board a spacecraft spinning about the earth vector. Two design approaches are described, an image dissector and a SEC vidicon system. The latter is dependent upon achievement of state-of-the-art performance while the first suffers from lower resolution and permits close approach photography only.

The image dissector television camera consists of a single-axis deflectable mirror, optical system, image dissector and processing electronics. The deflectable mirror is required to keep the planet within the camera field as the earth-probe-planet angle changes during the approach trajectory. The horizontal scan of the field of view is accomplished by electronic deflection of the dissector aperture. The primary vertical scan is generated by the spacecraft rotation, 21 degrees/sec due to the 5 rpm rotation at nominal earth-spacecraft-planet angle of 135 degrees. In addition, it will be necessary to partially compensate for the spin motion of the field of view by applying a vertical scan deflection in the image dissector to keep a constant net vertical scan period as the earth-spacecraft-planet angle changes.

Table 4.8-1. Summary of Sensor Parameters

	Three-Axis Stabilized Vehicle	Spin-Stabilized Vehicle	
Camera Tube	Conventional Vidicon	Image Dissector	SEC Vidicon
Field of View	$1^{o} \times 1^{o}$	$6^{o} \times 6^{o}$	$2^{o} \times 2^{o}$
Focal Length	25"	6.5"	20"
Relative Aperture	f/5	f/2	f/5
Scan Format	0.44" x 0.44" 500 lines	0.70" x 0.70" 500 lines	0.70 x 0.70" 500 lines
Approximate Total Weight	20 lbs	20 lbs	20 lbs
Approximate Power	10 watts	10 watts	10 watts
Gray Scale	64:1	64:1	64:1
Data Content per Picture	1.5×10^{6}	1.5×10^{6}	1.5×10^{6}
Exposure Time	0.25 sec	0.50 sec	0.1 msec
Readout Time	~1 minute	0.50 sec	0.2% of data in 5 msec pulses at arbitrary rep. rate
Approximate Size of Sensor Head	10" x 8" x 8"	14" x 4" x 4"	10" x 8" x 8"

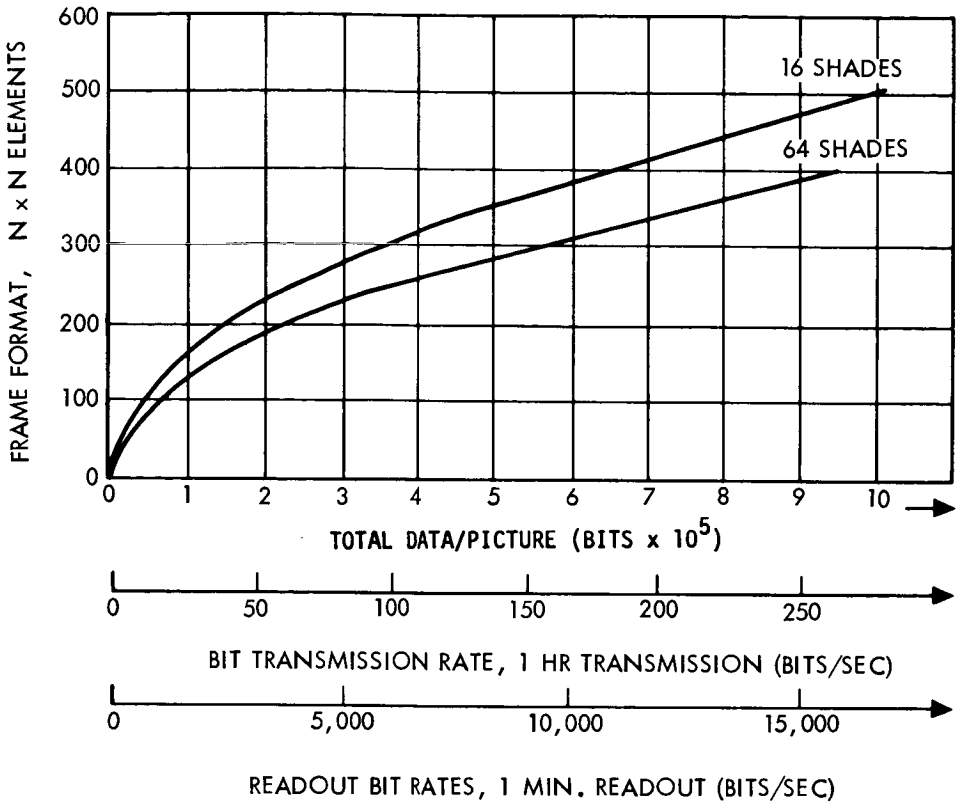

Figure 4.8-1. Data Requirements for Television Pictures

Due to sensitivity limitations of the image dissector this device will be able to provide full field pictures at 500 line resolution of the planet at 20 radii and less instead of the desired 100 radii range. The net photographic time period of the mission is thus somewhat reduced. In addition, the data output rate from the image dissector camera is extremely high, in the order of 3×10^6 bits/sec for 500 x 500 element picture with 6 bit gray scale. This output rate places a formidable constraint on the processing electronics.

It may be possible to overcome both the sensitivity and data rate problems associated with the image dissector by using an integrating camera. In order to accomplish this the camera must have an extremely short exposure time to avoid image smear. To limit image motion to less than one line during an exposure, the required exposure time is in the order of 0.1 msec, which is below the operating range of normal pickup devices. A special purpose television camera possessing the potential of operating reliably at this exposure time with reasonable illumination is the Westinghouse SEC vidicon. This camera tube has the

additional advantage of long duration image storage permitting reduction of the data readout rate. The drawback to a camera design based on the SEC vidicon is the lack of operational verification of its performance characteristics. If the SEC vidicon performance is verified in future testing, it is possible that this device would be the logical choice for the three axis stabilized vehicle camera.

The readout format described in Table 4.8-1 for the SEC vidicon is based on sequential readout of single line data separated by arbitrary time periods. An alternative to this mode is a pulsed single element read. In this mode the camera reads a single picture element in the normal 10 μsec dwell time but delays a fixed time period before reading the next element. The ultimate development of such a mode might permit real time transmission of the picture data. This alternative can be mentioned as a possibility only, however, since camera operation on this mode has not been verified. The SEC camera also requires a deflectable mirror to keep the planet within the field of view during the approach trajectory.

In summary, it appears that the television system is more compatible with the three-axis stabilized spacecraft than the spinning probe. The penalty realized upon going to the spinning vehicle will depend upon the degree of development in high sensitivity image tubes such as the SEC vidicon.

5. SPACECRAFT CONFIGURATIONS (SAMPLES)

5.1 MATCHING SPACECRAFT, LAUNCH VEHICLES AND MISSIONS

We are not yet at the point where the spacecraft, including science complement and matched data rate and storage, type of stabilization and degree of environmental protection can be satisfactorily matched to launch vehicles and missions. The missions include Jupiter, Saturn and Neptune, the latter by direct flight and by Jupiter swingby, and encompass flyby, orbiter and capsule delivery flights. Rather than attempt to make this synthesis at the present time, let us define the building blocks which we will try to match.

Starting from the science end, 50, 100 and 250-lb classes of science payloads will be considered. Sample 50 and 100-lb payloads were presented in Section 4. The 250-lb class will be associated with the list given in Technical Directive No. 1, dated March 7, 1966.

For purposes of this study, it will be assumed that the 250-lb class involves an attitude-stabilized spacecraft and that a planetary scan platform similar to that considered for Voyager will be employed to mount planet-pointing experiments such as TV, spectrometers, etc. Trainable antennas for the microwave radiometer, altimeter, etc., will either be mounted on the planetary scan package or separately gimballed.

The 50-lb class of payloads (including as a subset minimum payloads if necessary) will be tentatively associated with spin-stabilized spacecraft.

The 100-lb class of payloads will be mated to both spin and attitude-stabilized spacecraft. Both types of spacecraft stabilization will probably have to be retained throughout the study since it is believed they will offer different kinds of advantages and disadvantages and a selection would involve more factors than are currently available.

Assuming that the science payload fraction (sensors plus electronics) varies in the range from 10 to 20 percent of the basic flyby spacecraft weight, the corresponding spacecraft weights would be:

Payload Weight	Flyby Spacecraft Weight	
	10%	20%
50	500	250
100	1,000	500
250	2,500	1,250

where higher percentages are more probable in the heavier spacecraft.

It will be assumed that spacecraft heavier than the upper limit for each payload class are justified only if they are orbiters or carry a capsule.

Table 5.1-1 gives a selected spacecraft weight/mission/launch vehicle matrix. For simplicity, it will be assumed that the propulsion system for an orbiter should about equal the basic (flyby) spacecraft weight. Under these conditions Table 5.1-2 gives a related science payload class/mission/launch vehicle matrix. Entry capsule missions have not been shown in Table 5.1-2 but various possibilities can be inferred from Table 5.1-1.

It is within this kind of framework that, with the concurrence of JPL, the final spacecraft concepts will be selected and the designs refined.

5.2 SAMPLE CONFIGURATIONS

This section shows some exploratory conceptual designs. These sketches are meant to be representative of design possibilities and do not yet represent more than possibilities.

5.2.1 Summary Table

The table below indicates, in matrix form, the major items relative to each of the sample configurations pictorially illustrated in this report.

A more definitive description of each configuration is given in the sections immediately following the Summary Table.

Table 5.1-1. Spacecraft Weight/Mission/Launch Vehicle Matrix

C_3 km^2/sec^2	Time (yr)	Mission	Total Spacecraft Weight						
			F1	E	D	D1	C	B	A
			Atlas SLV3x/ Centaur/ TE-364	Atlas SLV3x/ Centaur/ HEKS	Titan IIICx/ Centaur	Titan IIICx/ Centaur/ TE-364	Saturn IB/ Centaur/ HEKS	Saturn V	Saturn V/ Centaur/ HEKS
90	1.8-2.0	Jupiter	570	940	1,600	2,250	4,300	21,000	29,000
100	1.6	Jupiter	480	790	1,000	1,950	3,850	17,500	26,500
110	3.4	Saturn via Jupiter swingby 1979	385	640	480	1,600	3,400	14,000	24,000
120	3.2 5.8 8.8	Saturn via Jupiter swingby 1979 Uranus via Jupiter swingby 1979 Neptune via Jupiter swingby 1979	300	510	100	1,350	3,000	11,500	21,500
130	2.8 3.1-3.3 8 10	Saturn via Jupiter swingby 1979 Saturn direct (1970, 71 and 72) Neptune via Jupiter swingby 1979 Uranus direct	220	390	--	1,150	2,600	7,900	19,500
140	2.8-3.1 7.2 7.5 18.5	Saturn direct Uranus direct Neptune by Jupiter swingby 1979 Neptune direct	--	280	--	970	2,300	6,800	17,500
170	2.3 5.3 6.8 10	Saturn direct Uranus direct Neptune by Jupiter swingby 1979 Neptune direct	--	--	--	600	1,400	1,900	13,400
200	8.3	Neptune direct	--	--	--	360	800	--	10,000

Launch Vehicle	Destination				Encounter Mode	Stabilization	Science Payload Class	Comments
	Jupiter	Saturn	Uranus	Neptune				
Atlas SLV3x/ Centaur/ TE-364	x				Flyby	Spin	50	
Atlas SLV3x/ Centaur/ HEKS	x				Flyby	Either	100	
	x				Orbiter	Spin	50	
	x	→ x			Flyby	Spin	50	1979 only
	x	→	x or x		Flyby	Spin	50	1979 only
Titan IIICx/ Centaur	x				Flyby	3-Axis	250-	
	x				Orbiter	Either	100	
Titan IIICx/ Centaur/ TE-364	x				Flyby	3-Axis	250	
	x				Orbiter	Either	100	
	x	→ x			Flyby	3-Axis	250-	1979 only
	x	→ x			Orbiter	Either	100	1979 only
	x	→	x or x		Flyby	Either	100+	1979 only
	x	→	x or x		Orbiter	Spin	50+	1979 only
			x or x		Flyby	Either	100	
			x or x		Orbiter	Spin	50	
Saturn IB/ Centaur/ HEKS	x				Orbiter	3-Axis	250	
	x	→	x or x		Flyby	3-Axis	250+	1979 only
	x	→	x or x		Orbiter	Either	100+	1979 only
		x			Flyby	Either	250	
		x			Orbiter	Either	100+	
			x or x		Flyby	Either	100	
			x or x		Orbiter	Spin	50	
SaturnV/ Centaur	x	→ x or	x or x		Orbiter	3-Axis	250	Dual spacecraft 1979 only
		x or	x or x		Orbiter	3-Axis	250	
Saturn V/ Centaur/ HEKS				x	Orbiter	3-Axis	250	Dual spacecraft 8-year flight

Table 5.1-2. Science Payload Class/Mission/Launch Vehicle Matrix

Table 5.2-1. Advanced Planetary Probe Summary Table

	Configuration					
	PD74-22A	PD74-23A	PD74-25A	PD74-26A	PD74-27	PD74-28
Launch vehicle	Atlas SLV3x/ Centaur	Atlas SLV3x/ Centaur	Atlas SLV3x/ Centaur/HEKS	Titan IIICx/ Centaur	Atlas SLV3x/ Centaur/HEKS	Saturn IB/ Centaur/HEKS
TE-364 solid motor for injection	x	x		x		
TE-364 solid motor for deboost						x
Nose fairing[1]	"B" Minimum Length (154 in.)	"B" Minimum Length (154 in.)	"B" Minimum Length (154 in.)	"B" Maximum Length (274 in.)	"B" Minimum Length (154 in.)	"A" Minimum Length (265 in.)
Stabilization	Spin	Spin	Spin	3-Axis	Spin	Spin
High gain antenna diameter	16 ft.	16 ft.	16 ft.	27 ft.	16 ft.	32 ft.
Total spacecraft weight[2]	450 lbs.	450 lbs.	500 lbs.	1,000 lbs.	700 lbs.	2,340 lbs.
Capsule			x			

Items common to all spacecraft:
- Earth-oriented
- RTG powered
- Large deployable sunflower antenna
- Monopropellant hydrazine midcourse correction propulsion system
- Two omni antennas (one on each end)

[1] See "Launch Vehicle Future Missions Study Guideline" by W. A. Ogram for definitions of Fairings "A" and "B"

[2] Includes spacecraft bus, deboost propulsion and capsule weights as applicable

5.2.2 Configurations in General

The following drawings are examples of some of the initial configurations developed for various missions. By employing such devices as interstage adapters, off-loading tankage and varying the payloads, the several spacecraft may be fitted to various boosters and be made adaptable to different missions.

As the missions involved take the probes many AU distant from the earth and sun, the tasks of providing a significant power supply and a meaningful data rate become a significant problem for the conventional solar cell power system and the relatively small communications antennas.

All configurations shown herein employ RTG units for the primary power supply in order to make the spacecraft independent with respect to its distance from the sun and to relieve the spacecraft of any sun pointing requirements during the major portion of the missions.

Relief from sun pointing requirements enables the mounting of large, body-fixed, earth-oriented antennas to the spacecraft. All configurations presented herein use large, deployable (TRW/Tapco), sunflower-type antennas for high gain communication. Designs with 24 petals have been selected for the early portion of the study. Tradeoffs involving different numbers of petals will be made in the latter stages of the study.

All configurations currently being shown use focal point feeds for the high gain antennas. Cassegrain antenna elements will be studied as to their advantages and disadvantages in the planetary probe systems.

All configurations currently utilize two omni antennas — one body-fixed to either end of the probe. The spacecraft orientation during early portions of the missions may prevent the forward mounted omni from viewing the earth, and during the remainder of the missions, the aft mounted omni may be earth occulted.

All spin-stabilized spacecraft use a forward-mounted, body-fixed conical scan antenna for the generation of spacecraft pointing error signals.

It is currently expected that a passive thermal control system can be devised for the probes, thereby making an active system unnecessary.

The number of spacecraft bus compartments will be minimized, the bus will be thermally insulated from the outside environment and from the RTG units, while all interior bus components will be thermally coupled.

During early portions of the missions when the probes are relatively close to the sun, it may be necessary to orient the probes so that the large antennas shadow the buses from the sun in order to minimize the sun's thermal input. During that portion of the mission the aft pointing omni antennas will be used.

Also common to all configurations is the liquid monopropellant hydrazine propulsion systems used for midcourse corrections. Nitrogen gas is currently used for the propellant pressurant. To minimize weight, the nitrogen supply is common with that of the attitude control system. Further studies will determine if a separate pressure system is required for reliability or if the propellant tank itself should be pressurized as in a simple blowdown system.

The precession propulsion system for the spin-stabilized probes, the attitude control system for the three-axis stabilized probe, and the spinup and spindown systems for all spacecraft use high pressure nitrogen as the propellant.

The booster and spacecraft thrust axes, the spacecraft axis of symmetry, the spin axis (or roll axis as applicable for the fully attitude-controlled configuration) and the spacecraft orientation axis are all coincident.

Future configurations will investigate the use of liquid monopropellants and bipropellants for precession, attitude control, spinup and spindown requirements and the application of yo's for spindown requirements.

The spacecraft buses are all essentially cylindrical in shape and provide a single platform for equipment mounting. Inspection of the configurations readily indicates that the buses are extremely flexible as to equipment mounting surface and volume. Their size may easily be increased and supplementary equipment mounting surfaces can be added as required.

However, increased size carries with it the weight penalties involved with providing micrometeoroid protection over larger areas and thermal control for larger volumes.

5.2.3 Specific Configurations

Figure 5.2-1 (Drawing PD74-22A) shows a configuration tailored for a Jupiter flyby mission using an Atlas SLV3x/Centaur booster with a TE-364 solid motor for injection. The spacecraft is housed within a minimum length "B" fairing and attaches to the booster via six "outriggers." Fairing load distribution[1] is accomplished with the aid of fittings incorporated into the fairing itself.

The spacecraft is fastened to the fairing three places with the aid of three tension capable bolts fitted with separation nuts and at three alternate locations with shear pins. All six attach points transfer compression loads.

Separation occurs when a signal actuates the three separation nuts and springs are used to provide the separation velocities required.

The spacecraft is spin stabilized, carries a 16-foot diameter high gain antenna and has a total weight of 450 pounds.

The RTG units are stowed within thermally insulated recesses of the bus and deploy after spacecraft/booster separation.

For design comparison purposes, thermal control louvers are shown installed on the aft surface of the bus. But, as noted earlier, it is believed that a passive thermal control system may be used.

A truncated conical shell section of RF transparent material supports the antenna feed, precession nozzles, and the conical scan and forward pointing omni antennas.

The single hydrazine tank is located on centerline within the truncated conical support noted above. This location provides the

---

[1] See Launch Vehicle Future Missions Study Guideline, by W. A. Ogram, for definitions of "A" and "B" Fairings.

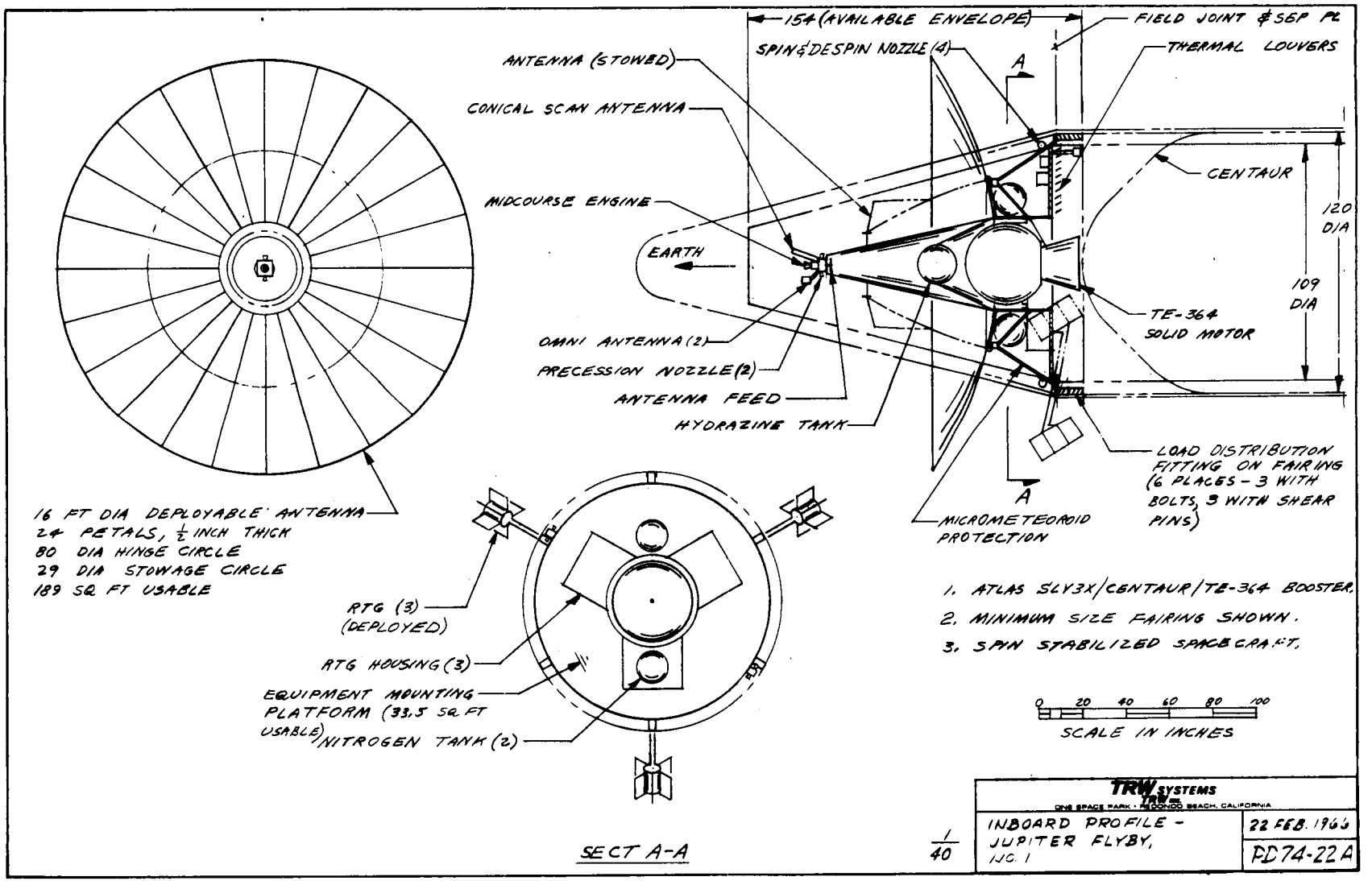

Figure 5.2-1 Inboard Profile - Jupiter Flyby, No. 1.

hydrazine poor thermal coupling with the other spacecraft components, and heaters may be required to prevent the propellant from freezing.

A single midcourse correction engine sized for up to 50 pounds of thrust is mounted on the forward end of the spacecraft. At remote sun distances, the engine and its supply lines may have to be heated to keep the propellant from freezing.

The configuration shown in Figure 5.2-2 (Drawing PD74-23A) is essentially identical in performance to PD74-22A. PD74-23A differs from PD74-22A as follows:

1) The spacecraft attaches to the booster through an interstage which in turn attaches to the 60-inch diameter attach ring on the Centaur forward dome. This method has been standard to date for attachments to Centaur and does result in a simpler and lighter spacecraft than the attach method of PD74-22A.

   "Launch Vehicle Future Missions Study Guideline" recommends the attach method of PD74-22A, but unless specifically directed otherwise by JPL, the contractor will attach the probe to the Centaur forward dome whenever applicable.

2) In order to improve the thermal coupling of the bus components, and to keep the propellant from freezing, the hydrazine tankage has been located within the equipment compartment. This procedure will be followed on all subsequent designs.

3) In order to minimize possible RF reflections, a tripod instead of the RF transparent truncated cone is used to support the antenna feed and the other probe components located forward of the feed. Where applicable, this design will be used in all other configurations.

Figure 5.2-3 (Drawing PD74-25A) depicts a Jupiter flyby mission configuration which incorporates a planetary capsule (including a sterilization container) into the design. All the aspects of a capsule mission have not been resolved as yet. The design shown merely indicates one possible spacecraft geometry if a capsule proves feasible. The capsule is located on the aft centerline to minimize lateral imbalance and spin instability of the spacecraft when the capsule is released.

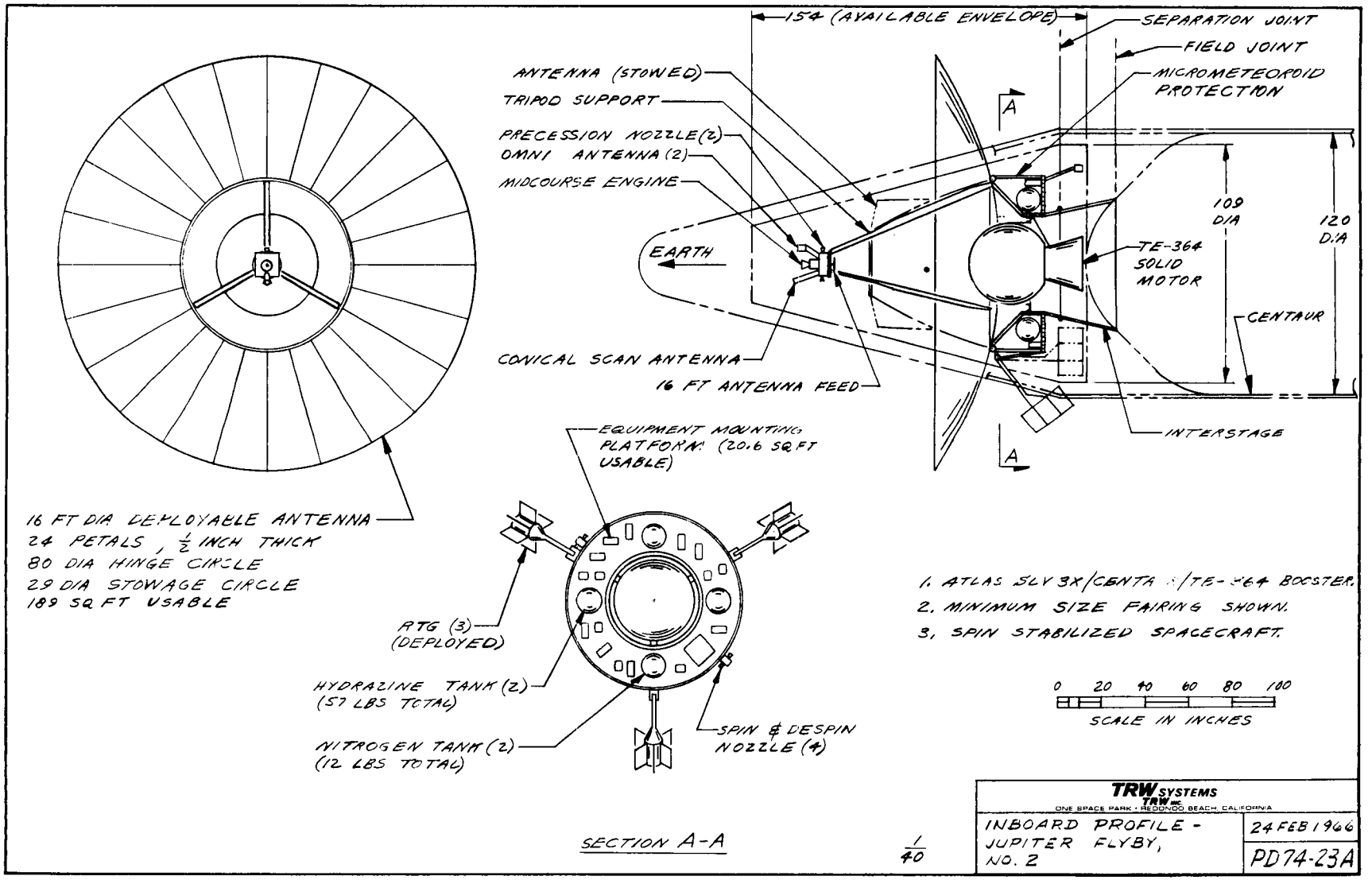

Figure 5.2-2 Inboard Profile - Jupiter Flyby, No. 2.

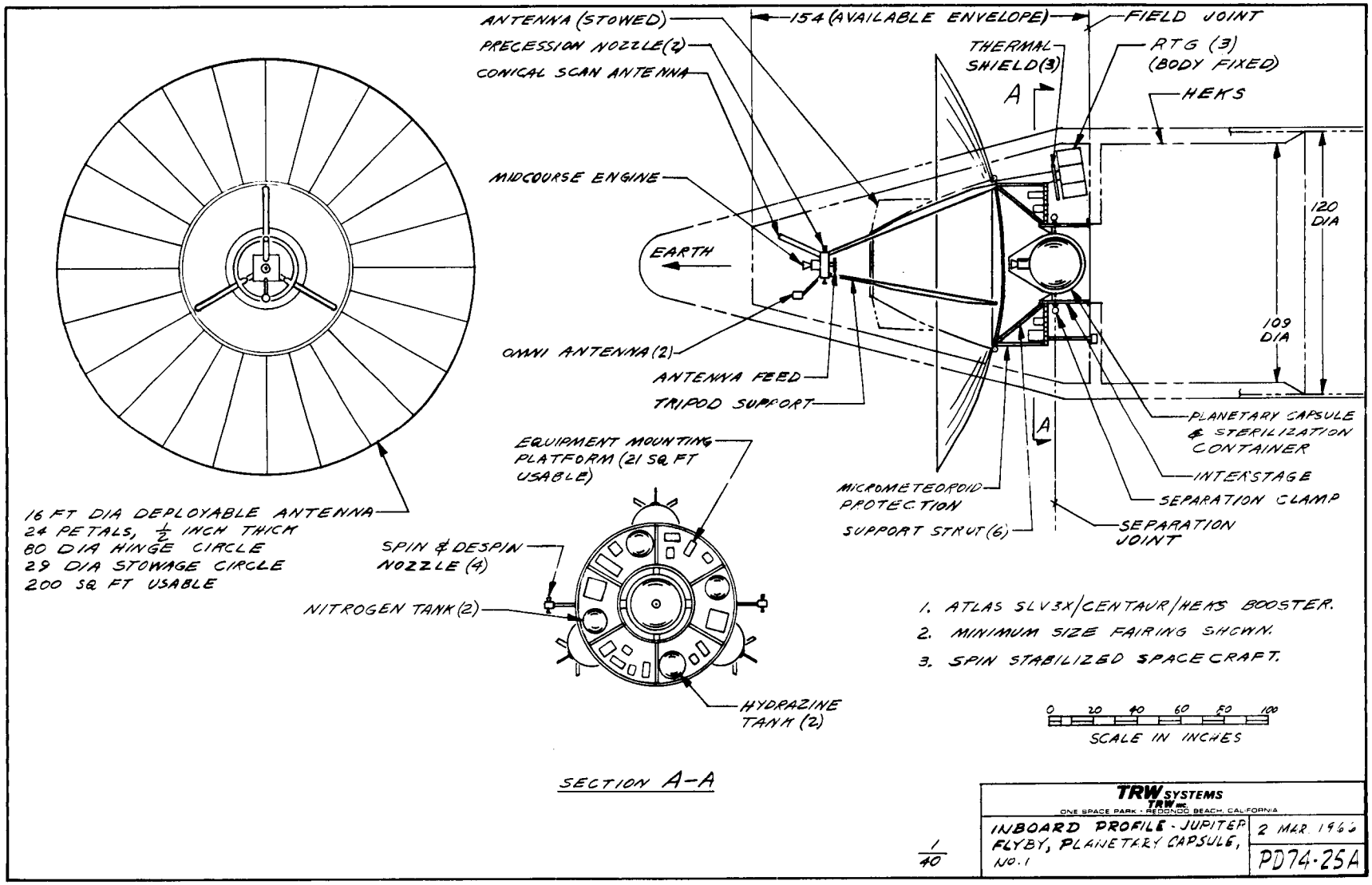

Figure 5.2-3 Inboard Profile - Jupiter Flyby, Planetary Capsule, No. 1.

The booster involved is the Atlas SLV3x/Centaur/HEKS and the spacecraft is protected during ascent by a minimum length "B" fairing. The spacecraft is spin stabilized, weighs 500 pounds and supports a 16-foot diameter antenna. The midcourse correction propulsion system is similar to those of PD74-22A and PD74-23A.

For design comparison and thermal study purposes, the RTG units are shown body-fixed to the aft end of the spacecraft. Such a nondeployable installation appears attractive from a weight and reliability point of view but its feasibility depends upon achieving an adequate inertia ratio and achieving acceptable shielding. The spacecraft is thermally protected by thermal insulating shields located between the RTG's and the probe. At remote distances from the sun, it may be desirable to allow RTG heat to enter the spacecraft by incorporating an active louver system into the thermal barrier.

Figure 5.2-4 (Drawing PD74-26A) is suitable for a Jupiter orbiter as the liquid monopropellant hydrazine midcourse correction system tankage has been increased in size to accommodate the propellant required for the deboost maneuver. The 50-pound thrust engines used for midcourse corrections are quite capable of handling the additional deboost operation.

Three thrusters have been provided: one is installed at the spacecraft forward end as in the configurations already described, and two are symmetrically located at the aft end. This installation would be used for midcourse corrections in that method of trajectory control which is accomplished by thrusting along the earth-oriented axis of the spacecraft.

The booster used with this configuration is the Titan IIICx/Centaur with a TE-364 solid motor for injection. The "B" fairing of maximum length is employed in order to maximize the size of the main antenna.

The 27-foot diameter antenna shown on the drawing is approximately the largest that can be stowed within the above noted fairing with the existing design ground rules. If a larger antenna is found to be desirable, some increase can be obtained by increasing the number of petals, reducing the petal thickness at their tips, and by reducing the stowage circle diameter.

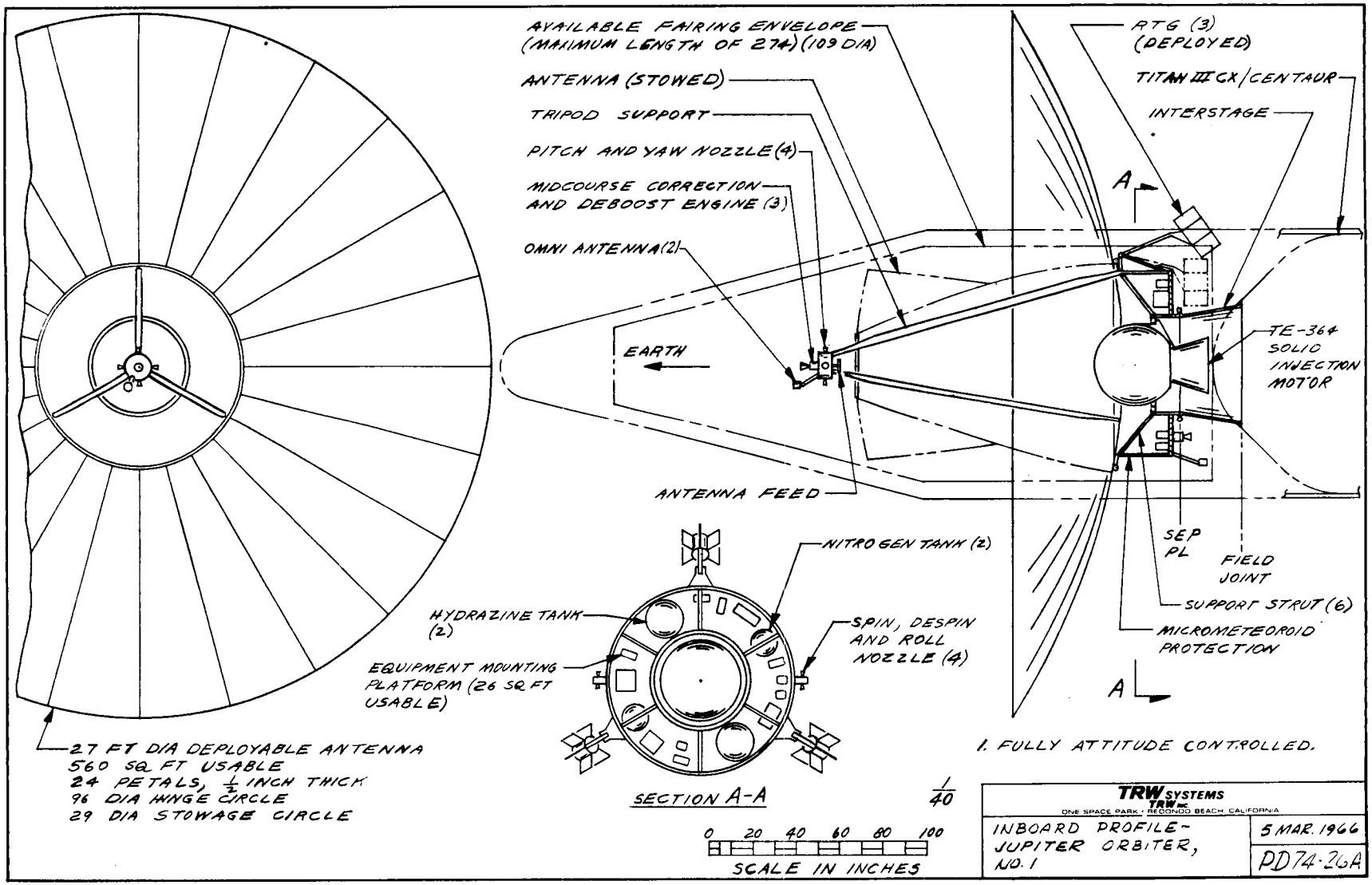

Figure 5.2-4 Inboard Profile - Jupiter Orbiter, No. 1.

The spacecraft has three-axis controlled stabilization but is spun up prior to the firing of the solid injection motor and despun afterward. The spacecraft weighs 1000 pounds which includes the deboost propellant. The RTG units are stowed aft of the bus and are deployed outboard after the fairing is jettisoned.

Figure 5.2-5 (Drawing PD74-27) illustrates another configuration suitable for a Jupiter orbiter mission and is launched by an Atlas SLV3x/ Centaur/HEKS booster. The spacecraft is stowed within the minimum length "B" fairing, weighs 700 pounds including the deboost propellant, is spin-stabilized and mounts a 16-foot diameter high gain antenna.

Similarly to the PD74-25A configuration, the RTG's are body-fixed with thermal shields for spacecraft protection.

The monopropellant liquid hydrazine system for midcourse corrections and deboost is similar to that described for the configuration of PD74-26A except for having a single "on centerline" propellant tank.

The configuration depicted in Figure 5.2-6 (Drawing PD74-28) is suitable for a Jupiter orbiter, is flown on a Saturn IB/Centaur/HEKS booster, and is contained within the minimum length "A" fairing.

The probe uses a solid motor for deboost into planetary orbit, is spin-stabilized and weighs 2340 pounds including the deboost engine. One outstanding feature of this design is the 32-foot diameter antenna which is currently believed to be the maximum size that will be of interest in this study. However, larger antennas can be physically accommodated by the fairing. The petal hinge circle and the petal stowage circle diameters are larger than those used on the previously described spacecraft.

Another design feature is that of mounting the RTG units to the nondeployable center section of the large antenna dish. This type of installation greatly increases the effective thermal radiating area of the RTG units. Additionally, a weight saving and reliability improvement should be realized as no deployment mechanisms or thermal shields are required.

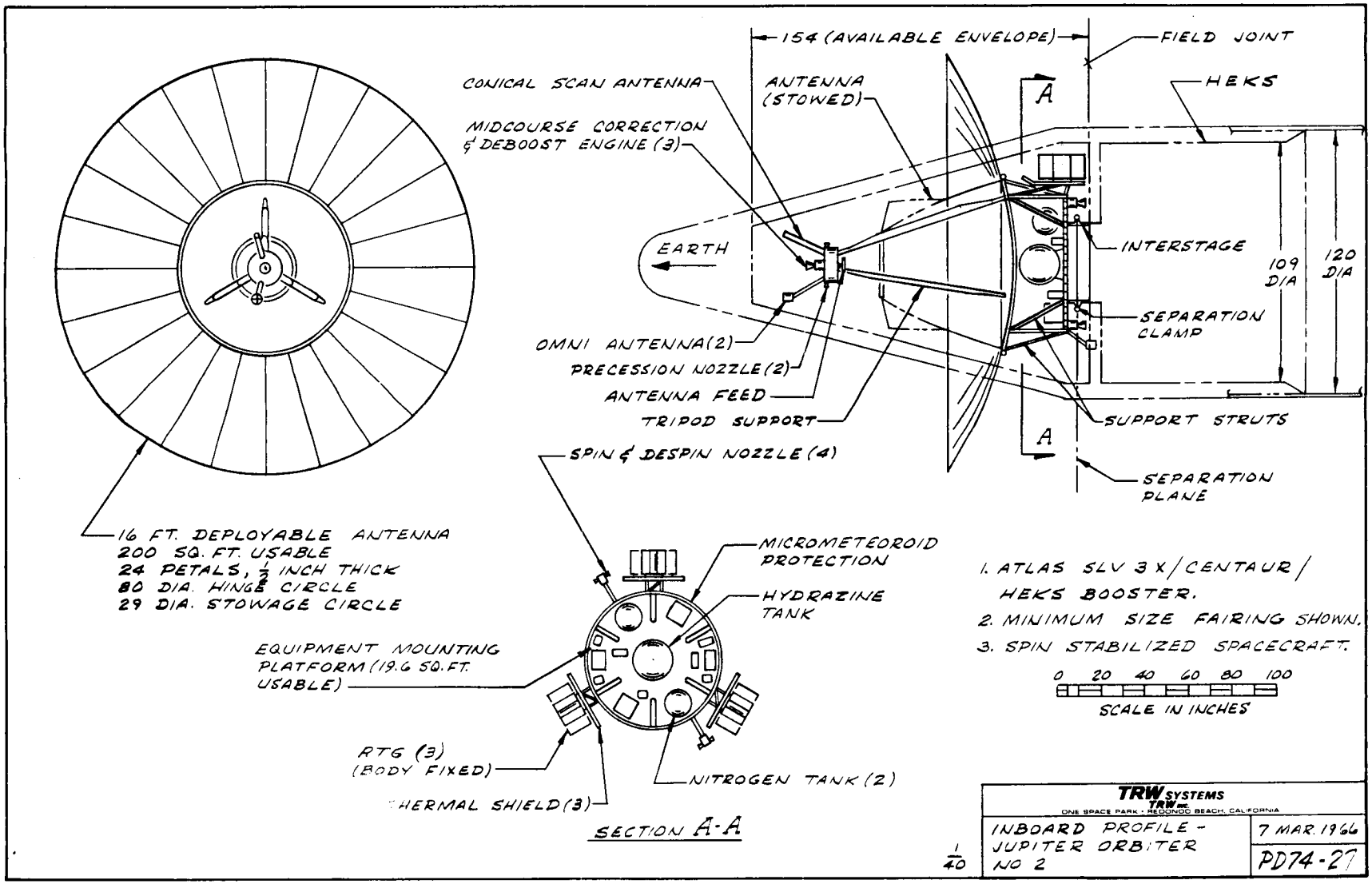

Figure 5.2-5 Inboard Profile - Jupiter Orbiter No. 2.

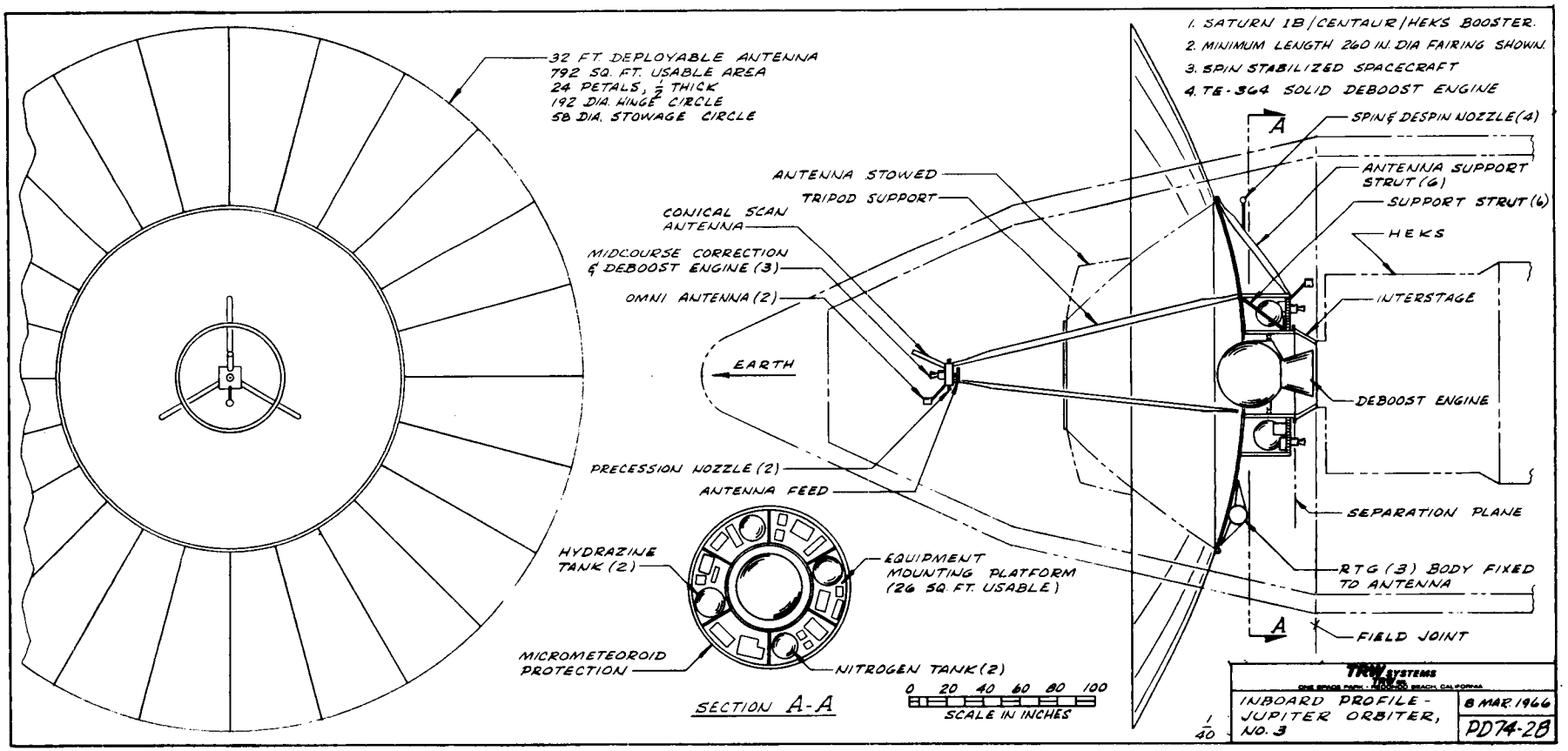

Figure 5.2-6 Inboard Profile - Jupiter Orbiter, No. 3.

The monopropellant liquid hydrazine system and engine geometry for midcourse corrections are similar to those described for the configuration of PD74-26A.

5.2.4 Sequence of Events

For illustrative purposes, the following event sequences are listed for various sample spacecraft configuration concepts. Only the events occurring from fairing separation to initial acquisition are of immediate concern.

5.2.4.1 Spin Stabilized Spacecraft with a Solid Injection Motor

1) Liftoff

2) Fairing separation. Occurs at approximately 350,000 feet and under low levels of acceleration.

3) RTG deployment. Where applicable, the early deployment of the RTG units is considered to be desirable in order to move the heat source away from the spacecraft and avoid possible damage to the spacecraft components. RTG deployment also affects the spacecraft spin stability favorably as the mass moment of inertia about the spin axis is increased.

4) Booster cutoff and coast

5) Spacecraft/booster separation. After correct spacecraft orientation by the booster, a signal releases the spacecraft/booster damping ring and springs impart a relative ΔV of approximately 2 feet per second to the spacecraft. The spacecraft is balanced so that its inertial axis is within 0.001 radians of the geometric axis of symmetry and the separation springs are matched to limit the tipoff rate to 0.5 degree per second.

6) Spinup. Spinup is initiated immediately after separation. A cold gas spinup system is shown on the example configurations but tradeoff studies will be required to determine if that system, a hot gas system or a solid rocket system is optimum. A spin rate requirement of from 0.5 to 1.0 rps is anticipated for the solid rocket burn. With the antenna in the stowed position, some of the sample configurations have favorable moment of inertia ratios and some do not. However, all configurations will remain stable during all operations required to complete acquisition.

7) Injection motor burn. After spinup to the desired rate has been accomplished, the solid motor is fired for spacecraft

trajectory injection. Additional studies will be required to determine if it is desirable to jettison the solid engine after burnout.

8) Partial despin. A cold gas despin system has been shown on the sample configurations but other systems such as hot gas, solid rockets and yo-yo's will have to be evaluated for this operation. It is desirable to despin the spacecraft down to a final spin rate of approximately 5 rpm. A minimum rate is required to maintain stability and a higher rate is costly in the precession gas required to change attitude. A partial despin is all that is required at this time as deployment of the large communications antenna will despin the spacecraft to the final desired rate.

9) Antenna deployment. Deployment of the antenna completes the despin operation.

10) Orientation. Firing of the precession jets orients the spacecraft to the desired attitude.

5.2.4.2 Spin Stabilized Spacecraft without a Solid Injection Motor

1) The sequence from liftoff through spinup is identical with the sequence described in Section 5.2.4.1 with the following exception:

As there is no solid engine burn, the spinup rate can be limited to a rate somewhat in excess of 5 rpm. It is desirable to have the spacecraft spin stabilized during antenna deployment to limit spacecraft perturbation during the operation. As before, the deployment of the antenna will despin the spacecraft to the desired final rate of approximately 5 rpm.

2) Antenna deployment. Final spin rate achieved.

3) Orientation. Spacecraft desired orientation accomplished.

5.2.4.3 Three-Axis Controlled Spacecraft with Solid Injection Motor

1) The sequence from liftoff through partial despin would be identical to the sequence described in Section 5.2.4.1 with the following exception.

As this is not a spin stabilized spacecraft, the partial despin becomes a total despin.

2) Antenna deployment. The antenna is deployed while the spacecraft is under three-axis control.

3) Orientation. The three-axis control jets align the spacecraft as required.

6. SUBSYSTEM STUDIES

6.1 STRUCTURE AND MECHANICAL

6.1.1 Function

The paramount purpose of the structure is to integrate the several subsystems of the spacecraft into a complete operating system with as little weight expenditure as possible.

In order to promote ease of assembly, test and maintenance as well as the ability to accommodate a mission or payload change, the structure must provide for ready access to the spacecraft interior and flexibility in its equipment mounting provisions and component alignment capabilities.

The structure must provide the physical load paths from the booster to the spacecraft and simultaneously provide strength and rigidity to sustain the static and dynamic loads of the launch environment.

After launch, the structure must provide the spacecraft components protection against the hazards of deep space such as micrometeoroids, radiation and high energy particles.

Structural and mechanical provisions have to be made for the various release and deployment mechanisms required by such components as the antenna petals and the RTG units.

To the maximum extent possible, the structural requirements will conform to the following guidelines:

a) Direct and optimum load paths will be used and masses will be located close to the thrust axis and spacecraft cg location to minimize induced loads and the resultant weight

b) Structure will be used for multiple functions such as employing micrometeoroid protection panels for equipment mounting and/or access doors

c) The spacecraft bus volume and surface area will be minimized to decrease the structural weight and the weight required for environmental protection and thermal control

d) Deployable components will be stowed so as to minimize structural requirements during thrusting and to minimize the number of deployed components and deployment distances in order to reduce structural weight

e) The number and size of joints will be minimized to increase the efficient use of structural weight

f) Material and structural geometries will be chosen to yield maximum strength-to-weight ratios and to minimize weight.

6.1.2 Conceptual Design for the Sample Spacecraft Configurations

Basically, the structural concept involved in all the configurations presented in this report divide the spacecraft into the following four major structural components: (1) a spacecraft/launch vehicle interstage; (2) a spacecraft bus; (3) a large deployable Sunflower type antenna; and (4) a support structure for the forward mounted equipment.

6.1.2.1 Spacecraft/Launch Vehicle Interstage

The optimum interstage is believed to be a short cylindrical or conical section that attaches to the booster at a small (3 to 5 ft) diameter bolted field joint and to the spacecraft at a circular separation joint. Separation of probe and booster would be achieved by actuating redundant separation bolts which release a "V" type clamping ring. Springs provide the required separation ΔV. As the interstages are relatively short structures, it is believed that they will be of semimonocoque construction to achieve good load distribution and will be made from conventional aircraft materials. The use of exotic expensive lightweight materials for members which remain with the booster does not appear justified at this time.

6.1.2.2 Spacecraft Bus

The bus consists of the equipment compartment and the attached structural members which support the various components mounted to the compartment. The equipment compartment consists of the equipment mounting platform, the cylindrical micrometeoroid protection walls, the fixed portion of the antenna dish and the various support struts.

The bus attachment to the interstage is made through a short, full monocoque cylindrical or conical section which is attached to the equipment platform. Where applicable, the section is extended forward as required to support either the TE-364 solid engine or capsule. Any structural members located forward of that joint are expected to be struts or truss members. The choice of materials for these members will be made later in the study.

All exterior surfaces of the equipment compartment will be fabricated from aluminum honeycomb sandwich panels in order to provide adequate structural strength and rigidity as well as superior micrometeoroid protection.

The bus provides the structural foundation for the RTG units, the large antenna, the forward support structure and various other components such as an omni antenna and the hydrazine motors.

The exact geometry of the support structure and deployment mechanisms for the RTG units and the supports for other miscellaneous equipment will be worked out at a later date.

6.1.2.3 Large Antenna

The large deployable TRW/Tapco Sunflower type antenna currently appears to be the most appropriate developed design for use on the Advanced Planetary Probe.

The deployable panels attach through hinges to a fixed mounting ring attached to the bus. The tips of the petals rest against a circular ring attached to the forward structure and are held in place by one or more clamping rings.

The clamping rings are severed on signal and springs and/or torsion bars located at the petal hinges rotate the petals to their deployed position. The larger antennas may require guides and locks at the petal extremities to insure accurate alignment of the petal surfaces.

If the deployed antenna is subjected to high centrifugal forces or high g loads, it may be necessary to provide RF transparent guy wires to limit the deflection of the antenna members.

6.1.2.4 Forward Support Structure

The large antenna feed, an omni antenna, a midcourse correction and/or deboost engine and a conical scan antenna and various gas nozzles, as applicable, are located some distance forward of the spacecraft bus. These items are supported by a structural tripod made probably of aluminum. The members are tapered and have cross sections which resist column deflection but provide minimum interference with the RF energy.

The lower end of the tripod structure has a broad base and attaches to fittings located on the bus.

The upper ends of the tripod members tie into a structural fitting which provides them with adequate moment capability at that point.

6.1.3 Alternate Conceptual Designs

Alternate conceptual design studies relative to structure will tend to involve detail design and material selection. For each particular configuration proposed, the basic structural load paths and the optimum types of structure can be readily determined.

6.1.3.1 Alternate Spacecraft/Launch Vehicle Interstage

The "Launch Vehicle Future Missions Study Guideline" by W. A. Ogram suggests that the spacecraft housed in the "B" fairing and which are launched by a booster with a Centaur upper stage, use a payload adapter which distributes the load uniformly over the cylindrical portion of the fairing.

The configuration concept shown on Drawing PD74-22A incorporates this type of attachment between the probe and the fairing. Six spacecraft "outrigger" type fittings extend from the bus to fittings mounted to the cylindrical section of the fairing. The outriggers shown are quite short, but when the bus is made compact (as is shown on PD74-23A), the outriggers become a significant weight item.

Additionally, the major weight items such as the solid motor are located near the center of the spacecraft thereby requiring a significant amount of structural weight to beam the load out to the fairing wall.

However, the use of an interstage design, such as that shown on Drawing PD74-23A, provides a more direct load path from the heavy elements of the spacecraft to the launch vehicle and a more efficient use of weight.

To date, the conventional method of attachment to the Centaur has been to the 58.5-inch diameter mounting ring on the Centaur forward tank dome.

TRW, therefore, proposes to use the Centaur forward dome attachment unless specifically directed otherwise by the customer.

6.1.3.2 Alternate Antenna Designs

As noted earlier, the Sunflower type antenna appears to be the best of the currently developed large antenna concepts for use on the Advanced Planetary Probe.

The contractor will continue to search for other suitable designs including its own independent in-house efforts.

6.1.4 State-of-the-Art Considerations, Reliability and Problem Areas

The structural design will involve well tested and proven airframe type concepts which may also be analyzed readily.

Structural reliability is of a high order and can be assured by a thorough and comprehensive testing program.

Appropriate materials must be carefully selected for particular jobs, such as the supports for the RTG units where long exposure to heat and low level radiation are factors.

Only well tested and successful types of deployment and separation devices will be used on the spacecraft.

The appropriate weight to be devoted to micrometeoroid protection has not yet been fixed; the uncertainty is due to a lack of knowledge of the meteoroid flux (see Section 3.8) rather than to uncertainty about the proper design techniques. Given the estimated environment, penetration probabilities may be deduced from equations presented in recent papers,

References 6.1.1 and 6.1.2. One pertinent indicator regarding tankage is given in Reference 6.1.3, which states that penetration of the tankage to one-fourth of the wall thickness of a pressure vessel does not destroy its integrity.

No other structural problem areas or development programs are anticipated.

REFERENCES

6.1.1 T. F. Lundeburg et al, "Impact Penetration of Manned Space Stations," Journal of Spacecraft and Rockets, Vol. 3, No. 2, Feb. 66, page 182.

6.1.2 T. F. Lundeburg, "Application of Hypervelocity Impact to Meteoroid Barrier Design," Journal of Spacecraft, Vol. 3, No. 2, Feb. 66, page 281.

6.1.3 J. A. Chamberlin, "Manned Spacecraft Design - The Problems Solved," Astronautics and Aeronautics, March 1966, page 27.

6.2 ELECTRICAL POWER SUBSYSTEM

6.2.1 Function

The function of the electrical power subsystem is to provide power to energize all electrical equipment aboard the spacecraft. Functional requirements are:

- Provide continuous electrical power during the entire mission lifetime from a primary power source using nuclear energy
- Condition the output from the primary power source to the proper forms for spacecraft use
- Provide centralized switching and distribution of power to spacecraft loads.

6.2.2 Conceptual Design

A simplified block diagram showing the conceptual design of the power subsystem appears in Figure 6.2-1. The design is based on the

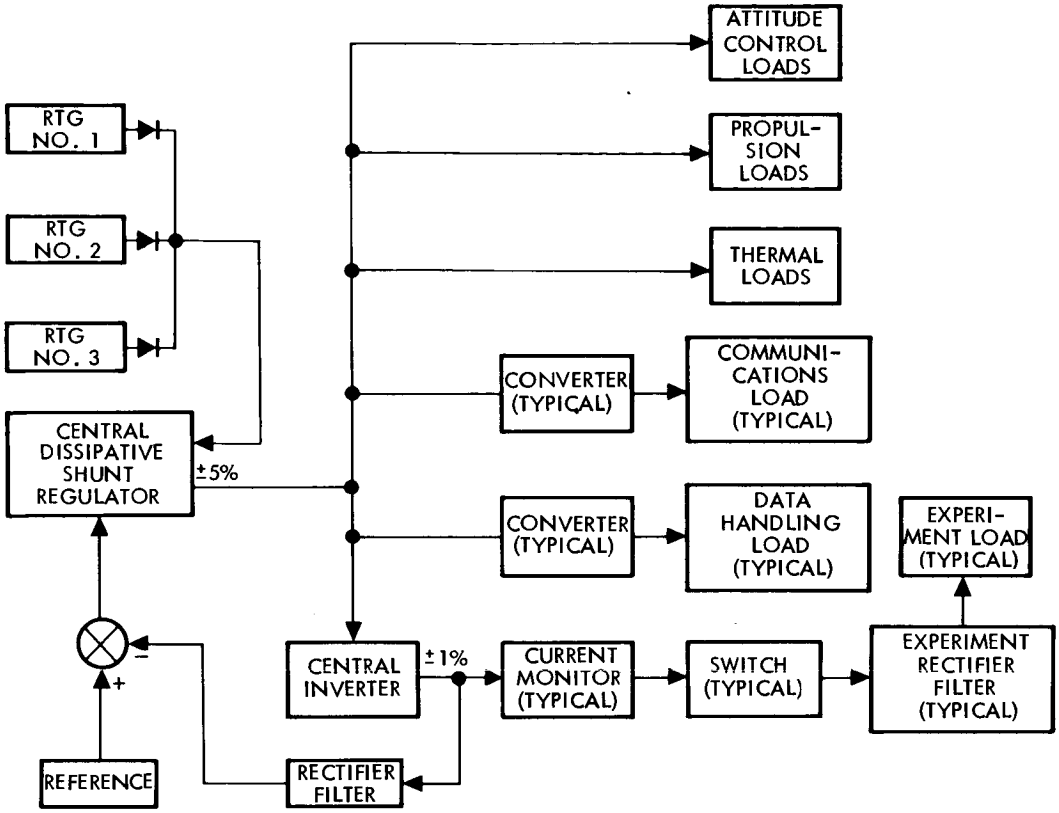

Figure 6.2-1. Conceptual Power Subsystem Block Diagram

use of radioisotope thermoelectric generators (RTG's) as the primary power source. The subsystem includes power control and conditioning equipment to supply the loads with electrical power at the required voltages and regulation. No secondary batteries have been included in this conceptual design, in view of the continuous nature of the RTG power source. The absence of a secondary battery and its associated charge-discharge circuitry improves the reliability of the subsystem. Peak load requirements such as for pyrotechnics can be satisfied with capacitors or small primary batteries.

The RTG output is shunt regulated by a dissipative shunt regulator to provide a central dc voltage regulated to ± 5 percent. If the SNAP 27 is used, the nominal voltage would be 14 vdc.

The central voltage regulator combines the following functions:

- Provides constant RTG operation in the full-power mode

- Provides constant spacecraft thermal profile (except for variations corresponding to RF power changes) in the presence of varying loads. This function is accomplished by the distribution of several power-sharing shunt elements around the vehicle

- Distributes semi-regulated dc power directly to attitude control, propulsion, and thermal subsystems

- Distributes semi-regulated input power to communications and data handling converters

- Functions as the regulating element of the central inverter, which supplies ± 1 percent regulated ac voltage to experiment loads. It may be noted that the shunt regulator output voltage tolerance is ± 5 percent rather than ± 1 percent because its feedback loop is closed around the inverter output; and some ± 4 percent regulation is required to maintain the inverter output constant in the presence of varying experiment loads.

The selection of the hybrid dc/ac distribution is intended to make maximum use of existing communications and data handling dc/dc converters from Pioneer, while providing ac distribution to experiments for maximum reliability, efficiency, and design flexibility.

Protection against single-point failures in spacecraft subsystem loads is provided by a mix of open circuit failure mode design, black box level redundancy with switching logic, and current limiters integral to circuits or boxes. Partial mission success in the presence of a catastrophic experiment failure is provided by disconnection of the faulted experiment. Current monitor and switch logic is indicated descriptively in the block diagram. In the case of overload, the current monitor produces an OPEN signal to the switch to disconnect the experiment. An overriding CLOSE signal may be applied by ground command, to determine whether the fault is transient.

The central shunt regulator is a fully redundant design which incorporates majority voting redundancy in error amplifier and voltage amplifier stages, and quad power amplifiers.

The primary power source will consist of one or more RTG's. The number of RTG's required for each spacecraft is a function of the total

load and the power output of each RTG. The estimated weight and raw power available from integral numbers of two representative RTG's (SNAP 19 & 27) are shown in Figure 6.2-2. (These two RTG's are discussed further in Sections 6.2.4 and 6.2.5.)

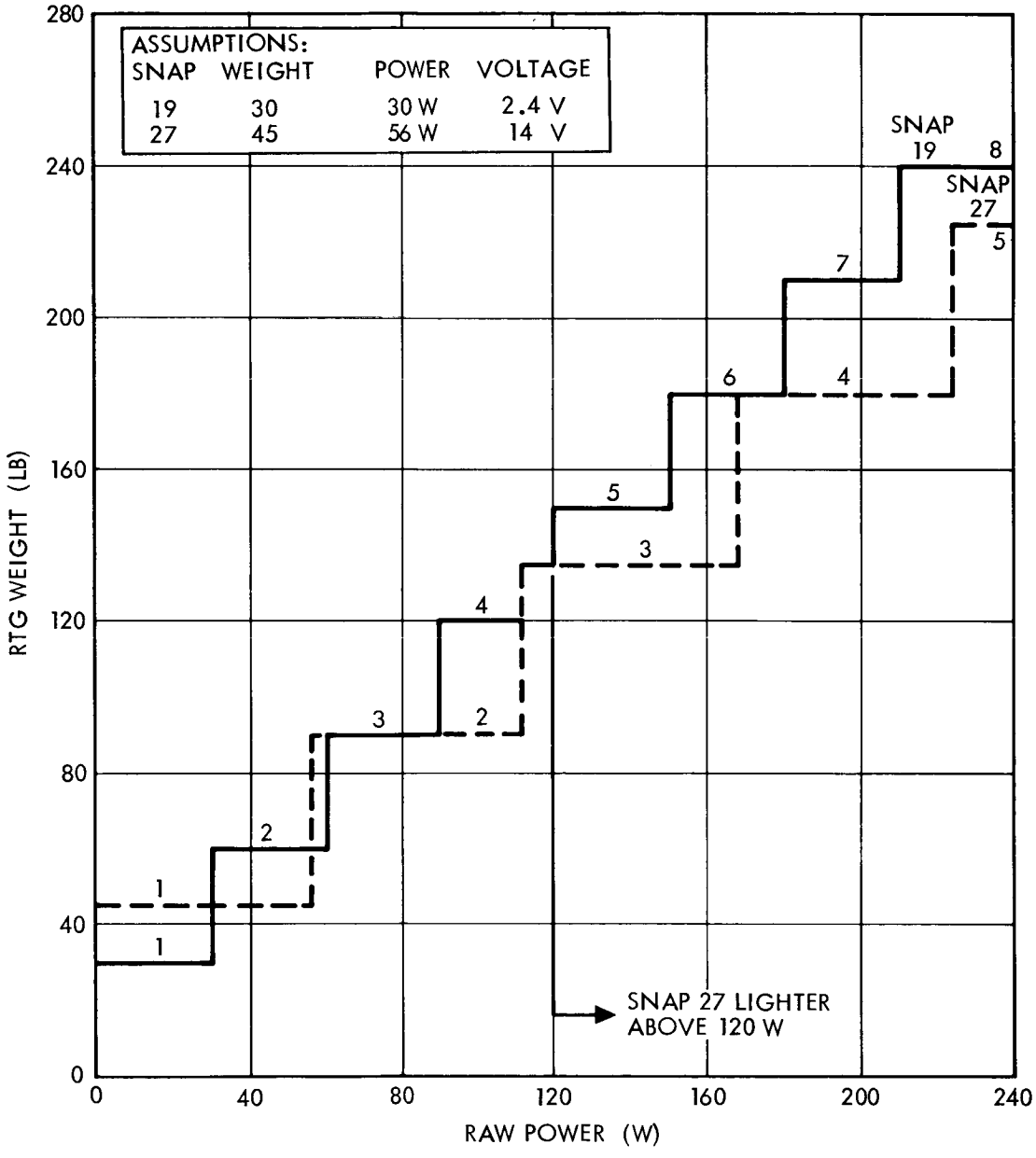

Figure 6.2-2. RTG Weight Versus Raw Power

Figure 6.2-2 may be used to select the number and type of RTG's to satisfy a particular load requirement. It is interesting to note that SNAP 19's need not be considered for loads greater than 120 watts (4 SNAP 19's) since it will always be lighter to use SNAP 27's above this power level. (The weight estimates for these two SNAP units will be refined further during the study.)

Spacecraft power load requirements have not been firmly established at this time. A probable minimum value is 70 watts. Detailed power requirements will be established during the remainder of the study.

6.2.3 Alternate Conceptual Designs

a. Solar Power Sources

Photovoltaic conversion for missions out to about 30 AU from the sun is not practical with currently available devices. Solar power systems using solar concentrators, such as solar thermionics, would require very large high quality concentrators as well as relatively precise sun pointing; hence these are also deemed impractical. Nuclear power is clearly the only satisfactory answer for this application.

b. Nuclear Reactor Power Sources

Reactor power sources are suitable for power levels of 500 watts or more. Below 500 watts reactor systems are not competitive with RTG's in terms of weight. Since the power requirements for Advanced Planetary Probes are on the order of 100-200 watts, reactor power sources will not be considered further in this study.

6.2.4 State-of-the-Art Consideration

Several RTG's are currently under development. Of these, the SNAP 19 and SNAP 27 are of interest to this study. Both are fueled with Pu-238, whose 86.4 year half-life and relatively low radiation make it the most suitable isotope for this application. The SNAP 19 and SNAP 27 are rated at 30 and 56 watts of raw output power, respectively. Both use lead-telluride thermocouples.

Electrically heated SNAP 19 generators have been undergoing tests at Goddard Space Flight Center since February, 1965. Two units are scheduled for flight on board the Nimbus-B in 1967.

The SNAP 27 is being developed for use in the ALSEP program. Flight qualification models are to be completed in December, 1966.

Thus, both RTG's would seem to be compatible with the APP program as far as development schedules are concerned.

There are, however, three significant problem areas which must be resolved before either unit can be considered satisfactory for Advanced Planetary Probes. These are:

- Radiation and magnetic interference between the RTG's and the scientific experiments onboard
- Provisions for complying with the nuclear aerospace safety requirements of the AEC
- Need for hermetic seals to prevent sublimation of lead-telluride thermoelements.

The interference problem is discussed in detail in Section 6.2.5. The aerospace safety problem is being studied at TRW Systems with the assistance of the RTG manufacturers. At present, our conclusions regarding aerospace safety are as follows:

1) Both SNAP 19 and SNAP 27 would be suitable (with minor modifications) if a safety philosophy of capsule burn-up and controlled dispersion of the isotope is acceptable to the AEC.

2) Neither unit as presently designed is satisfactory if intact reentry and complete containment of the isotope is required.

The possibility of RTG degradation or failure as a result of seal leakage is of concern in this application because of the long mission lifetimes involved and the probable exposure of the externally mounted RTG's to impacting particles during deep space missions. Mission reliability would be improved by using thermoelements (e.g., silicon-germanium) which can withstand a vacuum environment without degradation.

6.2.5 Problem Areas

The design of an Advanced Planetary Probe incorporating an isotopic power supply can be influenced significantly by the interaction of the power supply with the spacecraft. The presence of nuclear

radiation and magnetic fields from a radioisotope power supply aboard the APP can influence the spacecraft configuration and the types and/or positioning of instrumentation and experiments which might be integrated into the spacecraft. A comprehensive evaluation of the nuclear radiation environments of typical radioisotope generators is being conducted and the potential interactions of typical instrumentation and experiments to this nuclear radiation is being studied to aid in the spacecraft systems planning effort.

The radiation fields associated with an RTG are characterized by the radiations from the decaying isotopic source. The primary radiations from plutonium-238, the isotopic fuel used in the generators of interest, are neutrons, gamma rays, and alpha particles. Alpha particles have very short ranges in materials so they do not contribute to the exterior radiation fields. The gamma rays from plutonium-238 result from the alpha decay process and spontaneous fission. Figure 6.2-3 shows the basic radiations from a bare plutonium source. The six alpha decay gammas, designated by the circles on the graph, are emitted at discrete energies. The 0.76 Mev and 0.875 Mev alpha decay gammas contribute about 90 to 95 percent of the exterior gamma radiation field associated with a generator. The low energy alpha decay gammas are attenuated by the generator structural material. The fission product and prompt fission gammas, which are emitted in a continuous spectrum, are more than an order of magnitude less intense than the alpha-decay gammas. The combined spectrum of gamma rays is shown in Figure 6.2-4 as calculated at TRW and as presented in Reference 6.2.1. Good agreement was obtained between TRW results and the results presented in Reference 6.2.1.

The neutrons emitted by a plutonium-238 source are from spontaneous fission and from alpha-neutron interactions with impurities in the source. If a plutonium oxide fuel form with naturally occurring oxygen is used, the majority of the neutrons result from alpha-neutron reactions with the 0.208 percent oxygen-18 which occurs in natural oxygen. Spontaneous fission produces about 2.5×10^3 neutrons/sec-gm Pu-238 and alpha-neutron reactions produce about 1.8×10^4 neutrons/sec-gm Pu-238 making a total neutron production rate of about 2×10^4

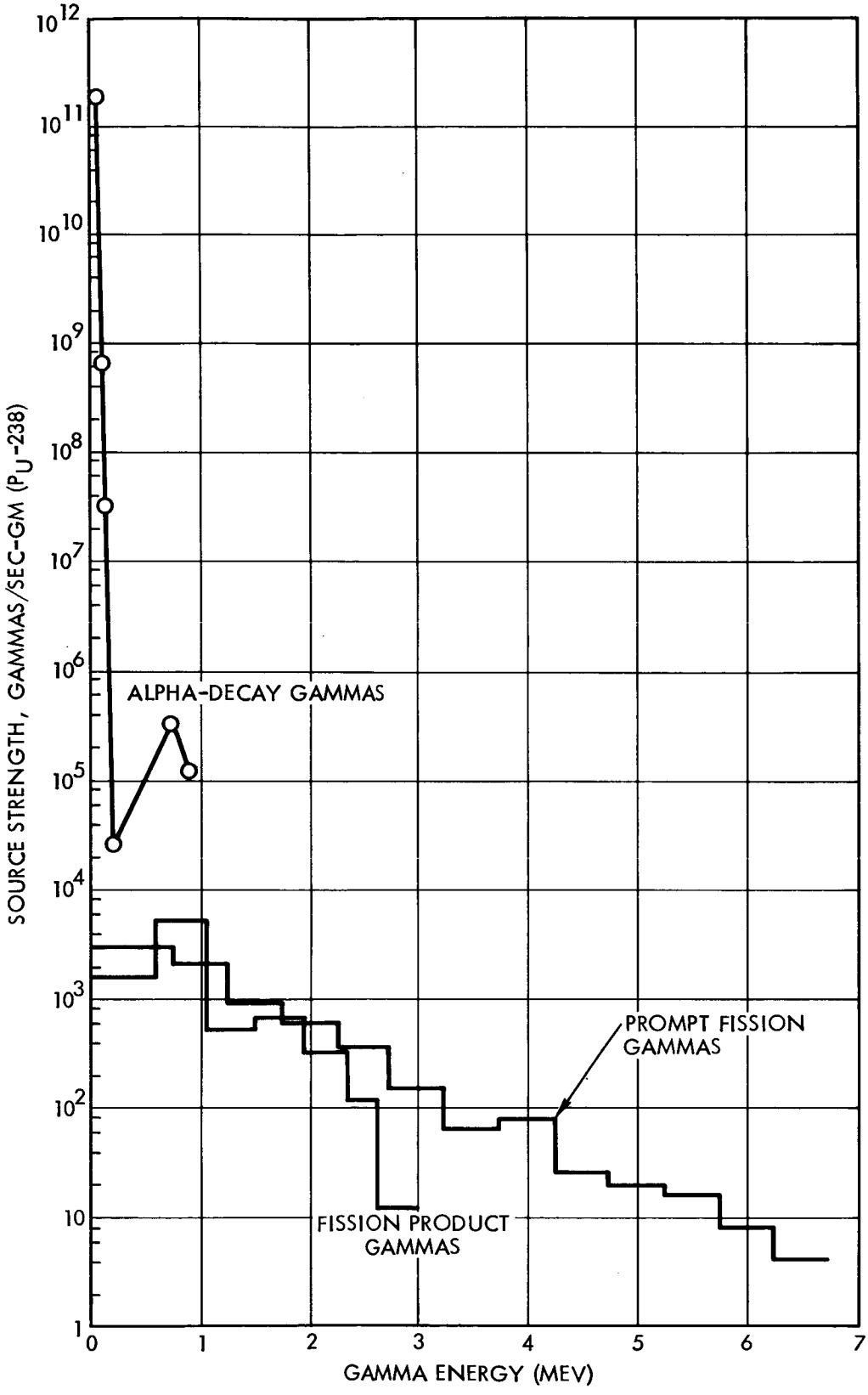

Figure 6.2-3. Gamma Radiation from Plutonium-238

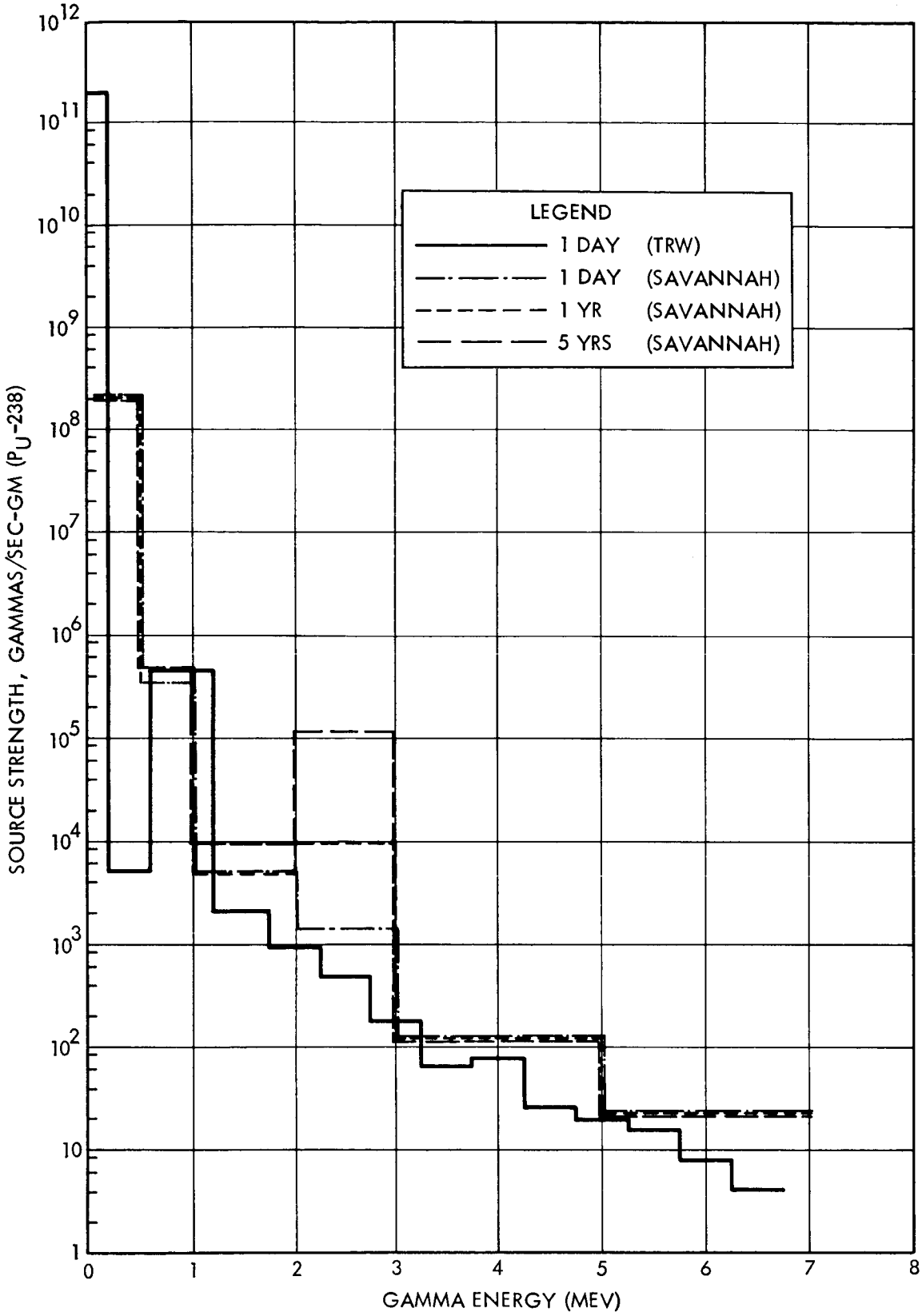

Figure 6.2-4. Total Gamma Radiation from Plutonium-238

neutrons/sec-gm Pu-238. Figure 6.2-5 shows the spectrum of neutrons from a PuO_2 fuel form using naturally occurring oxygen. The spectrum of neutrons from alpha-neutron reactions was obtained from Reference 6.2.1. Recent information from the Division of Isotopes Development indicates that the oxygen-18 content in the PuO_2 fuel form may be reduced, thus decreasing the total neutron production rate by a factor of 4.8 to 4.2 x 10^3 neutrons/sec-gm Pu-238. The neutrons produce approximately 80 percent of the total dose for a PuO_2 fuel form using naturally occurring oxygen while for a PuO_2 fuel form with reduced oxygen-18 the neutrons produce about 50 percent of the total dose.

The radiation spectra, dose rates and particle fluxes were obtained for the SNAP 19 RTG from References 6.2.2, 6.2.3, and 6.2.4, but since the results are classified CRD, they have been published in a separate classified report, Reference 6.2.5, which is furnished as Appendix A to this report. An independent check of the neutron and gamma fluxes was made at TRW and these results are also presented in Reference 6.2.5.

The scientific instruments which will be employed aboard the APP have been discussed in Section 4. The characteristics of each instrument are being studied to determine the sensitivity of the instruments to various types and intensities of radiation. Recent experiments performed at Ames Research Center were designed to measure the interaction of radiation from a SNAP 19 thermoelectric generator with experimental packages designed for the Pioneer spacecraft. The experimental packages aboard Pioneer consist of nuclear particle detection instruments and magnetic field measurement devices. The nuclear particle detection instruments which were tested by Ames were the Ames plasma analyzer, the MIT Faraday cup plasma experiment, the Graduate Research Center of the Southwest (GRCSW) cosmic ray detector and the University of Chicago cosmic ray experiment. The magnetic field measurement device which was tested was the fluxgate magnetometer provided by Goddard Space Flight Center. The radiation interference experiments conducted by Ames investigated the effects of separation distance, instrument orientation, and shielding on the instrument response to the radiation field surrounding the generator.

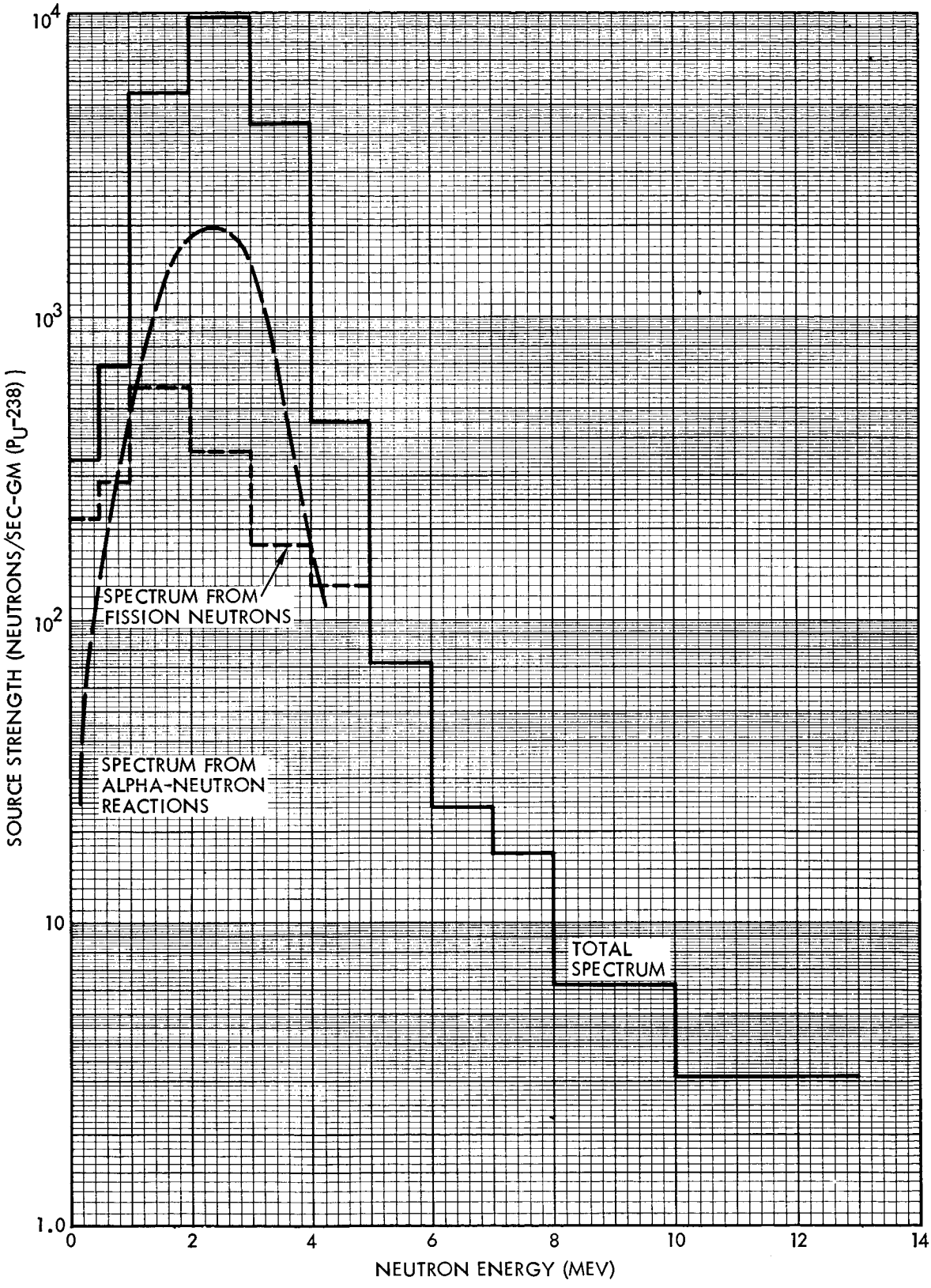

Figure 6.2-5. Neutron Radiation from Plutonium-238

The radiation interference experiments were conducted in a vacuum chamber at Lawrence Radiation Laboratory with separation distances between the spacecraft experimental package and the SNAP 19 generator varying from 0 to 9 feet. The plasma detectors tested by Ames were designed to measure relatively low energy protons in the 100 ev to 15 kev energy range and electrons in the 3 ev to 1 kev range. These instruments can normally measure a minimum flux of about 10^5 singly charged particles/cm^2sec. The secondary radiation produced by Compton scattering and photoelectric absorption of gamma rays from the generator and recoil atoms produced by neutron interactions produced no observable effects on either the Ames plasma analyzer or the MIT Faraday cup plasma experiment. Thus, these experiments indicate that the charged particle fluxes produced by radiation from the SNAP 19 generator are less than the minimum detectable level of 10^5 particles/cm^2-sec, and that there will be no radiation interference problem with the types of plasma probes used on Pioneer.

Two cosmic ray experimental packages were tested by Ames at LRL: the Graduate Research Center of the Southwest (GRCSW) cosmic ray detector and the University of Chicago (UC) cosmic ray experiment. The GRCSW detector was designed to detect protons and alpha particles in the 7.5 to 90 Mev energy range and additional cosmic ray particles in the 150 to 350 Mev range. The UC cosmic ray experiment was designed to detect cosmic rays in the 0.8 to 190 Mev energy range with several channels which allowed a crude spectrum measurement within this overall energy range. The GRCSW detector appeared to be sensitive to secondary particles, e.g., ionized recoil atoms, produced by neutron interactions with surrounding materials. The UC cosmic ray experiment was found to be very sensitive to gamma ray radiation in the lower 0.8 to 8 Mev energy range, but was found to be relatively insensitive to radiation in the higher energy ranges above 8 Mev. The high sensitivity of the instrument to the low energy gamma rays caused the instrument to saturate under certain modes of operation. The use of up to 4 inches of lead shielding significantly reduced the radiation sensitivity of the University of Chicago cosmic ray experiment.

Another method which may possibly be used to reduce the sensitivity of the UC cosmic ray experiment is to eliminate the low energy channel and measure cosmic rays in the 8 to 190 Mev energy range. In conclusion, it appears that there may be a radiation interference problem with the cosmic ray experiments; however, methods may be found to circumvent these problems by changing the instrument range, modifying the experiments, or by shielding.

The influence of the radiation field and the magnetic field associated with a SNAP 19 generator on a magnetometer was experimentally investigated by Ames Research Center. The experimental results showed that there was no change in the sensitivity of the magnetometer due to nuclear radiation fields at separation distances as close as 18 inches. However, the magnetic interference with the magnetometer was significant for the SNAP 19 generator. This may have been due to either the iron shoes or the metallic fasteners used on the particular generator employed for the experiments. Although the measurements of the influence of the magnetic fields surrounding the SNAP 19 generator on a magnetometer were cursory, the experiments indicated that significant interference can exist. The possibility of this interaction had been anticipated, and the Martin Company and General Electric had already been requested to evaluate means by which the magnetic fields surrounding their generators could be reduced and to estimate the magnitude of the reduced fields.

At present experimenters object to the use of isotopic generators aboard spacecraft due to the uncertainty associated with the interactions of the generator's radiation and magnetic fields with experiment packages aboard the spacecraft. Intuitively, experimenters feel that any additional radiation or magnetic fields are harmful and will degrade the effectiveness and accuracy of the experimental measurements. Since isotopic power sources appear attractive for deep interplanetary probes, deep space probes and solar probes, accurate definition of any interactions between the generator radiation and magnetic fields and spacecraft experiments is very important. After accurate definition of any interactions has been accomplished, methods of circumventing the interactions will be evaluated.

Another consideration requiring investigation is damage to materials and equipment aboard the spacecraft which may be a function of mission time. For example, materials such as structural metals, ceramics, polymeric materials and electronic components are sensitive to time integrated gamma and neutron fluxes. Neutron and gamma damage thresholds for materials, i.e., radiation doses for which detectable changes in material properties occur, vary, but the most sensitive to neutron and gamma irradiation damage are electronic components such as semiconductors, solar cells, and electron tubes which have neutron and gamma threshold damage levels of about 10^{10} n/cm^2 and 10^4 rads, respectively. For a neutron flux of 100 n/cm^2-sec, a gamma flux of 100 gammas/cm^2-sec, and a mission time of five years, the integrated neutron and gamma fluxes (1.6×10^{10} n/cm^2 and 6×10^3 rads, respectively) approach the threshold damage values for sensitive electronic components. Thus, for long mission times the gamma and neutron fluxes from the radioisotope power supply must be integrated over mission time, and the radiation flux values obtained must be compared with tolerable values for the components of interest.

6.2.6 Studies to be Performed

a. Power Requirements

Peak and average power requirements for all subsystems will be defined as a function of mission phases. Power quality requirements will be established. Load profiles will be constructed from these requirements.

b. Power Subsystem Configuration

Subsystem studies will be made to result in a recommended design which satisfies all requirements, including the best method of supplying peak power. A preliminary subsystem specification will be generated defining sizes, weights, performance, and reliability.

c. RTG Power Source

Modifications required to adapt SNAP 19 and SNAP 27 to APP applications will be examined, particularly with respect to aerospace safety and interaction with experiments. The advantages to be gained

by going to a new RTG design which incorporates advanced technology will be investigated. Possible approaches include (1) elimination of lead-telluride thermocouples to improve magnetic cleanliness, (2) use of silicon germanium thermocouples to eliminate the need for hermetic seals, and (3) improvements in isotope purity and capsule design.

d. Detailed Distribution Studies

Based on the results of Item a., power distribution will be refined to optimize reliability, efficiencies, weight, and performance. Should ac distribution to communications loads appear advantageous, approximate design cost tradeoffs will be examined.

e. Circuit Design

Elimination of integral preregulators from existing converters will be considered. Need and implementation of central inverter redundancy will be studied.

f. Peak Power Capability

The need for a primary or secondary battery, or passive energy storage will be investigated based on valve and squib requirements. Use of a thermal battery will be considered as an alternate.

g. Experiment Disconnect Switch

A tradeoff study will be conducted on static switches versus magnetic latching relays. The magnetic latching relay requires minimum auxiliary circuitry, but may present too great a magnetic field problem.

h. Electromagnetic Compatibility

EMC constraints will be incorporated into ac/dc distribution tradeoffs. ac frequency will be compatible with satellite spectrum usage. Square wave rise time will be constrained as required and active filtering will be compared to passive filtering.

REFERENCES

6.2.1 D. H. Stoddard and E. L. Albenesius, "Radiation Properties of 238 Pu Produced for Isotopic Power Generators," Savannah River Laboratory, DP-984, July 1965.

6.2.2 A. M. Spamer, and K. G. Davenport, "SNAP 19 Program Generator Radiation Analysis," MHD-3169-15, Martin Company, August 1964. (CRD)

6.2.3 K. Davenport, "Radiation Dose Rates, SNAP 19 Phase III Generators," MHD-3607-4, 4 October 1965. (CRD)

6.2.4 K. Davenport, "Radiation Dose Rates, SNAP 19, Phase III," MHD-3607-4, Rev. 1, 12 January 1966. (CRD)

6.2.5 J. R. McDougall, "SNAP 19 Radiation Field," TRW Systems, TRW 9990-7237-T5000, March 1966. (CRD)

6.3 ATTITUDE CONTROL SUBSYSTEM

6.3.1 Functions and Performance Requirements

High information rates in the communication system can be achieved most efficiently by using a high-gain microwave antenna on the spacecraft. As high gain usually implies small beamwidth, the attitude control system must be able to point this antenna to the earth with sufficient accuracy.

During midcourse maneuvers, if conducted according to the normal program of Section 3.5, specific attitudes are required in order to obtain velocity increments in the appropriate directions. The attitude control system must be capable of positioning the spacecraft in any commanded orientation and then return it automatically to the earth-pointing mode. Scientific experiments might also require the establishment of fixed or programmed attitudes during transit or in the proximity of the target planet. In addition, the attitude control system should provide stabilization against disturbances of internal and/or external origin. Attitude stabilization can be accomplished by spinning the spacecraft about the principal axis of maximum moment of inertia or by resorting to active 3-axis stabilization. Either approach has its own advantages, depending upon the mission requirements and spacecraft configuration under consideration.

For a maximum allowable loss of 1 db in antenna gain, the pointing error for a 16-foot diameter paraboloidal antenna should not be greater than 0.55 degree. In order to obtain the same gain tolerance with a 32-foot paraboloidal antenna the pointing error should not exceed 0.287 degree. These figures will be considered as typical design objectives for preliminary design calculations.

Among all the references that may be used for antenna pointing, closed-loop RF links seem to be the most accurate, but they have the disadvantage of being complex and requiring large powers in the ground stations. (However, for a spin-stabilized spacecraft during most of the interplanetary phase, RF signals are necessary for attitude error sensing only a small percentage of the time, and the spacecraft could be unattended for possibly days at a time.) Optical sensors for fine control have the disadvantage of pointing the antenna geometrically, not electronically, but their main advantage is that they do not require ground stations. If the optically sensed references are other celestial objects than the earth, a stored program is necessary to determine antenna aiming directions in spacecraft coordinates.

The tradeoff between spin-stabilized and 3-axis stabilized approaches is not only influenced by mission requirements or communication system performance but also by midcourse guidance requirements. As data on these guidance maneuvers are not available yet, only the problems of sensing and actuation have been considered during this phase of the study.

Electronic methods for attitude sensing are expected to improve considerably in the decade ahead and for this reason as well as for their accuracy they will be given special consideration in the present study.

6.3.2 Conceptual Design for Spin-Stabilized Spacecraft Configuration

Spin-stabilized configurations in which the spin axis coincides with the symmetry axis of the antenna system have the advantage of simplifying the mechanization of RF angle-tracking systems. Conventional conical scanning can be implemented without the need of rotary coupling devices or slip rings. Attitude control of spinning

spacecraft is usually accomplished by means of transversal impulsive torquing, which results in stepwise angular displacements of the resultant angular momentum vector. This results in nutation of the spin axis about the new angular momentum vector. Damping of this "wobble" can be accomplished by means of a passive damper or by an active scheme consisting of two gas jets, one for initiating nutation and the other for terminating it after the spin axis has described a 180 degree arc about the angular momentum vector resulting after the first moment impulse. This last approach is preferable because it not only reduces wobble but also minimizes spin speed changes. To accomplish large angular displacements a sequence of a number of such pulse pairs is required.

Attitude control systems for spin stabilized spacecraft configurations will then be assumed to consist of a conventional conical-scan system for attitude sensing in the earth-pointing mode and a two-pulse torquing system for attitude corrections. Additional attitude sensing devices are required for operation modes in which other attitudes are to be established, such as for midcourse maneuvers and/or scientific experiments. The orientations for these maneuvers may be accomplished open loop or closed loop. The total precessing impulse required to give the desired angular displacement of the spin axis is computed, based on the estimated moment of inertia and spin rate, and torquing pulses of appropriate timing and magnitude are commanded. In the open-loop method, it is taken on faith that the desired orientation has been attained, and the operation proceeds. In the closed-loop method, the attitude after precession is sensed, and a final correction is made if necessary. The attitude sensor may consist of an optical device for recording the passage of stars as it scans in a plane perpendicular to the spin axis. This sensor not only locates the spin axis by identification of the stars observed, but also provides indexing to establish the orientation of the spacecraft at any instant in the rotation cycle. The implementation of this mode of attitude control for maneuvers depends on whether 2-way communication is available in the off-cruise attitude, and therefore on the distance from earth at the time of the maneuver.

Earth acquisition is another problem that may require additional sensing devices. Initial acquisition is a simple maneuver when the actual spacecraft attitude and position are known and there is an auxiliary communication link. Acquisition at distances greater than the range of this communication system requires another device to determine spacecraft orientation with respect to the earth or a new reference such that, after it is acquired, the angle between the spin axis and the earth is within the range of the conical-scan system. The sun could be such reference, after 50 or 60 days from launch date, provided the conical-scan system has an acquisition range of from zero to about 25 degrees. (Figure 3.3-5 shows that, for three sample trajectories, the sun-spececraft-earth angle remains under 27 degrees after the first 50 days.)

This requirement implies an antenna beamwidth of the same order of magnitude, which might result in some deterioration of the system pointing accuracy. Depending on the mission, pointing accuracy and distances involved, two conical scan antennas may be required, one with a beamwidth of about 25 degrees for acquisition and another one for fine pointing control. Other references in place of the sun might be required for deep space missions or where the possibility of eclipses or confusions makes this reference undesirable. Figure 3.3-5 shows that the sun would periodically come very close to the spin axis of an earth-pointing spacecraft, as the earth goes through successive conjunctions, as seen from the spacecraft.

Acquisition must be an automatic process to be initiated when the spacecraft is in the earth pointing mode and the target gets out of the range of the wide-beam conical-scan antenna. Assuming the sun is the auxiliary acquisition reference, the sequence of operations would be as follows:

a) Acquire the sun

b) After the sun has been acquired, signals should be received by the wide-beam conical-scan antenna. An earth acquisition with this antenna should follow.

c) Once the earth has been acquired with the wide-beam antenna, the narrow-beam antenna is used for fine pointing.

This acquisition method is illustrated in Figure 6.3-1. If the wide-beam antenna system fails to receive signals after step a), the spacecraft will remain pointed to the sun until the sun-earth angle comes within the range of the fine-control antenna.

A block diagram of the attitude control system concept developed for the earth-pointing mode is shown in Figure 6.3-2.

The ground station is assumed to consist of a 210-foot diameter transmitting antenna radiating 100 kw in the 2.3 gc band. Ground stations involving smaller antennas are also being considered in view of the high signal-to-noise ratios obtained with high-gain on-board antennas.

Three types of conical-scan receiving antennas have been considered in order to compute the errors due to thermal noise as a function of beamwidth.

A summary of antenna characteristics and the corresponding RMS angular errors at Jupiter and Neptune is given in Table 6.3-1.

For these calculation the noise power spectral density was assumed to be -164 dbm and the demodulator output filter bandwidth was supposed to be 1 cps.

These errors are due to thermal noise only and have been computed assuming coherent detection.

A lower bound in the error due to thermal noise could be obtained by assuming an equivalent servo bandwidth for the tracking system. For instance, if this bandwidth is of the order of 0.02 cps, the corresponding error figures may be obtained from the 1 cps values by dividing by $\sqrt{50}$.

The conical-scan process results in amplitude modulation of the received carrier. For non-zero attitude error the resulting modulating signal consists of a fundamental component at the spin frequency and even and odd harmonics. These harmonics are all in phase with the fundamental component and the peak value of the complex waveform occurs when the beam axis is closest to the target axis. Assuming ideal components, for an impulsive torquing system this is the time

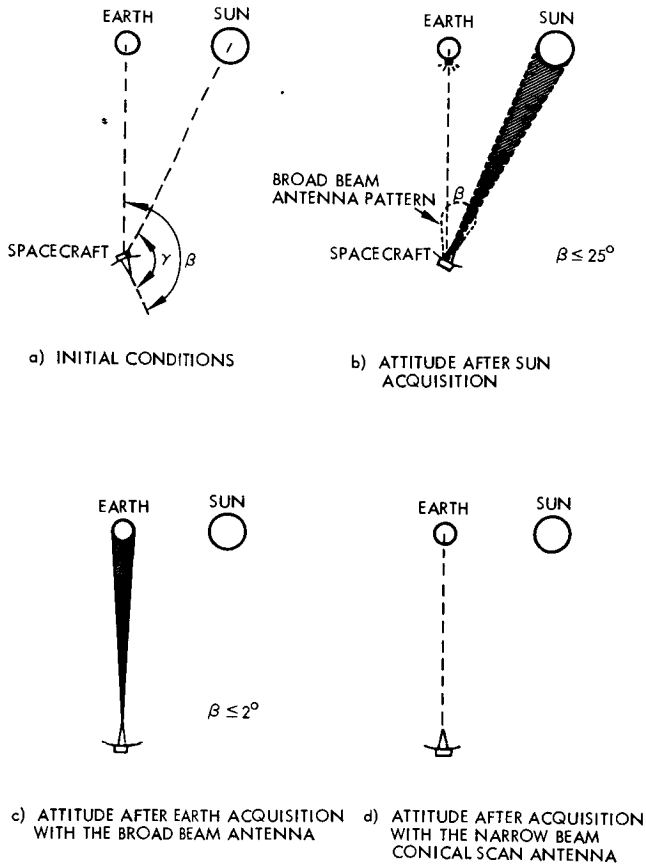

Figure 6.3-1. An Acquisition Scheme with the Sun as Secondary Reference

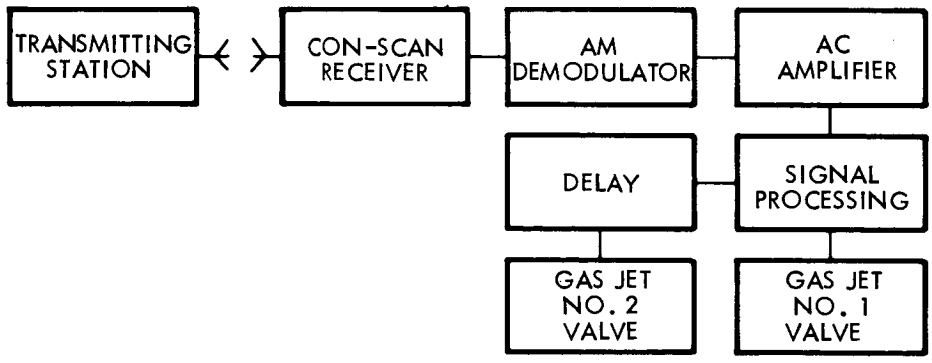

Figure 6.3-2. Control System Block Diagram for the Earth-Pointing Mode

Table 6.3-1. RMS Angular Errors Due to Thermal Noise in Conventional Conical-Scan Attitude Sensing Systems

PARAMETERS	ANTENNA TYPES		
	30" Helix	4' Paraboloidal	16' Paraboloidal
Peak Gain [db]	13	23	38
Boresight Gain [db]	10	20	35
Beamwidth [degrees]	25	8	2
R.M.S. Angular Error at Jupiter [degrees]	0.5	0.05	0.0016
R.M.S. Angular Error at Neptune [degrees]	31	0.32	0.01

when the train of control pulses should be initiated to decrease the existing attitude error. For small error angles, the peak value of the ac component of demodulator output is a linear function of the error angle. For each value of signal-to-noise power ratio there is an optimum value of beam offset angle, normalized to beamwidth units, which minimizes the RMS error angle due to thermal noise.

The signal processing consists in finding the time at which the amplified domodulator output reaches its maximum value.

The first gas jet is offset with respect to the antenna beam plane in order to account for the delay introduced by the finite actuation time of the pneumatic system.

Relative positions of the gas jets with respect to the antenna beam are shown schematically in Figure 6.3-3, where

$\mu = \omega_s t_a$

t_a = delay due to actuator dynamics

$\Delta\phi = \frac{A}{C}\pi$

C = spin moment of inertia

A = transverse moment of inertia

The angular displacement after a pair of impulses is approximately given by

$$\Delta\Psi \simeq \frac{2M}{C\,\omega_s} \quad \text{(rad)}$$

where

M = moment impulse (ft-lb-sec)

C = spin moment of inertia (ft-lb-sec^2)

ω_s = spin angular frequency (rad/sec)

which shows the desirability of operating with small inertia and spin rate to minimize gas consumption. The maximum rate obtainable is given by

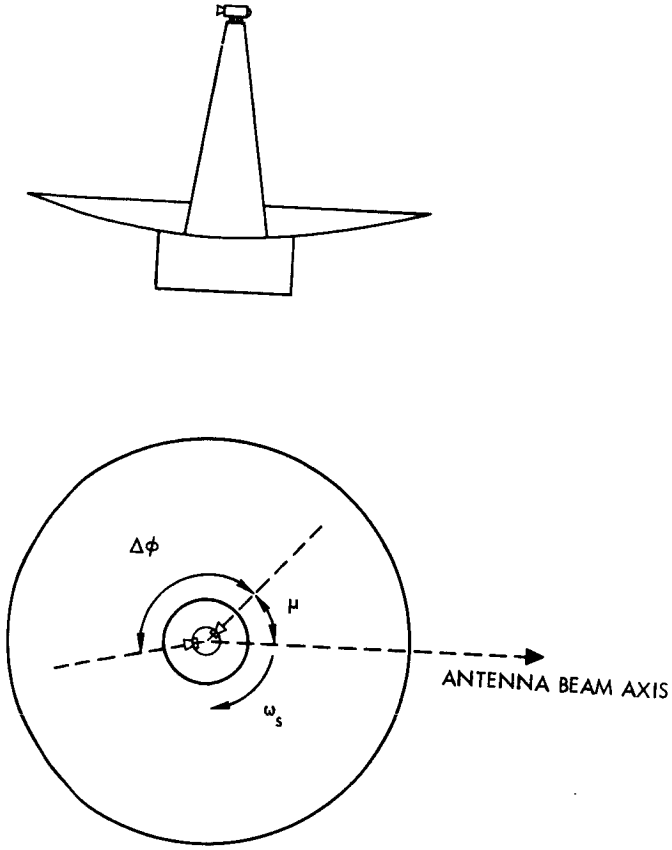

Figure 6.3-3. Gas Jet Nozzle Locations

$$\frac{\Delta\Psi}{\Delta T} = \frac{\omega_s}{2\pi} \quad \Delta\Psi \simeq \frac{M}{\pi C}$$

which shows it is independent of the spin rate. The gas consumption per degree for the 2-pulse system is given by

$$\frac{M_p}{\Delta\Psi} = \frac{C\,\omega_s}{57.3\, I_{sp}\, \ell}$$

where M_p is the gas consumption per step displacement, I_{sp} is the specific impulse and ℓ is the moment arm.

An error analysis of the torquing system has shown that the residual wobble originated by the 2-pulse system may be minimized by selecting an adequate value for λ, which is defined by

$$\lambda = \frac{C - A}{A}$$

Although the 2-pulse torquing system is characterized by a very small residual wobble angle, an additional passive damper may be required to take care of this residual wobble as well as the wobble induced by mid-course maneuvers or solid rocket injection motor operation.

Attitude control system design parameters computed for the sample spacecraft configurations are given in Table 6.3-2.

6.3.3 Three-Axis Stabilized Spacecraft Configurations

Three-axis attitude stabilization requires two references, one of which might be the earth if RF angle tracking systems are used. Trade-off studies are being conducted to determine the relative advantages of the following approaches:

1) Two-coordinate, amplitude-comparison monopulse for pitch and yaw - and single star tracker

2) Two-coordinate, phase-comparison monopulse for pitch and yaw and single star tracker

3) Electrically or mechanically gimballed sun and Canopus sensors.

6.3.4 Alternate Conceptual Designs

Alternate conceptual designs have been discussed in the preceding sections. However, there is an alternative torquing approach for spin stabilized spacecraft that is worth investigating: a two-pulse system in which the angle between gas jets is not $\frac{A}{C}\pi$ but π. Wobble damping may not be as good in this case, but the attitude control system reliability might be increased due to the possibility of operating with either one of the gas jets individually in a single-pulse failure mode.

6.4 TELECOMMUNICATIONS

6.4.1 Function

The function of the telecommunication system is tracking, telemetry, and command. In addition, for some attitude control approaches, the telecommunication system has to provide angle tracking data to the attitude control system.

APP Configurations	PD74-22 PD74-23 PD74-25	PD74-26 (1)	PD74-27	PD74-28
Total spacecraft weight (lb)	450-500	1000	700	2340
Spin moment of inertia (sfs)	200	714 (roll)		1071
Transverse moment of inertia (sfs)	129	555		723
Moment arm (feet)	8.1	16		13.25
Assumed spin rate (rpm)	5	-		5
Moment of inertia (λ)	0.55			0.482
Optimum λ for minimum wobble	0.50	-	0.50	0.50
Antenna diameter (ft)	16	27	16	32
Allowable error (deg)	0.57		0.57	0.287
Angle Step Size (deg)	0.2	-	0.2	0.1
Deadzone amplitude (deg)	0.2-0.5		0.2-0.5	0.1-0.25
Moment impulse (ft-lb-sec)	0.183			0.49
Thrust impulse (lb-sec)	0.023			0.037
Gas consumption (lb/deg)	0.0038			0.0123
Maximum rate (deg/sec)	0.0081			
Acquisition antenna BW (deg)	25			
Fine control antenna gain (db)	20			

(1) The configuration of PD74-26 is 3-axis stabilized, the others are all spin stabilized.

Table 6.3-2. Attitude Control System Design Parameters

Tracking of the probe by the DSIF station is required in order to determine accurate vehicle trajectory. Tracking information is obtained from the measurement of the two-way doppler frequency shift, apparent angles of arrival of the signal transmitted by the probe, and the ranging. It will be assumed in this study that ranging information is not absolutely necessary and may be provided only during initial portion of the mission. Two-way doppler measurement and angle tracking, however, is required throughout the mission.

The telemetry link is required to transmit spacecraft performance parameters and the experiment data. The telemetry rate that can be supported is a function of the communication range. To provide maximum bit rate, the information rate will have to be changed at appropriate flight times. For the telemetry link information rates from 1 bps to 10 kbps will be considered with the bit error probability not more than 5×10^{-3}.

The command link is required for the flexible control of the spacecraft and for the correction of failure modes. The required data rate for the command system is low, with one bps quite adequate. The accuracy requirement, however, is much more severe than for the telemetry link. The bit error probability of at least 1×10^{-5}, without error detection or error correction coding, is normally required.

For the spin-stabilized spacecraft, a modified conical scan radar technique is used for pointing antenna at the earth. In this case the RF carrier transmitted by the DSIF is tracked by the probe receiver and pointing error signals are provided for the attitude control system.

For a three-axis stabilized spacecraft, the sun and Canopus can be used for attitude references although electrically or mechanically gimballed sensors are required. Alternatively, simultaneous lobing techniques can be used to point the spacecraft at the earth, Canopus providing the third axis reference.

6.4.2 Conceptual Design of Telecommunication Systems

6.4.2.1 Introduction

The APP concept under study utilizes a 16 to 32 foot transmitting antenna. Antennas of these sizes will have beamwidths between 2 degrees

and 1 degree, and therefore require accurate pointing. In the case of spin-stabilized spacecraft, angle tracking can be obtained most easily by using the conical scan methods. For the 3-axis stabilized spacecraft, offset sun/Canopus sensors are preferred but simultaneous lobing methods can also be used to obtain accurate antenna pointing toward the earth. Indeed, the main difference between Mariner 4 (as well as Pioneer 6) and the APP communication systems considered, is this requirement for accurate attitude control. Therefore, the most natural classification of the communication systems is according to the method used for obtaining attitude references. The emphasis here is placed on the spin stabilized spacecraft, however, 3-axis stabilized probes are briefly considered.

6.4.2.2 Telecommunication Systems for Spin-Stabilized APP

A simplified baseline communication system for the spin-stabilized APP is given in Figure 6.4-1. The receiver, exciter, and the power

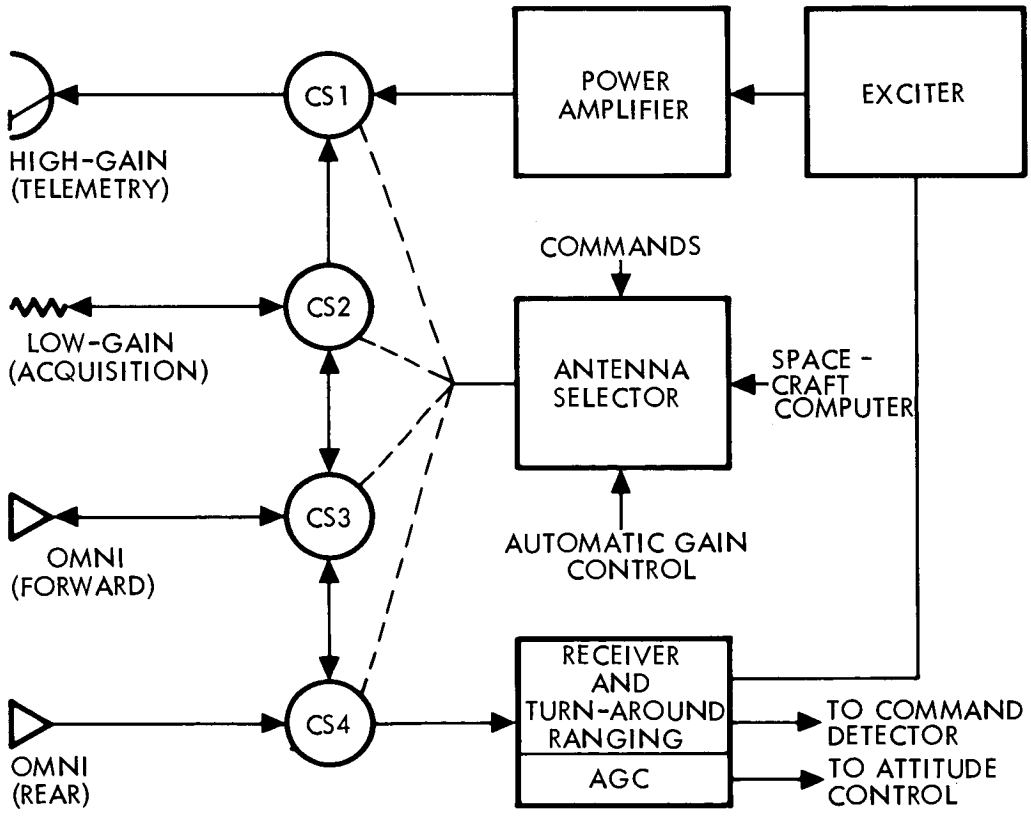

Figure 6.4-1. Baseline Telecommunication System for Spin Stabilized APP

amplifiers can be similar to those of Mariner 4. Although a transistorized 10-watt amplifier can be designed even for 1970 launch, the efficiency would be of the order of 20 percent. The TWT power amplifier used by Mariner and Pioneer would have an efficiency of the order of 30 percent. Further reliability studies are necessary to select between these alternates. Circulator switches are used for switching of antennas. Antenna selection would be controlled by ground commands, programmed central computer and sequencer events, or receiver automatic gain control, AGC. It is estimated that the weight of the system for 1970 launch, excluding antennas, would be about 20 pounds, and about 35 watts of power would be required for a 10 watt TWT.

The receiver AGC a-c component is proportional to the spacecraft axis pointing error and will be supplied to Attitude Control System (ACS). Furthermore, it appears that a coherent AGC channel of the type employed by the Mariner 4 receiver could provide an optimum angle tracking signal without any significant additions or modifications. The only addition to the communication system due to the angle tracking requirement is the helix antenna, A_2. The beam of the helix antenna is to be tilted about 10 degrees off the spin axis and would be used for acquisition and positioning of the high-gain antenna, A_1 when signal-to-noise ratio is adequate. Such an antenna would be about 22 inches long with an on-axis gain of 14 db. For fine positioning, in the presence of low signal-to-noise ratio, the high-gain antenna, A_1, with an offset feed would be used. The use of the 16 to 32 foot paraboloid high-gain antenna for fine angle tracking has a gain disadvantage. Because of the offset feed, there is a transmitting pointing loss which could be as high as 3 db. It should be pointed out that there is no room for locating two feeds in order to completely avoid the 3 db loss. Ways around this problem are under investigation. The omnidirectional antennas A_3 and A_4 are required during the initial part of the mission and would be used as long as communication distance permits. Antenna A_3 provides forward hemisphere coverage while A_4 has backwards hemisphere coverage. A_4 would be used only immediately after launch.

Aside from the possible problems mentioned, the baseline system of Figure 6.4-1 must be augmented to improve system reliability. To

improve the probability of mission success, at least a second receiver, power amplifier, and an exciter should be added. Such a system is indicated in Figure 6.4-2. In addition to the redundant receiver and

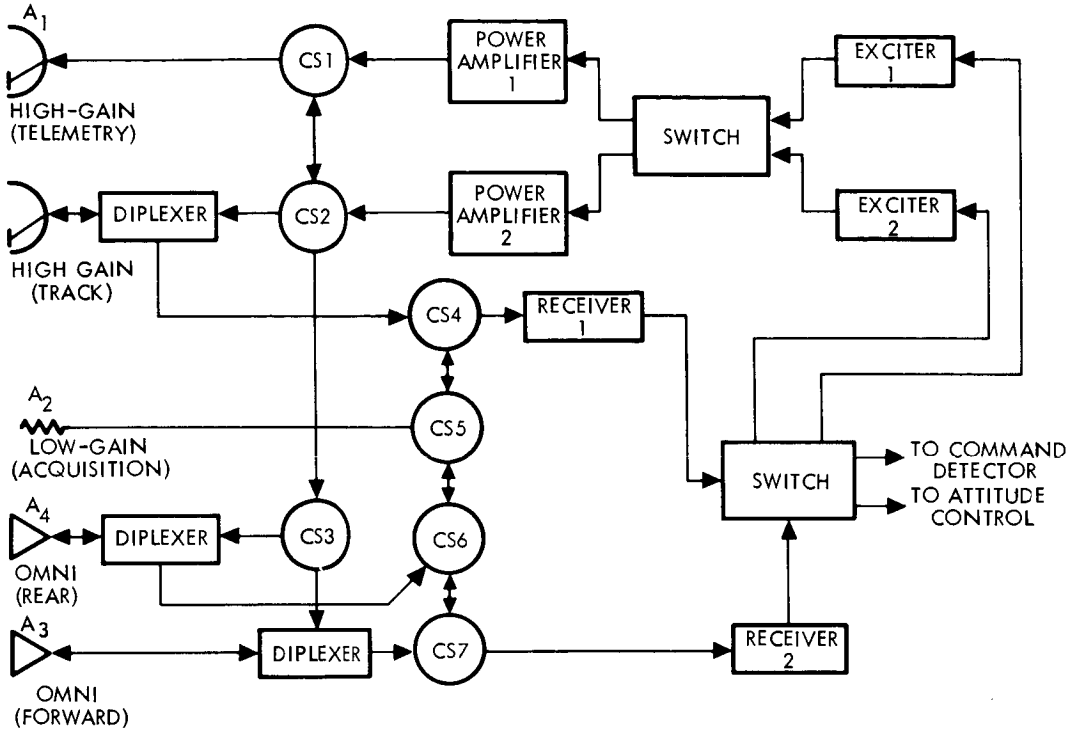

Figure 6.4-2. Telecommunication System for Spin-Stabilized Spacecraft

transmitter, this configuration also includes a fifth antenna. The main problem with this system is the complexity of the antenna- switching hardware. The antenna-switching arrangement shown should be considered preliminary. Antennas A_1, A_3, A_4, and A_5 may be used for telemetry while A_2, A_3, A_4, and A_5 can be used for reception. The helix antenna would be used for coarse angle tracking while the paraboloid antenna, A_5, with the diameter of about four feet is designed for fine angle tracking. It appears advantageous to use Cassegrain feed for the high-gain paraboloid. The back part of the medium-gain paraboloid antenna could be contoured to a hyperbola and used as part of the Cassegrain feed. One advantage of the Cassegrain feed is reduction in cable losses. However, about 1 db decrease in antenna gain is caused

by aperture blocking and the net advantage of the Cassegrain feed is less than 1 db.

It appears that the support members for the medium-gain paraboloid, the helix, and the feed should be made from aluminum and form a tripod. A large conical dielectric tubular column (typically fiberglass) is not recommended. It is possible that the column would act as a dielectric horn guiding the radiation away from the feed and resulting in improper illumination of the paraboloid. Also, the aluminum support struts could accommodate the transmission lines from the helix and the medium-gain antenna feed.

It is estimated that the weight of the system shown in Figure 6.4-2, excluding antennas, would be 33 pounds and the required power 40 watts.

6.4.2.3 Telecommunication Systems for Three-Axis Stabilized APP With RF Tracking

In this section monopulse radar tracking techniques for obtaining antenna pointing at the earth will be briefly considered.

Extensions of the TRW Voyager studies of sun/Canopus 3-axis stabilization indicate that gimballed sensors can readily provide adequate accuracy. Boresight errors can be eliminated by applying a bias whose value is determined by maximizing ground received power. Smaller attitude control limit cycle motions than those used for Mariner are, however, required. An alternate tracking system based on simultaneous lobing techniques is also possible to point the antenna at the earth. As with the spin-stabilized probes, the RF signal transmitted by the DSIF would be tracked. Single channel mechanizations for the angle trackers, resulting in minimum weight system, have been described by JPL[1] and TRW.[2] Even so, the antenna mechanization is complex and many RF components probably would have to be located at the antenna feed. A second acquisition or coarse angle tracking antenna in this case is not needed. The mechanizations of these angle trackers will be defined in detail in the future reports in order to facilitate tradeoffs.

---

[1] EPD-139, Vol. III.

6.4.3 Performance

Both telemetry and command modulation methods can be described as PCM/PSK/PM. The JPL-developed two-channel PN synchronization techniques are assumed in the calculations of the system performance given in Tables 6.4-1, 6.4-2, and Figure 6.4-3. Spacecraft parameters are based on Mariner 4 performance. For DSIF a 210-foot diplexed, low-noise antenna with 100 kW transmitter power is assumed for maximum spacecraft ranges. This is a planned and required capability for Voyager. During the major portion of the mission to Jupiter the 85-foot antenna would be sufficient for both uplink and downlink. The DSIF receiver loop noise bandwidth, $2B_{LO}$, was taken to be 12 cps and is as presently implemented.

Table 6.4-1 indicates that with a 16-foot spacecraft antenna and a 10-watt transmitter reliable 400 bps transmission rate at about maximum Jupiter range (6 AU) is possible. In Figure 6.4-3 a plot of a bit rate versus communication distance for various power gain products, PGP, is presented. PGP is here defined as the product of transmitter power and actual antenna gain, not peak gain. PGP is also equal to effective radiated power minus circuit loss. From Figure 6.4-3 the size of the antenna and/or the required transmitter power for a specified information rate can be obtained. A sample uplink performance calculation is presented in Table 6.4-2. This design control table indicates that the 210-foot transmitting antenna would not be required if a 22 inch helix is used. The signal-to-noise ratio needed for the angle tracking, however, may dominate the uplink requirements.

At low bit rates the single-channel PN systems may be used advantageously. For example, at 10 bps telemetry rate, the use of single-channel could result in 1 db performance improvement. Similarly, for the 1 bps command link, about 0.8 db improvement over two-channel system may be obtained. Perhaps more important for the command system, automatic acquisition can be more easily provided for the single channel. With automatic acquisition, the time to acquire

---

[2] Huang, R. Y., "Analysis of a Single-Channel Monopulse Receiver," TRW IOM 9330.11-52, dated 20 December 1965.

Table 6.4-1 Telecommunications Design Control Table

Project: APP
Channel: Spacecraft-to-Earth
Mode: 400 bps, 16 ft S/C Antenna, 10 W

No.	Parameter	Value	Tolerance		Source
1	Total Transmitter Power	40.0 dbm	+1.0	-1.0	NOTE 1
2	Transmitting Circuit Loss	-2.0 db	0.8	0.8	
3	Transmitting Antenna Gain	38.5 db	1.0	1.0	
4	Transmitting Antenna Pointing Loss	-1.0 db	1.0	1.0	
5	Space Loss	-278.8 db	0.0	0.0	
6	2300 Mc R = 6.0 AU Polarization Loss	-0.1 db	--	--	
7	Receiving Antenna Gain	61.7 db	1.0	0.5	EPD-283
8	Receiving Antenna Pointing Loss	-0.5 db	--	--	EPD-283
9	Receiving Circuit Loss	-0.2 db	0.1	0.1	EPD-283
10	Net Circuit Loss	-182.4 db	3.9	3.4	
11	Total Received Power	-142.4 dbm	4.9	4.4	
12	Receiver Noise Spectral Density (N/B)	$-183.8 \frac{\text{dbm}}{\text{cps}}$	0.8	0.7	EPD-283
13	T System = $30^{\circ}K \pm 5^{\circ}K$ Carrier Modulation Loss $\theta_D = 1.25 \pm 5\%$ $\theta_S = 0.32 \pm 5\%$	-10.5 db	1.5	1.9	
14	Received Carrier Power	-152.9 dbm	6.4	6.3	
15	Carrier APC Noise BW($2B_{LO}$ = 12 cps)	10.8 db·cps	0.5	0.0	MC-4-310A
	Carrier Performance Tracking (one-way)				
16	Threshold SNR in $2B_{LO}$	0.0 db	0.0	0.0	MC-4-310A
17	Threshold Carrier Power	-173.0 dbm	1.3	0.7	
18	Performance Margin	20.1 db	7.7	7.0	
	Carrier Performance Tracking (two-way)				
19	Threshold SNR in $2B_{LO}$	2.0 db	1.0	1.0	MC-4-310A
20	Threshold Carrier Power	-171.0 dbm	2.3	1.7	
21	Performance Margin	18.1 db	8.7	8.0	

NOTE 1 - To facilitate addition of tolerances, the adverse tolerance is always placed in the right-hand column.

No.	Parameter	Value	Tolerance		Source
	Carrier Performance				
22	Threshold SNR in $2B_{LO}$	6.0	+0.5	-1.0	MC-4-310A
23	Threshold Carrier Power	-167.0 dbm	1.8	1.7	
24	Performance Margin	+14.1 db	8.2	8.0	
	Data Channel				
25	Modulation Loss	-0.9 db	0.2	0.2	
26	Received Data Subcarrier Power	-143.3 dbm	5.1	4.6	
27	Bit Rate (1/T) 400 bps	26.0 db·bps	0.0	0.0	
28	Required ST/N/B $P_e{}^b = 5 \times 10^{-3}$	8.5 $\frac{\text{db·bps}}{\text{cps}}$	0.7	0.7	
29	Threshold Subcarrier Power	-149.3 dbm	1.5	1.4	
30	Performance Margin	+6.0 db	6.6	6.0	
	Sync Channel				
31	Modulation Loss	-20.1 db	1.9	2.3	
32	Receiver SYNC Subcarrier Power	-162.5 dbm	6.8	6.7	
33	SYNC APC Noise BW ($2B_{LO} = \frac{1}{2}$ cps)	-3.0 db·cps	0.2	0.2	
34	Threshold SNR in $2B_{LO}$	14.0 db	0.3	0.3	
35	Threshold Subcarrier Power	-172.8 dbm	1.3	1.2	
36	Performance Margin	10.3 db	8.1	7.9	

Table 6.4-1 Telecommunications Design Control Table (Contd)

Project: APP
Channel: Earth-to-Spacecraft
Mode: 210-ft Antenna, 100 KW, S/C M.G. Antenna

No.	Parameter	Value	Tolerance		Source
1	Total Transmitter Power	80.0 dbm	--	--	EPD-283
2	Transmitting Circuit Loss	-0.4 db	+0.1	-0.1	EPD-283
3	Transmitting Antenna Gain	60.6 db	1.0	0.5	EPD-283
4	Transmitting Antenna Pointing Loss	-0.5 db	--	--	EPD-283
5	Space Loss	-278.1 db	0.0	0.0	
6	2115 Mc R = 6 AU Polarization Loss	-0.5 db	--	--	EPD-283
7	Receiving Antenna Gain (Helix)	14.0 db	0.5	0.5	
8	Receiving Antenna Pointing Loss	-2.0 db	1.0	1.0	
9	Receiving Circuit Loss	-1.3 db	0.2	0.2	
10	Net Circuit Loss	-208.2 db	2.8	2.3	
11	Total Received Power	-128.2 dbm	2.8	2.3	
12	Receiver Noise Spectral Density(N/B)	-165.3 $\frac{\text{dbm}}{\text{cps}}$	1.0	1.0	
13	T System = Carrier Modulation Loss	-3.2 db	0.3	0.3	
14	Received Carrier Power	-131.4 db	3.1	2.6	
15	Carrier APC Noise BW ($2B_{LO}$ = 20 cps)	13.0 db·cps	0.5	0.0	
	Carrier Performance Tracking (one-way)				
16	Threshold SNR in $2B_{LO}$	0.0 db	0.0	0.0	
17	Threshold Carrier Power	-152.3 dbm	1.5	1.0	
18	Performance Margin	20.9 db	4.6	3.6	
	Carrier Performance Tracking (two-way)				
19	Threshold SNR in $2B_{LO}$	3.8 db	0.0	0.0	MC-4-310A
20	Threshold Carrier Power	-156.1 dbm	1.5	1.0	
21	Performance Margin	17.1 db	4.6	3.6	

Table 6.4-2 Telecommunications Design Control Table

Table 6.4-2 Telecommunications Design Control Table (Contd)

No.	Parameter	Value	Tolerance		Source
	Carrier Performance				
22	Threshold SNR in $2B_{LO}$	8.0 db	+1.0	-1.0	MC-4-310A
23	Threshold Carrier Power	-148.3 dbm	2.5	2.0	
24	Performance Margin	12.9 db	5.6	4.6	
	Data Channel				
25	Modulation Loss	-8.5 db	0.6	0.6	
26	Received Data Subcarrier Power	-136.7 dbm	3.4	2.9	
27	Bit Rate (1/T) 1 bps	0.0 db·bps	0.0	0.0	
28	Required ST/N/B $P_e^b = 1 \times 10^{-5}$	15.7 $\frac{db \cdot cps}{bps}$	1.0	1.0	
29	Threshold Subcarrier Power	-149.6 dbm	2.0	2.0	
30	Performance Margin	12.9 db	5.4	4.9	
	Sync Channel				
31	Modulation Loss	-5.5 db	0.5	0.5	
32	Receiver SYNC Subcarrier Power	-133.7 dbm	3.3	2.8	
33	SYNC APC Noise BW ($2B_{LO}$ = 2 cps)	3.0 db·cps	0.8	0.8	
34	Threshold SNR in $2B_{LO}$	15.7 db	1.0	1.0	
35	Threshold Subcarrier Power	-146.6 dbm	2.8	2.8	
36	Performance Margin	12.9 db	6.1	5.6	

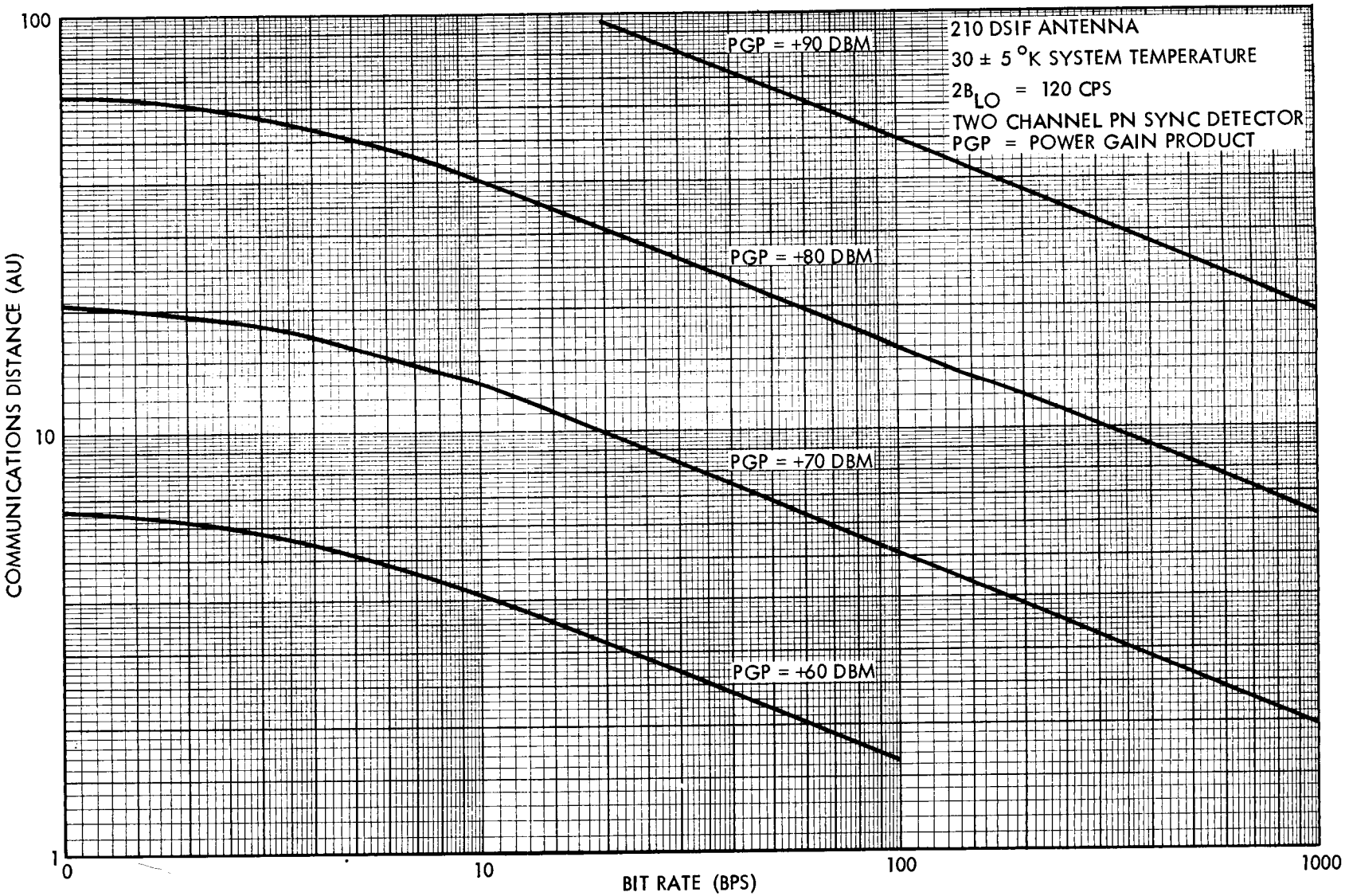

Figure 6.4-3. Bit Rate Versus Communication Distance

lock could be reduced when the clock frequencies are not accurately known.

One of the problems in accurately predicting uplink performance is the uncertainty regarding system noise temperature or noise spectral density (item 12 of Table 6.4-2). For the APP it may not be possible to avoid having the sun in the spacecraft antenna beamwidth when pointing at the earth. It has been determined that at Jupiter the high-gain antenna temperature (and therefore the system temperature) would appreciably increase in case the disturbed sun is in the main antenna beamwidth. For instance, in the case of a 16-foot antenna and a maximum receiver noise figure of 10 db, the noise spectral density would be -151 dbm/cps, an increase of 14 db. The helix antenna temperature will not be affected by the sun.

6.4.4 Preliminary Comparison of Considered Systems and Problem Areas

The main problem with all telecommunication systems for the APP is the complexity of the antenna-antenna switching hardware. Also, the need for a second omnidirectional antenna, which provides backward heisphere coverage, contributes to this complexity.

Preliminary investigation seems to indicate that the telecommunication system for the spin-stabilized probe is somewhat simpler than those for the 3-axis stabilized spacecraft. The disadvantage of using the spin-stabilized spacecraft, as well as the 3-axis stabilized one using angle tracking attitude control, is the fact that the failure of the uplink may mean complete loss of telemetry data. In the case of the optically 3-axis stabilized spacecraft, telemetry at reduced bit rates could be possible even if the uplink fails. The probe could be mechanized to automatically switch bit rate in case of uplink failure. It is clear that for the two angle tracking stabilized systems the uplink has to be made at least as reliable as downlink.

Another possible problem with the systems considered here is the prolonged, although intermittent, commitment of the transmitters, beacons, in support of the APP. It appears that beacon support requirements would be minimum, for the reasons previously discussed, for the 3-axis optically stabilized spacecraft.

6.4.5 Studies to be Performed

During the remaining period the following tasks will be performed:

1) Detailed description of the systems considered, including block diagrams, hardware description, estimated weights, and power.

2) Transmitter study to predict optimum choice of a power amplifier.

3) State-of-the-art study for the remainder of the telecommunications equipment to predict components and materials used and to estimate weight, power, and reliability for later launches.

4) Computation of the signal-to-noise ratio of angle tracker error signal provided to the attitude control system.

5) Perform an extensive parametric study, the end product of which would give bit rate, signal-to-noise ratio, system temperature, etc., as a function of range, antenna size, transmitted power, etc.

6) Consideration of single-channel PN synchronization systems.

7) Study of applicability of coding to APP.

8) Investigation of other modulation techniques.

6.5 COMMAND DISTRIBUTION SUBSYSTEM

6.5.1 Function

The function of the command distribution subsystem (CD) is to receive, process, and output various commands and data as required by the spacecraft operation. The following requirements are basic to all missions:

- Accept and decode received ground commands
- Accept and decode spacecraft commands
- Store commands for execution at designated times
- Store data to be issued at designated times.

6.5.2 Conceptual Design for the Sample Spacecraft Configurations

A command subsystem for such missions as proposed for the Advanced Planetary Probe can range considerably in complexity depending on the function it is called upon to perform. The basic conceptual design will be the same for a spin-stabilized spacecraft or for a 3-axis stabilized spacecraft. The type and multiplicity of commands and data will vary with the spacecraft configuration. The mechanization of the command subsystem must be configured to handle all timing and sequencing control functions. A clock is needed to issue timing pulses, and a decoding tree or matrix is necessary to interpret commands and issue discretes. Since some of the commands and data may be stored onboard the spacecraft a memory device may be necessary to hold the information.

The generalized electrical interfaces are shown in Figure 6.5-1. The input commands may either be issued by the earth ground station or

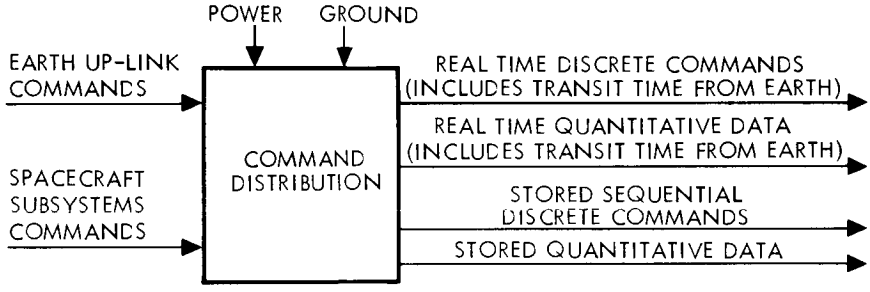

Figure 6.5-1. Generalized Command Distribution Electrical Interfaces

by other spacecraft subsystems. Because of the long communications delay time (over 1 hour), many spacecraft operations must be initiated by commands originating in spacecraft sensors. These input commands may be discrete or quantitative, real time or stored in the various subsystems. These commands will be processed by the command distribution to provide real time or stored, discrete or quantitative commands to the various spacecraft subsystems.

a) Real Time Discrete Command

This command is a direct command, including transit time from earth, that provides a designated spacecraft subsystem with a discrete pulse.

The discrete pulse is issued by the command distribution as soon as the incoming command is decoded.

b) Real Time Quantitative Data

This is a direct command, including transit time from earth, that provides a designated spacecraft subsystem with serial data. This serial data is issued by the command distribution as soon as the incoming command is decoded.

c) Stored Sequential Discrete Command

This command provides a designated spacecraft subsystem with a sequence of discrete pulses after the receipt of the command. The command is stored in memory until its execution time, at which point the discrete pulses are issued to the designated subsystem.

d) Stored Quantitative Data

This provides a designated spacecraft subsystem with serial data after the receipt of the command. The same format is used as for the stored sequential discrete command.

6.6 DATA HANDLING SUBSYSTEM

6.6.1 Function

The data handling subsystem is required to perform the following functions:

a) Sample and encode engineering and science data into a time multiplexed PCM signal for real time transmission or for storage.

b) Store high rate science data (TV) and low rate science and engineering data into data storage during periods when data input rates exceed transmission rates (also during transmission blackout).

c) Mix (or interleave) stored scientific data (vidicon, low rate science) with real time engineering data into a serial PCM bit stream.

A simplified block diagram of the data handling subsystem and its system electrical interfaces are shown in Figure 6.6-1. The system consists of a PCM encoder and several buffer data storage units. The

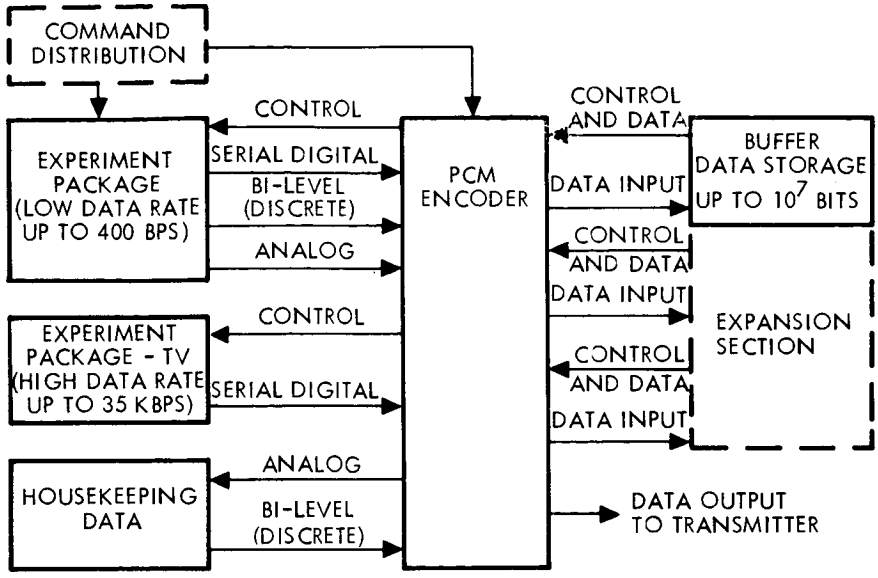

Figure 6.6-1. Data Handling Subsystem

PCM encoder format is data from both low and high rate experimental packages as well as engineering data. The PCM encoder provides three types of data formats for different modes of operation. These are:

1) TV data plus low rate science and engineering
2) Low rate science plus engineering - flare and interplanetary cruise mode
3) Engineering data during launch and diagnostic periods.

The data storage acts as a buffer to match the high rate TV data to the transmission rate. Also, the buffer is used to store low rate science during transmission blackout. As indicated in the block diagram expansion sections (redundant) storage may be added to increase reliability or to be used to increase the overall storage capacity. Figure 6.6-2 shows an approximate data input profile and data output profile for the Jupiter mission and is summarized in Table 6.6-1. The maximum transmission rate in the vicinity of Jupiter is 500 bps. This data rate has been assumed as a constant for the total flight since this data rate is adequate for all data requirements up to the planet encounter period.

Data Mode	Input Data Rate Bits/Sec	Duty Cycle	Transmission Average Bit Rate Bits/Sec
Engineering Data	60 to 240	Continuous Diagnostic	60 to 140 10 or 240
TV	Intermittent – 10^6 34K	2 x 10^6 bits/picture	≈ 400
Special Occurrence (Solar Flares)	360	48 hours	360
Low Rate Science	100 - 200	Continuous over most of mission	100 - 120
Flyby Science	350	Continuous during flyby	350
Blackout Mode	200	Continuous during blackout	Storage
Spacecraft Downlink Data Transmission Capability			(Maximum) 500 bits/sec (Minimum) 180 bits/sec

Table 6.6-1. Summary of Data Profile

The PCM encoder will operate in several modes of operation to conform to the data profile of Figure 6.6-2. These modes are as follows:

Interplanetary flight mode. During most of the interplanetary phase the experimental data rate will be about 120 bps. This represents the most common mode of operation.

Special occurences, solar flare observance, mode. This mode will require an increased sampling rate up to about 360 bps.

Launch and diagnostic mode. After launch and several times during the interplanetary flight the housekeeping data will be read out to check the condition of all systems.

Planet encounter mode. This mode is characterized by high rate data input, (TV) with maximum transmission rates utilized to empty the memory between TV pictures. Interleaved with the TV data is the low rate experimental inputs and engineering.

Planetary flyby mode. The experimental data input (low rate) increases to approximately 350 bps during flyby.

Transmission blackout mode. The spacecraft transmission is cut off as it passes behind Jupiter for about one hour. The

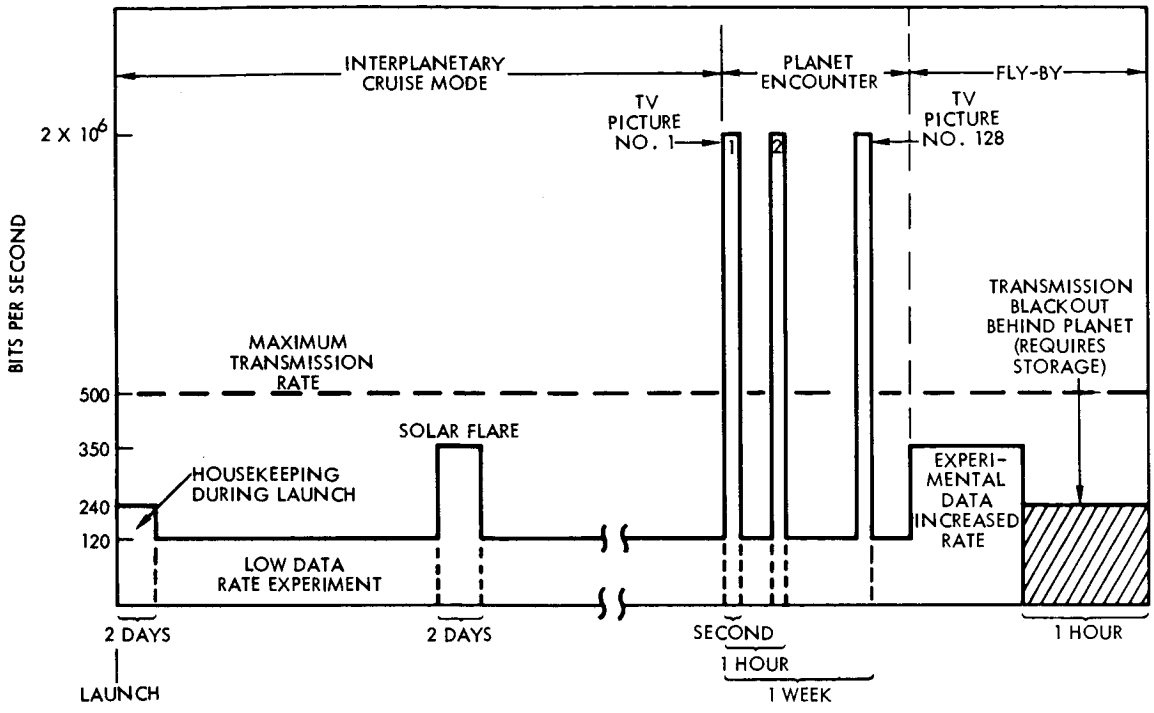

Figure 6.6-2. Typical Data Profile

data rate during this mode is approximately 200 bps with all data going into storage.

Final mode. Readout of stored data, interleaved with real time engineering.

6.6.2 Conceptual Design for the Sample Spacecraft Configuration

The conceptual design of the DHS discussed here is based on the requirements of the sample spacecraft configurations of Section 5 with the consideration that the designs will allow for increasing the number of data inputs as well as storage capacity, modes of operation (i.e., number of formats, mix ratio of science and engineering data). Redundancy techniques will be used to increase the reliability and to minimize the effects of failures. Integrated circuits will be used for weight and volume reduction.

The modes of operation outlined in Section 6.6.1 dictate the relationships of the PCM formats used during the mission trajectory. Several main-multiplexer formats will be used to time-multiplex the

experimental data. Each main-multiplexer will be linked to sub-multiplexers for handling slower sampling rate inputs, housekeeping and the low frequency sampled experiments. The housekeeping data sub-multiplexer will be capable of being used as a main-multiplexer for diagnostic analysis of this data.

A tape recorder memory of 10^7 bits and/or a small size core memory buffer will be included as part of the DHS for buffering between the incoming data rate and the transmitter data rate. The memory will be required to operate up to 34K bps rate during storage. During read-out the memory will operate at a 500 bps rate.

6.6.3 Alternate Conceptual Designs

There are several alternate data storage methods which have been considered for the APP program. The choice of storage will depend on several factors: the data input rate - output rate ratio, the instantaneous data input rate, the total bit capacity required, and the weight, volume, and power requirements. The physical characteristics of various storage units are shown in Table 6.6-2.

Another factor effecting the memory choice is the type of TV experiment to be included in the mission. The vidicon readout rate and mode of readout (by individual lines or continuously through the complete picture) and the time between pictures fix lower limits on the storage. The possibility of storage on the vidicon and readout rates from the vidicon slow enough to match the transmission rate would greatly reduce the memory capacity requirement. The bits per picture and transmission time required for TV pictures of various resolutions and constrasts are shown in Table 6.6-3. This table indicates the storage required, in bits, for single pictures.

6.6.4 State-of-the-art Considerations

Improvements in the state-of-the-art in memories and integrated circuits should have a large effect on the DHS design. Integrated and thin film circuits for space applications are currently in development and are considered in the design of the APP data handling subsystem. Special integrated circuits for analog-to-digital conversion and for

Table 6.6-2. Storage Units

Type of Memory	Bits of Storage Capacity	Write Cycle		Read Cycle		Standby Power (watts)	Not Including Power Converter	
		Bit/Sec	Power (watts)	Bit/Sec	Power (watts)		Weight (lb)	Volume (cu. in.)
Cores	100K	500	< 1	500	< 1	.075	3.5	120
Cores	200K	4096	< 1	500	< 1	.075	7.0	200
Cores	10^6	4096	< 1	500	< 1	.075	24.0	500
Cores	10^6	100K	< 5	500	< 1	.075	24.0	500
Tape Recorder	10^6	500	4	500	4	.075	5.0	90
Tape Recorder	10^7	16K	6	1000	4.4	.075	7.5	271
Tape Recorder	10^8	50K	7	1000	3	.075	11.0	600

Table 6.6-3. TV Transmission

Picture Lines	Resolution Samples/Line	Bit Per Picture		Transmission Time/Picture (Including Line ID) at 400 bps	
		5 Bit/* Sample	6 Bit/* Sample	5 bit*	6 bit*
600	600	1.8×10^6	2.16×10^6	75.3 minutes	90.3 minutes
500	500	1.25×10^6	1.5×10^6	52.3	62.7
400	400	0.8×10^6	0.96×10^6	33.5	40.2

* Bits per picture element to establish gray levels

analog gating are presently available, but further evaluation is required before their use would be proposed. Integrated arrays of metal oxide semiconductor (MOS) circuits for use as buffer memories are also available, although a large reduction in power loss per bit must be made before large arrays will be practical for use in space. Power reduction studies are being made on these circuits.

The results of recent studies for NASA indicate that lower power thin film and core memories are feasible. These memories could have a definite effect on programs planned for the 1970 to 1980 period. The lower power per bit of cores and higher reliability are the tradeoffs against the lower volume of tape storage in bit capacity ranges of 500K to 2×10^6 bits. Also, the flexibility of the write/read ratio is better for cores.

General improvements in such fields as the radiation resistance of semiconductors, speeds and size of tape recorders, package concepts and connectors will further affect the design concept over the 1966 to 1980 period.

6.7 PROPULSION SUBSYSTEM

6.7.1 Function and Requirements

The function of the vehicle propulsion subsystem is to reliably provide the necessary velocity increment for midcourse and retro maneuvers.

The preliminary midcourse requirements are for a velocity increment of 100 meters per second for a spin stabilized spacecraft and 75 meters per second for a three axis stabilized platform. The retro velocity increment was initially assumed as 600 meters per second. Impulse repeatability was assumed as requiring 1 percent of delivered impulse.

6.7.2 Conceptual Design

Based on the above requirements, analysis was performed on a solid retro and monopropellant midcourse propulsion system and a monopropellant system to perform both functions. Bipropellant systems were not considered initially because the small total impulse requirements,

3,000 to 61,000 pound seconds, did not appear to warrant it. In general, bipropellant systems do not become competitive in terms of weight until about 50,000 pound seconds. Therefore, a bipropellant system would only become competitive for the 800 to 1000 pound spacecrafts and with the additional system complexity involved it appeared reasonable to not consider it at this time.

Using the above requirements propellant quantities were calculated and the results presented in Figures 6.7-1 and 6.7-2. Using these results, propellant tank weights and pressurization gas weights were calculated as shown in Figures 6.7-3 and 6.7-4. The initial system considered was a blowdown monopropellant system as shown schematically in Figure 6.7-5 since it encompassed the least number of components as well as very simple, reliable ones and therefore promised the highest reliability.

With the total impulse range of 3,000 to 61,000 pound seconds, a 50 pound thrust level was selected for the combustion chamber. This results in a 60 to 1220 second burn time. The 1220 second burn time is easily attainable with a spontaneous catalyst hydrazine monopropellant engine and the impulse repeatability of the 50 pound thrust engine of better than 1 percent would easily satisfy the minimum impulse accuracy requirements.

Based on weights of units tested at TRW, the weight of the thrust chamber was determined. A curve of chamber weight versus thrust level using actual chamber weights for plotting the curve is shown in Figure 6.7-6. Fixed weights which include lines, fittings, filter fill and drain valves were estimated, and propulsion system weights were determined as a function of spacecraft initial weight as shown in Figure 6.7-7.

A second system, employing a solid retro and a monopropellant midcourse engine, was subjected to preliminary analysis. The propulsion system weights are also presented in Figure 6.7-7. The mass fractions for the solid motor employed are presented in Figure 6.7-8.

A pressure regulated monopropellant hydrazine system, schematically shown in Figure 6.7-9, was also reviewed. Over the range of propellant quantities involved, 13.5 to 264 pounds, the weight difference between the blowdown system and the regulated system was only a few

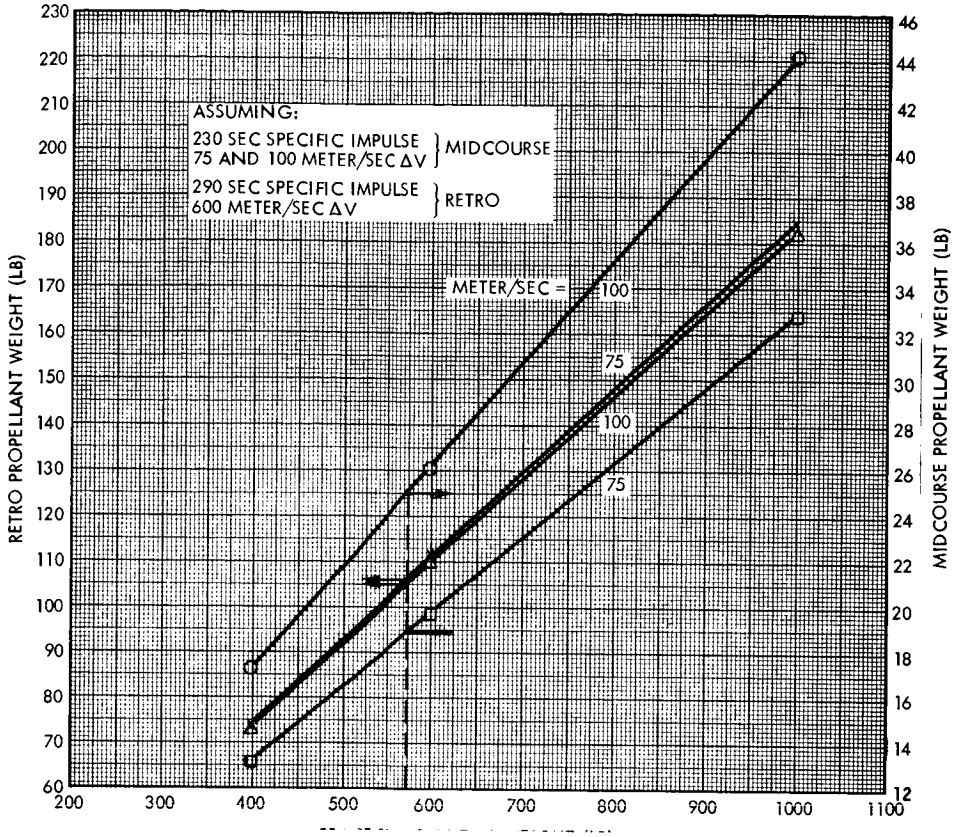

Figure 6.7-1. Propellant Weight Versus Spacecraft Initial Weight

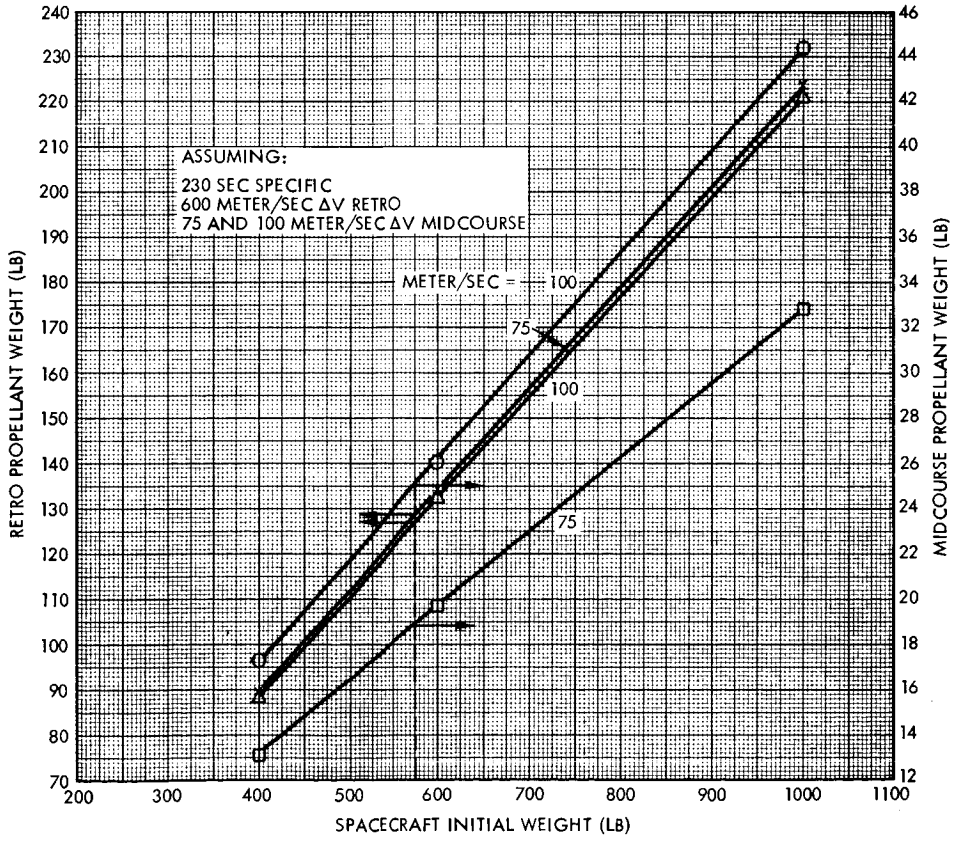

Figure 6.7-2. Monopropellant Midcourse and Retro Propellant Weight Versus Spacecraft Initial Weight

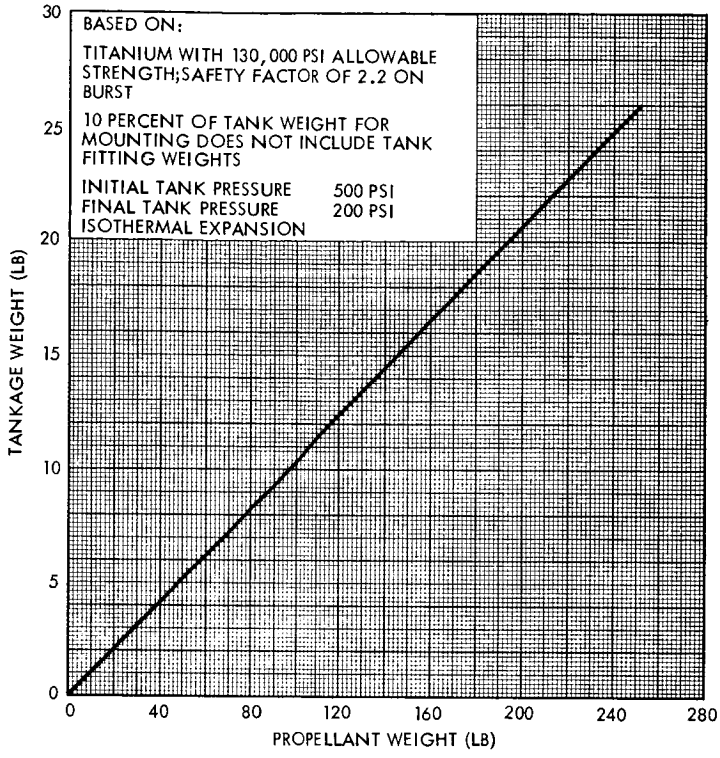

Figure 6.7-3. Blowdown System Propellant Tank Weight Versus Propellant Weight

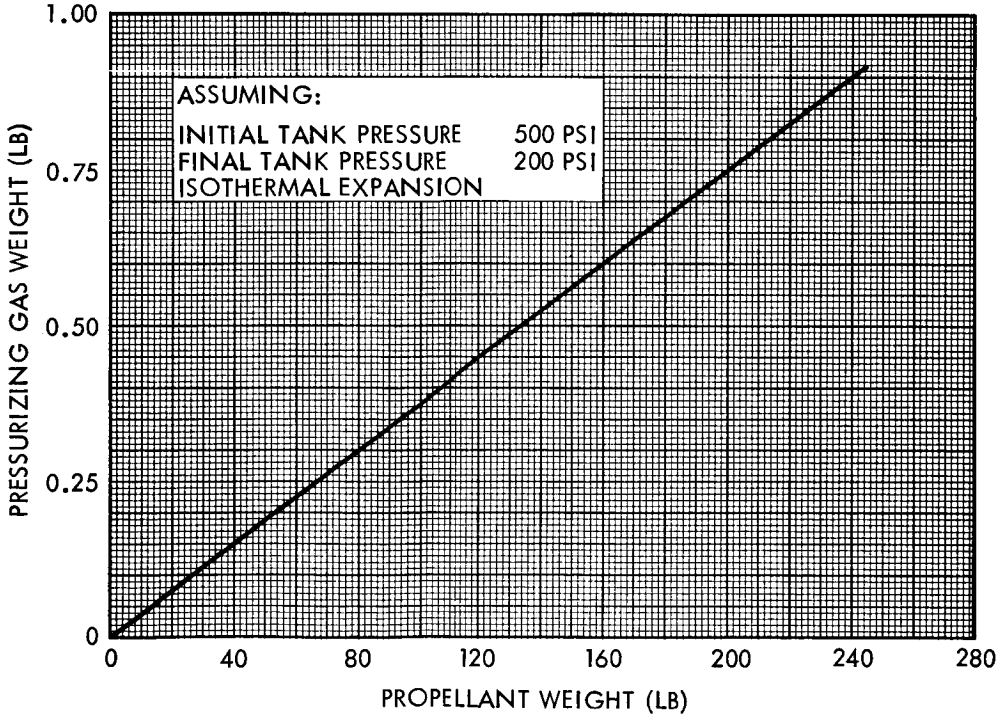

Figure 6.7-4. Blowdown System Propellant Tank Pressurizing Gas Weight Versus Propellant Weight

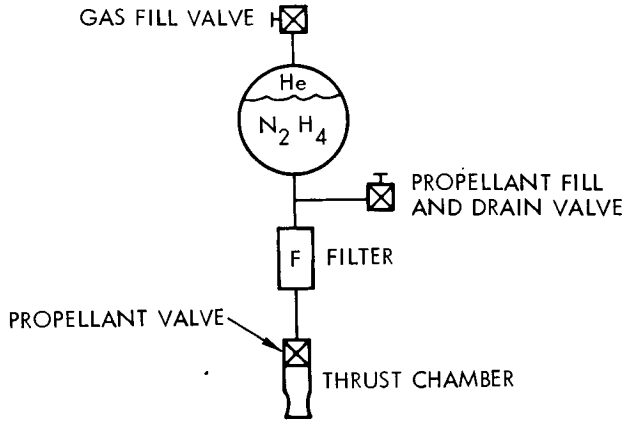

Figure 6.7-5. Monopropellant N_2H_4 Blowdown System (A positive expulsion bladder will be required for the three-axis stable platform vehicle)

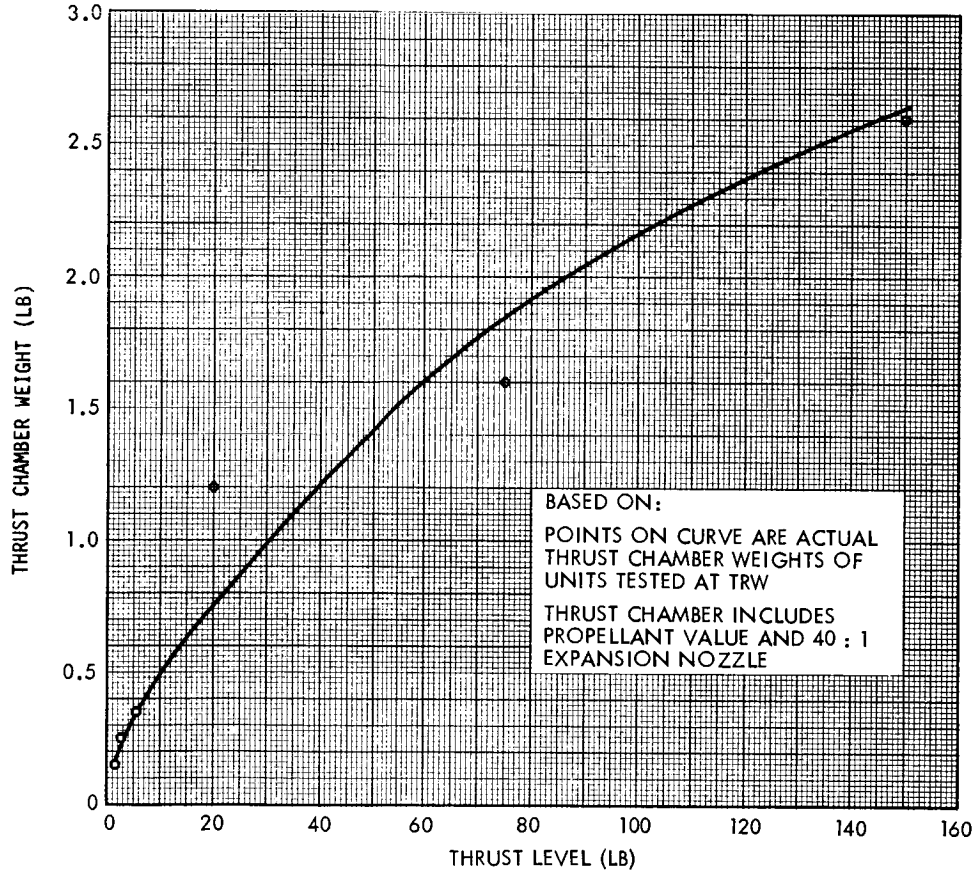

Figure 6.7-6. Monopropellant Thrust Chamber Weight Versus Thrust Level

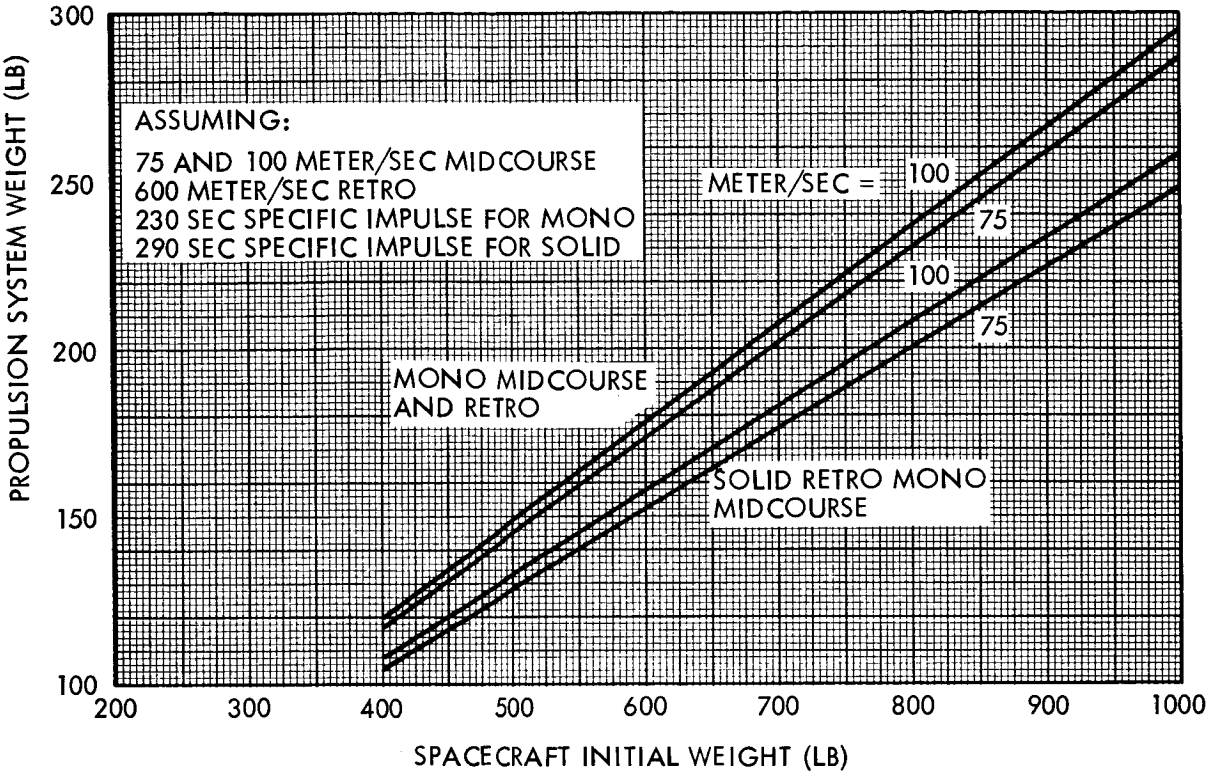

Figure 6.7-7. Propulsion System Weight Versus Spacecraft Initial Weight

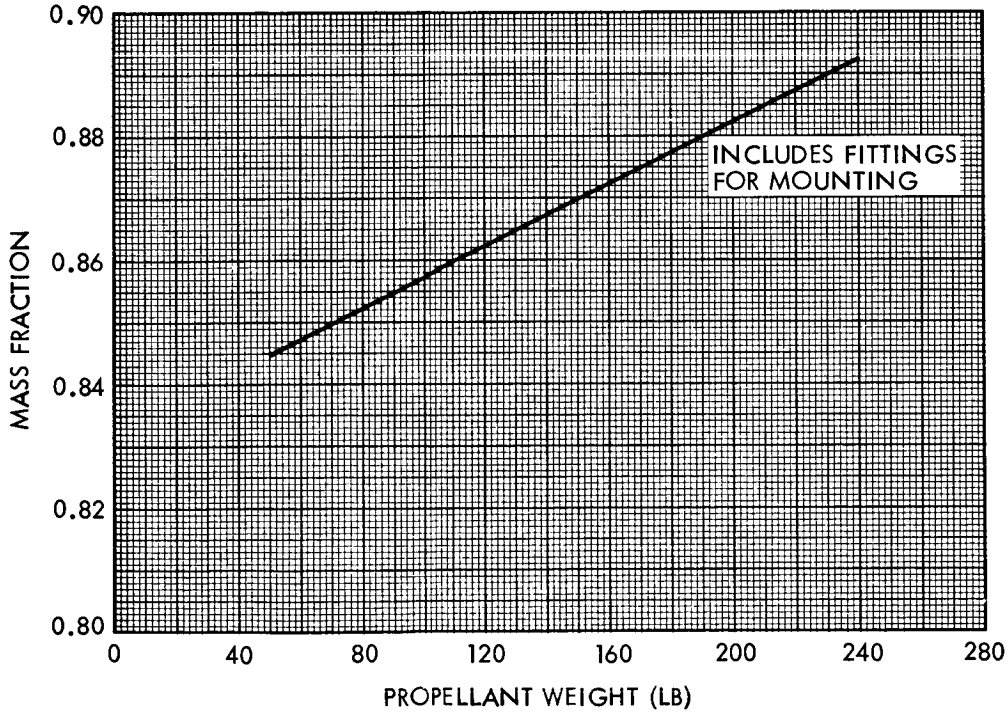

Figure 6.7-8. Solid Propellant Mass Fraction Versus Propellant Weight

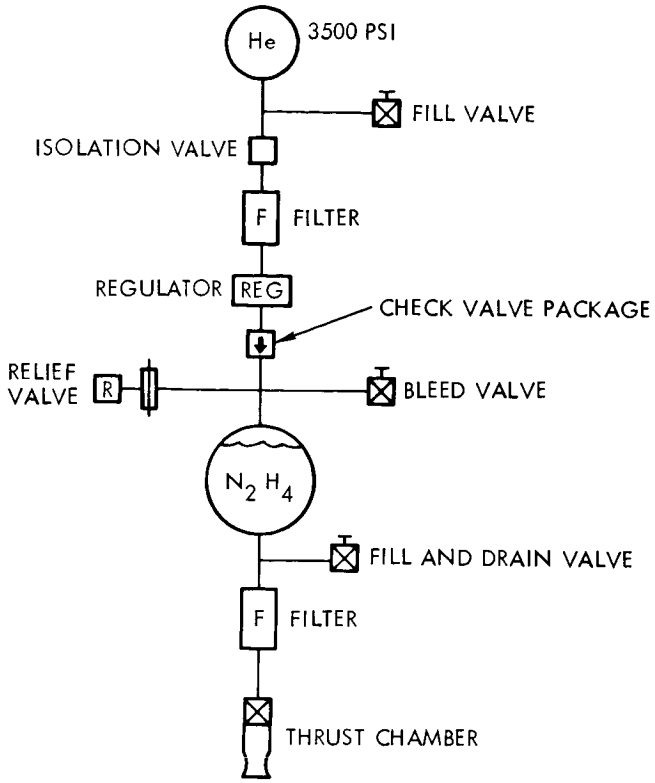

Figure 6.7-9. Monopropellant N_2H_4 Regulated System

pounds. The blowdown system was lighter by 3 pounds at the smaller propellant quantities and equal in weight to the regulated system at the higher propellant quantities. Therefore, the regulated system with the additional components and system complexity does not appear to be a contender for this application.

6.7.3 Alternate Conceptual Designs

In addition to the high thrust engines considered to date it appears advisable to include low thrust systems in the applicability study. A decomposed ammonia radioisotope thrust system (DART) has excellent duty cycle flexibility, can use multiple thrust nozzles of different thrust levels, has a very efficient propellant storage technique and delivers a specific impulse of 250 to 360 seconds. The problems associated with employing thrust levels of approximately 0.03 pound for this mission will, however, have to be analyzed.

6.7.4 State of the Art Considerations

The spontaneous catalyst hydrazine propulsion systems will probably be qualified for the 1970 to 1980 period since they are presently finding extensive proposed applications on current programs. To date extensive development testing has been performed at TRW, Walter Kidde, and other companies.

One problem encountered is mechanical breakdown of the catalyst during extended use and under vibration loading. Catalysts in pellet form are particularly vulnerable to this latter condition. Use of porous inert pellets as a catalyst carrier yields a surface area far greater than the mechanically rugged screen type carrier but also increases the likelihood of damage from internal reaction and shattering of the pellet by the gases generated in its interior. This problem is currently under investigation.

The main area of concern in applying the radioisotope heated thrusters is the problem of obtaining an encapsulated fuel form capable of reliable operation at the high temperatures needed to obtain the higher specific impulse values. Present systems are capable of about 250 sec with thrust levels limited to approximately 0.025 pound. The above problem should be solved, however, so that systems capable of specific impulses in the 300 sec range will be available during the 1970-1980 period.

6.7.5 Reliability Consideration

From a reliability standpoint, the blowdown spontaneous catalyst hydrazine system appears to hold the highest potential. It is the simplest system and employs very reliable components. The bipropellant system with its multitude of components would be far less reliable. The regulated monopropellant system with the same basic components as the blowdown system, but including many additional ones, would inherently be less reliable. Since the solid retro still requires a liquid midcourse system, it also cannot match the reliability of the blowdown hydrazine system.

The mission times of 1.5 to 5 years will require zero leakage systems. Therefore, ganged explosive valves will have to be considered as a replacement for the solenoid propellant valve shown in Figure 6.7-5.

All brazed lines and fittings will also be mandatory. The ability to store hydrazine confined by a bladder for this long period of time will also need review.

6.7.6 Problem Areas

In addition to the problem areas discussed in the preceding paragraphs, because of the great distance from the sun, problems will be encountered in keeping the propellants within acceptable temperature limits. Hydrazine, for instance, freezes at 35°F. Long term exposure of the spontaneous catalyst to vacuum will also have to be considered. However, flight experience from other programs should be available by 1970-1980 to form a more solid base for this consideration.

6.7.7 Studies to be Performed

In addition to the work performed to date, the following effort will be required to meet the requirements of the Advanced Planetary Probe Study:

- Develop additional conceptual designs based on more definitive requirements and perform tradeoff studies which shall include cost effectiveness
- Investigate the state of the art of the above conceptual designs
- Identify additional problem areas and approaches to their solution
- Review the concepts in terms of the Mariner and Pioneer system designs
- Develop block diagrams, operational sequences, detailed weight and power estimates
- Review redundancy considerations in light of lifetime reliability design considerations and perform reliability analysis
- Investigate means for modularization of the propulsion system so as to provide orbiter and capsule entry capabilities to the basic flyby design
- Prepare preliminary schedule and costs for the selected systems.

6.8 THERMAL CONTROL SUBSYSTEM

6.8.1 Function

The thermal control subsystem will maintain the temperature of the following items within an acceptable operating range:

a) Electronic components

b) Experiments

c) Spinup system

d) Orientation system

e) Orbit injection motor

f) Midcourse engine

g) Antennas

h) Planetary probe and container

The subsystem will provide the required temperature control during all phases of the mission including launch, coast, orbit, midcourse correction, and transit.

6.8.2 Conceptual Design for the Sample Spacecraft Configuration

All electronic components will be located within a central compartment which is suitably isolated from solar heat input by multilayer aluminized Mylar insulation blankets and low thermal conductivity structural attachments. The components are mounted on an all aluminum honeycomb panel that is designed to reject internal electronic heat dissipation to space at a predetermined rate. It will not be necessary to use louvers or thermal switches in the system to provide a means of varying the established heat rejection rate as long as the internal power level is relatively constant and structural heat leaks are kept small. If the transmitter has to be duty cycled, a constant power dissipation can be maintained within the compartment by using internal shunt resistors or flexible electric heaters to make up the power decrease that occurs when the TWT is switched off.

Experiments will be located within the temperature controlled compartment unless their requirements dictate otherwise. Since it is quite

probable that some of the compartment experiments will be equipped with windows that look out into space, it will be necessary to intimately mount the experiments to the electronic component mounting platform to maintain acceptable temperatures. Local electric heaters will be used to control the temperature of experiments located outside the controlled compartment.

External equipment such as the midcourse and orbital engines, and orientation nozzles and lines will require heater power. In addition, a black Cat-a-lac paint (absorptivity, $\alpha = 0.95$; emissivity $\epsilon = 0.86$) is required on the sunlit surface of the deployable antenna to achieve the proper temperature range and prevent focussing of the solar energy on the feed. The rear surface of the antenna is left bare to obtain a near-earth temperature of about $265^{\circ}F$ and $-135^{\circ}F$ at Jupiter. A black front surface not only establishes acceptable antenna temperatures but also reduces temperature gradients across the aluminum honeycomb antenna structure because practically all the absorbed heat is re-emitted from the same surface and little conduction takes place between the face sheets. The spin stabilized configurations eliminate gradients over the antenna dish by averaging the heat input to alternately irradiated and shaded points on the antenna. Fully attitude controlled configurations will subject the antenna to spanwise temperature gradients which can produce distortion that is minimized by controlling the extent of structural shadowing, and using proper orientation and mechanical design constraints. If the antenna position is not controlled and the axis is normal to the sun vector, a gradient of $270^{\circ}F$ could exist under steady state conditions.

The RTG units can be isolated from the spacecraft by low conductivity structure and multilayer insulation blankets. However, during the detailed design it may be found that the waste heat from the RTG units can be utilized to provide a more satisfactory temperature level within the controlled compartment. Also, the waste heat can be used to lower the temperature gradient across the antenna dish for a fully attitude controlled system.

6.8.3 Alternate Conceptual Design

If power is limited, it is possible to replace electric heaters with radioisotope heaters in some instances. However, an associate weight penalty will be incurred if this type of heater is used. The exact weight penalty per watt of heating is not firm since most of the weight is associated with the conductive distribution system that is unique for each use. As an example, though, a 5 watt radioisotope heater/ distribution system will weigh on the order of 12 ounces. This is about 8 ounces heavier than a comparable flexible electric heater.

Louvers or thermal switches may be required if the compartment heat leaks cannot be adequately controlled. This situation could exist if many experiments have large window areas. Thermal switches are potentially far superior to louvers because they have an open to close resistance ratio of over 40 compared to a louver ratio of 3. The switches also require less volume, but will be heavier since an external radiator is needed in addition to the internal component mounting panel.

6.8.4 State-of-the-Art Considerations

All proposed thermal control subsystem items except the thermal switch and radioisotope heater have been successfully used on previous TRW spacecraft. A thermal switch prototype is currently undergoing tests in the Systems Heat Transfer and Thermodynamic Department and it appears that the switch will be operational by the end of the year. The technology of fabricating radioisotope heaters is well established. However the design of these heaters is dependent upon many non-thermal considerations such as handling, mission abort, re-entry, and possible payload interaction. The radioisotope material itself is readily available now and heaters can be made available by 1970 if the above problems are resolved.

6.8.5 Reliability

The recommended system is primarily passive in nature and will have a high reliability. Similar types of systems have operated, and are still operating, on other TRW spacecraft that have been in orbit longer than 2 years. Active elements such as the electric heaters

have been flown on the OGO spacecraft. Of the 22 heaters utilized on OGO there appears to be one heater failure. This represents a 95.5 percent success rate. For the Advanced Planetary Probe this rate should be even higher since the heater cycle rate will be reduced.

Radioisotope heaters are conceptually extremely reliable because there are no moving parts. The thermal switch is less reliable since it requires a bellows displacement which subjects the materials to fatigue. The bellows is filled with a fluid which could be expelled to space if any type of minute fracture exists in the bellows wall. Therefore, a significant portion of the switch qualification testing is concerned with the vibration and cyclic integrity of the bellows. Preliminary laboratory tests, along with bellows manufacturer data, indicates that the prototype switch design should be reliable for long life missions.

6.8.6 Problem Areas

Specific surface thermal properties are required to maintain acceptable spacecraft temperatures. The desired properties are normally obtained through chemical films, paints, and deposited coatings. In each instance, the surface covering is quite thin, usually about 3 mils. For the proposed missions this coating thickness may not be sufficient if cosmic dust erosion is a problem. The extent to which the various surface coatings will be eroded by the cosmic dust is not known. Therefore, it will be necessary to study this problem in more detail, both in defining the expected cosmic dust density and developing coating methods that will survive dust erosion.

Improper orientation of the Probe can produce excessive temperature gradients within the vehicle and over the antenna. Solar irradiation of the honeycomb radiator panel can drive the electronic temperatures above their acceptable upper limit. For these reasons, it is imperative that the final trajectory and vehicle orientation be consistent with thermal constraints.

The requirement that the entry probe be sterilized can affect the capsule design. The extent of change will depend upon whether

heat is used as the sterilization process and the nature of the capsule mission. The effect of the sterilization requirement is most pronounced if the capsule has internal electronics that have to be checked out on-stand prior to launch. An inert cooling gas will have to be circulated near the capsule in this case to remove the electronic heat dissipation. The container around the capsule should be maintained continously at a pressure higher than ambient, especially during boost through the atmosphere.

6.8.7 Studies to be Performed

The following design studies and efforts will be performed:

a) Analysis and sizing of insulation

b) Heat leak analysis and system/experiment requirements

c) Thermal balance studies

d) Evaluation of the possible use of RTG waste heat (antenna heating, for example)

e) More detailed subsystem design

7. GROWTH TO ORBITER AND LANDER MISSIONS

As indicated in Section 2.2, the Advanced Planetary Probe missions are basically the planetary flyby missions. However, we are to examine the growth potential of the basic concepts to perform orbiter and planetary capsule missions. For the purpose of considering these other missions, only Jupiter will be considered as the target planet, although the extension to Saturn and Neptune is not conceptually difficult.

7.1 ORBITER MISSION DESCRIPTIONS

In an orbiter mission, the interplanetary trajectory is directed close enough to the target planet so that a transfer into a planet center orbit can be achieved without an unduly large expenditure of propellant. For entry into orbits about Jupiter optimum transfer techniques will permit the attainment of useful orbits with a transfer velocity increment as low as 600 meters/second. Of course, any of the following changes would increase the propulsion requirement: arrival at Jupiter at a higher relative velocity; attainment of a more circular orbit about Jupiter; transfer from the approach to the orbit at a higher altitude above Jupiter; and transfer from the approach trajectory to the elliptical orbit at points other than periapsis of these trajectories.

In any event, the value of those experiments associated with planetary phenomena increase as their useful period is extended from the brief duration of proximity to the planet in a flyby mission, to the continuous opportunities associated with repetitive orbital passages.

7.2 SYSTEM IMPLICATIONS

For the orbiter missions, the emphasis is on the capability of the spacecraft to transmit scientific data to the earth continuously at a large rate, in comparison with the ability of a flyby spacecraft to store large total quantities of data for later transmission to the earth.

Another consequence of the orbiter mission is that the spacecraft would operate for extended periods in a region close enough to Jupiter to be influenced by the possibly very strong radiation environment of that planet. Of course, the measurement of that environment is one of

the primary objectives of the Advanced Planetary Probe missions, and it is presumed that the first missions would be flybys, with this measurement being the primary goal. As a consequence the full description of the nature of the planetary environment for an orbiter mission can be estimated only very roughly now, but would be refined during the course of the program.

Other system implications of the orbiter mission are the following:

- The periodic interruption of the communications path between the spacecraft and the earth with each orbital passage
- The variation in thermal inputs to the spacecraft due to eclipse of the spacecraft of the sun by Jupiter, and by proximity of the sunlit disc of Jupiter to the back side of the spacecraft
- The importance of mission guidance and control in the execution of the orbit transfer maneuver
- The possibility of determining gravitational harmonics of Jupiter by continued tracking of the orbiting spacecraft.

7.3 LANDER MISSIONS

The purposes which might be logical for lander missions to Jupiter are associated with direct measurements to be made in the atmosphere of the planet. The design of a lander capsule to perform these measurements is complicated by the great mass of the planet, and the extreme entry speeds resulting from the gravitational attraction.

The escape velocity at the surface (actually the outer atmospheric layers) is 60 km/sec. The entry velocity of a capsule on a ballistic trajectory stemming from spacecraft arrival asymptotic velocities of 6 to 10 km/sec is essentially 60 km/sec. It is beyond the state of propulsion system technology to make more than a minor dent in this entry velocity by any rocket braking techniques; the use of chemical rockets reduce the payload mass by a factor of e for every 3 km/sec detriment in velocity. Furthermore, the scale height of the atmosphere of Jupiter is variously estimated at about 8 km for the outer layers, and less at lower altitudes, so that a capsule entering at any angle other

than a grazing trajectory will be very quickly subjected to extremely high deceleration and atmospheric heating.

Preliminary investigation indicates that at these entry speeds a solid ablation sphere of conventional materials is likely to be completely consumed on direct entry. High temperature ablators such as carbon or graphite might, in principle, survive better but all extrapolations to such entry velocities are yet speculative. There are even extreme structural integrity problems since deceleration should approach 10,000 g's. Direct entry into Uranus and Neptune is much more feasible although still speculative.

On a direct entry, the time before blackout while in a detectable atmosphere is probably of the order of one second so that pre-entry measurements of the atmosphere appear unattractive.

Another class of lander mission would attempt to extend the life-time of the entry vehicle by the use of grazing trajectories. From the point of view of entry dynamics, this is equivalent to increasing the scale height of an atmosphere entered vertically, so that the rate of penetration into denser layers of the atmosphere is reduced. Of course, the ability to achieve the very low entry angles associated with grazing trajectories depends on the attainment of a very high guidance accuracy, because the entry corridors are extremely thin. In fact, if the top of the corridor corresponds to the limit of trajectories which skip out of the atmosphere, and the bottom of the corridor corresponds to the imposition of the maximum deceleration and thermal environments which can be withstood by the capsule, it is not certain that the width of the entry corridor is a positive number. Thus, the only certain possibility of capsule survival after blackout is on a skipout trajectory. Even this kind of capsule mission places extreme emphasis on orbit determination and guidance capability, and on the ability of the entry capsule to survive the substantial deceleration and thermal effects associated with the grazing skipout trajectory. Another possibility, attractive from an orbiting spacecraft, is to place a capsule in a decaying orbit about Jupiter. This could lead, as with the Echo balloon, to definitive high altitude density determinations providing the capsule could be tracked.

In view of these extreme requirements, both for the entry capsule and the parent spacecraft, an exhaustive analysis of the growth potential to this type of mission is outside of the scope of this study.

8. THE FUTURE COURSE OF THE STUDY

This section outlines what we envision to be the scope and direction of effort to be applied during the remaining period of the Advanced Planetary Probe Study. It is intended to be consistent with the Work Statement, and, of course, is subject to the cost and man-hour limitations of the contract. JPL's comments and suggestions are solicited.

8.1 MISSION ANALYSIS

In the area of mission analysis, the following are among the tasks to be addressed:

a) Science requirements. The interpretation of the scientific objectives of the mission and the establishment of sample science complements to fulfill these objectives will be expanded. The objective will be to provide the basis of a more definitive statement of the functional requirements imposed on the spacecraft by the scientific objectives. These requirements include weight, volume, power, data handling, commands, thermal control, geometrical (look angle) and trajectory requirements.

b) Comparison of midcourse correction programs for spin stabilized spacecraft. The normal and special programs outlined in Sections 3.5 and 3.6 for midcourse trajectory corrections will be compared for spin-stabilized spacecraft. Accuracy estimates for the corrected trajectory will be made, both for this comparison, and for a three-axis stabilized spacecraft.

c) Guidance and propulsion requirements for swingby trajectories. The special guidance requirements for swingby trajectories discussed in Sections 3.1 and 3.7, and the propulsion requirements for the consequent trajectory correction programs will be identified and estimated.

d) Encounter geometry. Analyses of the trajectories of the spacecraft when in proximity to the target planet will be made, with emphasis on the utilization of the geometrical characteristics in achieving the scientific objectives of the mission.

e) Orbit insertion analysis. For orbiter missions, analyses will be made similar to those identified in the preceding paragraph for the flyby missions. The orbit

insertion geometry and propulsion requirements will be analyzed.

f) Trajectories. The displays of Section 3. 3 will be completed for the remaining trajectories D and E, defined in 3. 3. 2.

8. 2 SYSTEM DESIGN TASKS

The following system design tasks will be undertaken:

a) For those configurations retained for detailed studies,

i) Detailed weight breakdowns will be generated,
ii) Detailed spacecraft power budgets will be generated,
iii) Reliability-weight-redundancy analyses will be performed, to indicate the optimum program of component redundancy, and to assess the probabilities of mission success.

b) A study will be performed to optimize the matching of the generation of data (the output of spacecraft diagnostic sensors and science sensors), the storage of data aboard the spacecraft, and the transmission of data to the earth.

c) The assessment of the interactions of RTG power supplies and the spacecraft subsystems and science sensors will be completed.

d) A more definitive conceptual design of the program of attitude control of the spin-stabilized spacecraft will be generated. It will cover initial establishment of the cruise attitude, maintaining the cruise attitude, conducting maneuvers in the cruise attitude and away from the cruise attitude, and re-establishment of the cruise attitude from other attitudes which may be either intentionally or unintentionally attained, emphasis is on the attitude control and communication subsystem requirements and implementation.

e) Criteria for micrometeroid protection will be established.

8. 3 SUBSYSTEM STUDIES

The subsystem studies will be sustained so as to attack the areas which have been variously outlined in Section 6 of this report. The results of these studies are intended to:

a) Support the system design tasks outlined in Section 8. 2

b) Satisfy paragraph 1 (b) (3) of the Work Statement, in providing descriptions of the subsystem designs.

8.4 GROWTH TO ORBITER AND CAPSULE MISSIONS

To establish the capability of spacecraft designs for growth to support orbiter and capsule entry missions the following tasks will be performed:

a) Science requirements. To utilize the orbiter mission it is likely that the science complement will be altered somewhat, compared to the flyby mission. In addition to changes in the complement of the instruments themselves, changes are expected in the relative emphasis between data storage capability and data transmission rate, and in the geometrical constraints permitting the instruments to fully exploit the orbital characteristics.

b) Oribt insertion requirements. In addition to the mission analysis of Section 8.1 d), leading to the geometrical characteristics and the propulsion requirements of the orbit insertion, other spacecraft subsystem requirements will be identified.

c) Capsule requirements. Although we consider the feasibility of a meaningful entry mission to be doubtful (see Section 7.3), a brief examination of the requirements of such a mission on the spacecraft design will be made.

8.5 RELIABILITY

The reliability studies prescribed by the work statement, paragraph 1 (b) (5), will be undertaken. It is anticipated that the principal use of these studies will be to support the studies of Section 8.2 a) iii).

8.6 COST EFFECTIVENESS

The cost effectiveness analysis prescribed by the work statement, paragraph 1 (b) (6), will be performed.

8.7 SCHEDULE AND COST ESTIMATES

The schedule and cost estimates prescribed by the work statement, paragraph 1 (b) (7), will be performed.

RE-ORDER NO. 66-107

March 28, 1966

MID-TERM TECHNICAL PROGRESS REPORT

ADVANCED PLANETARY PROBE STUDY

15 March 1966

ERRATA

p 13	The last paragraph of p 14, which ends on p 15, should be removed from that location and inserted on p 13, after the heading "3.2.3 Injection Accuracy"
pp 20, 21, 23, 24	After "SCALE:" change from "1 au = 0.25 inch" to "1 au = 0.14 inch" (4 places)
p 26	Replace entire page with new page (attached)
p 28	Replace entire page with new page (attached)
p 31	In the first line of the second paragraph, replace "through" by "into"
p 34	In the third column heading of the table, insert "σ" to make it read "1σ Semi-Major Axis"
p 70	In the column heading under A, delete "/HEKS" to give "Saturn V/ Centaur"
p 71	In the column heading "Launch Vehicle", next to last entry of the table, delete "/Centaur" to give "Saturn V," last entry of the table delete "/HEKS" to give "Saturn V/Centaur"
p 117	In the row titled "Maximum rate (deg/sec)" change "0.0081" to "0.0167" and insert in the right-hand column "0.00834"
p 121	In Figure 6.4-2, the second antenna from the top should be labeled "A_5"
p 153	In the third line from the bottom, change "detriment" to "decrement"
p 157	In subparagraph d), make an additional sentence by changing "attained, emphasis" to "attained. Emphasis"

JPL Contract 95 13 11

This work was performed for the Jet Propulsion Laboratory, California Institute of Technology, sponsored by the National Aeronautics and Space Administration under Contract NAS7-100.